NBSIR 77-1213

Skid Resistance Measurement Tests of New FHWA Reference Systems at the Eastern Field Test Center

R. W. Kearns and J. F. Ward

Engineering Mechanics Section
Mechanics Division
Institute for Basic Standards
National Bureau of Standards
Washington, D.C. 20234

February - April 1976

Final

Issued March 1977

Prepared for
Federal Highway Administration
Office of Development
Washington, D.C. 20590

NBSIR 77-1213

SKID RESISTANCE MEASUREMENT TESTS OF NEW FHWA REFERENCE SYSTEMS AT THE EASTERN FIELD TEST CENTER

R. W. Kearns and J. F. Ward

Engineering Mechanics Section
Mechanics Division
Institute for Basic Standards
National Bureau of Standards
Washington, D.C. 20234

February - April 1976

Final

Issued March 1977

Prepared for
Federal Highway Administration
Office of Development
Washington, D.C. 20590

U.S. DEPARTMENT OF COMMERCE, Juanita M. Kreps, ***Secretary***

Dr. Betsy Ancker-Johnson, ***Assistant Secretary for Science and Technology***

NATIONAL BUREAU OF STANDARDS, Ernest Ambler, ***Acting Director***

Federal Highway Administration Policy

CONTENTS

ILLUSTRATIONS

TABLES

SKID RESISTANCE MEASUREMENT TESTS
OF
NEW FHWA REFERENCE SYSTEMS
AT THE
EASTERN FIELD TEST CENTER

February - April, 1976

ABSTRACT

The Federal Highway Administration (FHWA) is developing a program to improve the method of measuring wet weather pavement skid resistance (SN) and to reduce the variation in results. At the national level, an interim reference system (IRS) is maintained and operated by the National Bureau of Standards. At the regional level, an area reference system (ARS) is maintained and operated at each FHWA Field Test Center. Intercomparisons between these reference systems and the highway measuring systems at the state level provide measurement assurance.

In this report, the first correlations between three identical, newly manufactured systems (ARS 1, 2, 3) and the IRS are given. Computed standard deviations of mid-range predicted SN values are typically less than 0.1 SN. SN is given as a function of test speed for each system, on two test surfaces. Speed gradients of SN are found to be characteristic of the surface.

The test program is explained, from preparations and calibrations of subsystems through dynamic measurement on the surfaces. Controlled and uncontrolled variables are identified, discussed, and in some cases, investigated experimentally. A ranking of the sources of dispersion is given.

A ground station for improved SN calculation precision and on-site statistical analysis, operated in parallel with traditional SN data acquisition methods, is found to perform reliably.

Key Words: Accident reduction, skidding; correlation, skid resistance; highway safety; measurement, skid resistance; pavement, skid resistance; pavement wetting system; skid resistance, measurement; tire-pavement interface forces; wet pavement skid resistance.

1. INTRODUCTION

The measurement of the skid resistance of highways, under wet weather conditions, is part of the Federal Highway Administration (FHWA) skid accident reduction program. Currently, the majority of state highway departments measure pavement skid resistance with locked-wheel skid measurement systems, which are reported to be in substantial compliance with the requirements of ASTM Designation E 274-70 [1].* To reduce the variability between measurement results from different designs of systems meeting these requirements and to improve the precision of the measurements made by a given system, FHWA is developing a hierarchical system for the measurement of pavement skid resistance [2]. At the national level, the FHWA program provides for an interim reference system (IRS) maintained by the National Bureau of Standards (NBS). At the regional level, the program provides for area reference systems (ARS) maintained at FHWA Field Test Centers (FTC). At the state level, skid resistance measuring systems are maintained to inventory and rank the condition of the highways in accordance with their skid resistance. The plan to assure measurement consistancy between the states includes the monitoring and development of test procedures and equipment by NBS to relate the measurements made within the hierarchical system to the national measurement system.

The measurement assurance program for FTC and ARS includes the periodic evaluation of test facilities and procedures, determination of the performance characteristics of the ARS and its subsystems, measurement of selected reference surfaces maintained at the FTC with the IRS, and correlation of the measurements made by the ARS and IRS. The program also includes the evaluation of new test equipment and procedures, and experimental studies for the development of numerical data, where appropriate, to identify and quantify sources of difference in the skid number measurements. As a result, improvements in procedure and equipment are expected as the program develops with the increased measurement capabilities being transferred to the highway measurement systems at the FTC.

This report describes tests conducted under the direction of NBS personnel at the FHWA Eastern FTC (EFTC), East Liberty, Ohio, in the spring of 1976. At that time, three new skid measurement systems were

---

* Numerals in brackets denote the literature references cited at the end of this report.

tested along with the IRS. The new systems were designed and manufactured for use as area reference systems. Subsequently, FHWA has assigned the unit described herein as ARS 1 to the Central/Western FTC (C/W FTC), College Station, Texas, and has assigned the unit described as ARS 3 to the EFTC.

2. PREPARATION, MEASUREMENT, AND ADJUSTMENT OF SUBSYSTEMS

Previous results from skid trailer test programs indicated the measurements lacked precision, agreement among trailers using self-watering systems was poor, and the causes for the differences between trailer measurements were difficult to define [3]. To identify sources of these differences, certain preparations were made and auxiliary equipment and experiments were designed to measure, and intercompare with the IRS, the performance characteristics of the components and subsystems. When conditions were found to be outside the ASTM requirements or conditions were found that would adversely affect the total performance of the ARS, adjustments and modifications were made or recommended.

2.1. Test Preparations

Auxiliary test equipment was prepared at NBS to supplement the facilities of the Field Test Center. Test tires were obtained and prepared by examination and break-in.

2.1.1. Auxiliary Test Equipment

Skid resistance is reported in terms of skid number (SN), which is determined from the force required to slide a locked test tire at a stated speed in the presence of a water layer applied to the pavement ahead of the test tire, divided by the effective wheel load and multiplied by 100. The speed, the thickness of the water layer, and forces at the tire-pavement interface are the principal quantities to be measured. To relate these measurements to the national measurement system, auxiliary test equipment was designed, using component types which are routinely calibrated in various NBS laboratories.

A differential radar speed meter, whose time base was calibrated against a standard frequency and whose radiated frequency is specified to be well within limits required for its 0.1 miles per hour (mph) (0.16 kilometers per hour (km/h)) resolution was used to record the speed of the system during a skid resistance measurement (sec. 2.4).

A turbine flow rate meter was calibrated to a 0.6 gallons per minute (gpm) (2 liter per minute (l/min)) uncertainty in the Fluid Meters Section. Calibrations were obtained for the turbine both alone and as part of a digital differential flow rate system having a 0.1 gpm (0.4 l/min) resolution. The system is part of the on-board IRS instrumentation, but is adaptable to measuring the flow rate in the ARS (sec. 2.5).

Two load cells, calibrated to a 0.25 pounds-force (lbf) (1.1 newton (N)) uncertainty in the Engineering Mechanics Section, were utilized in a test fixture to apply simultaneously known traction and load forces to a force plate during its calibration [4]. The force plate was used subsequently to calibrate the force transducers of the trailers (sec. 2.6).

Other auxiliary test equipment included a voltmeter, calibrated to 1 millivolt uncertainty by the Electrical Instruments Section; an inflation pressure gage, calibrated to 0.05 pounds-force per square inch (psi) (345 pascals (Pa)) uncertainty by the Pressure and Vacuum Section; and an automatic sequential displacement recording system (sec. 2.7).

2.1.2. Test Tires

In preparation for the testing at EFTC, each of the ASTM E 501 test tires [5] to be used was mounted on a wheel, balanced and broken in with a drive of approximately 200 miles (320 km). In addition, a representative sample of the tires was examined at NBS to verify the nominal radial spring rate of 1280 lbf/in (224 kN/m) at 24 psi (165 Pa) inflation pressure under 1085 lbf (4800 N) load after break-in. The value was determined from radial load versus deflection data obtained with the test setup shown in figure 1.

2.2. Skid Trailer Weight Distribution

To measure the static weight distribution of the test trailer, a vertical load cell was placed under the hitch and a force plate was placed under each tire of the trailer. E 501 test tires were used. The fifth wheel, in the ARS trailer design, bears part of the load when in operation and was placed in operating position during the measurement. The piping of the left nozzle was filled with water, the air-bearings of the force plates were inflated, and the trailer was oriented. Load readings were then taken simultaneously and weight adjustments were made to bring the readings into the range of desired values.

The ARS trailers were not provided with adjustable trim weights or fastenings for weights. Each measurement was interrupted while EFTC personnel fabricated the weights needed. To minimize delay, other testing proceeded after the desired weights had been temporarily taped in place. Later the weights were fastened more securely but time did not permit a re-check of the static loads.

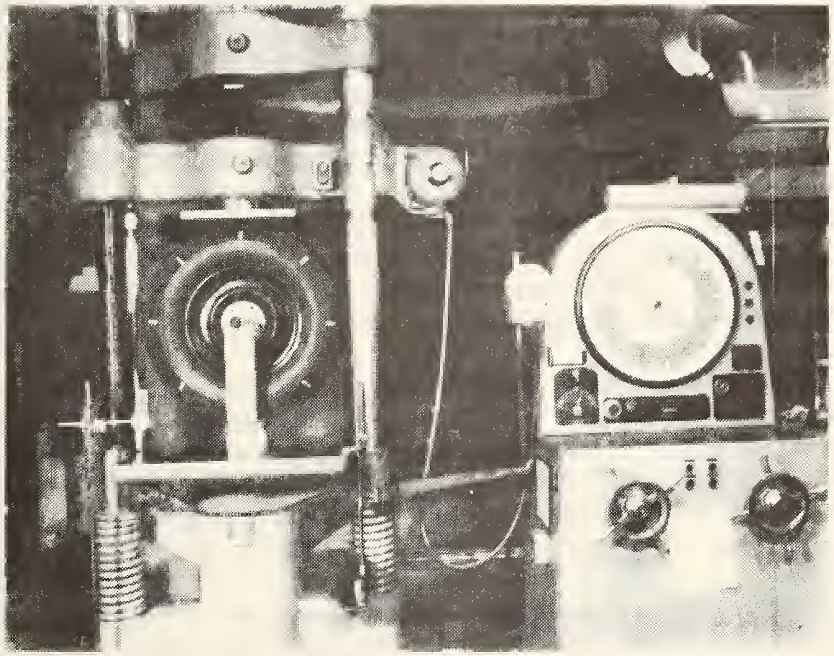

Figure 1. Test tire radial spring rate test set-up.

It is believed that all equipment contributing to the weight of the new ARS trailers had been installed by the time of the load measurements. However, they had only a prime coat of paint. An undetermined weight due to finish coats was added to ARS 1 after the static testing period. ARS 2 and ARS 3 went through dynamic testing with the prime coat only.

The measured load distributions are shown in table 1.

2.3. Tow Vehicle Displacements

Changes in the tow vehicle hitch height and rear wheel radius were measured as a function of crew weight and water load. Changes in hitch height affect the skid number measurement in two ways; the vertical load reduction factor is altered and the transducer is rotated such that a component of the vertical load may be measured as traction (sec. 2.6). Changes in tow vehicle rear wheel radius change the water pump rate.

Figure 2 shows the results for hitch height. For ARS and IRS, a rise on the order of 0.2 in (0.5 cm) occurred with removal of 800 lbf (3560 N) water load. The hitch was more sensitive to water load changes than to equal crew load changes.

Figure 3 indicates rear wheel radius changes. Data are shown for the left wheels; right wheel behaviour was similar. The radius change of the ARS units, which have dual rear wheels, amounted to 0.7 percent of the nominal 15.5 in (39.4 cm) radius over the range of water load. The ARS radius was less sensitive to crew load changes than to equal water load changes.

The single rear wheels of the IRS changed by 1.9 percent of the nominal 14.4 in (36.6 cm) radius over the range of water load. IRS wheel radius was roughly as sensitive to crew load changes as to equal water load changes.

2.4. Speed Measuring Subsystem

Each ARS employs a commercial fifth wheel in a modified mounting within the trailer frame. The wheel is instrumented for speed readout. The speed signal is recorded as a step function on the ARS strip chart recorder.

One speed recording range was operational in the ARS: 0 to 100 mph (0 to 161 km/h) in 50 scale divisions, each 0.8 mm wide. Each division represented 2 mph (3.2 km/h). Apparent 0.2 mph (0.3 km/h) signal steps could be discerned on the chart with the aid of a 7X hand lens. However, because the width of the line drawn by the pen was equivalent to about 0.8 mph (1.3 km/h), a more sensitive recording range would have been appropriate.

Table 1. Skid trailer static load distributions

Trailer	Left wheel weight	Right wheel weight	Hitch weight
	lbf[a]	lbf	lbf
ARS 1	1085	1085	146
ARS 2	1085	1085	141
ARS 3	1085	1085	148
IRS	1086	1085	149

[a] 1 lbf = 4.448 N.

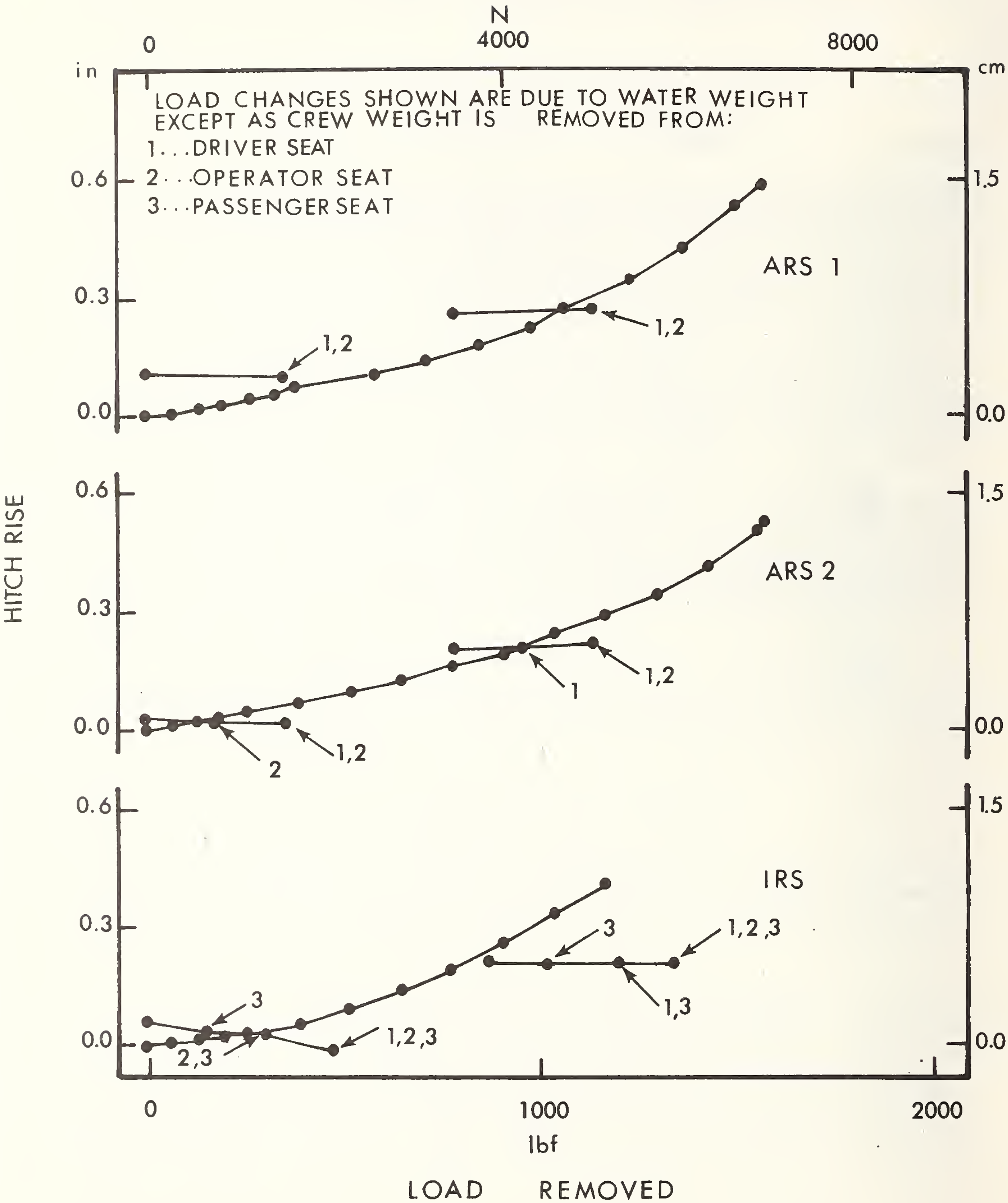

Figure 2. Change in tow vehicle hitch height with load.

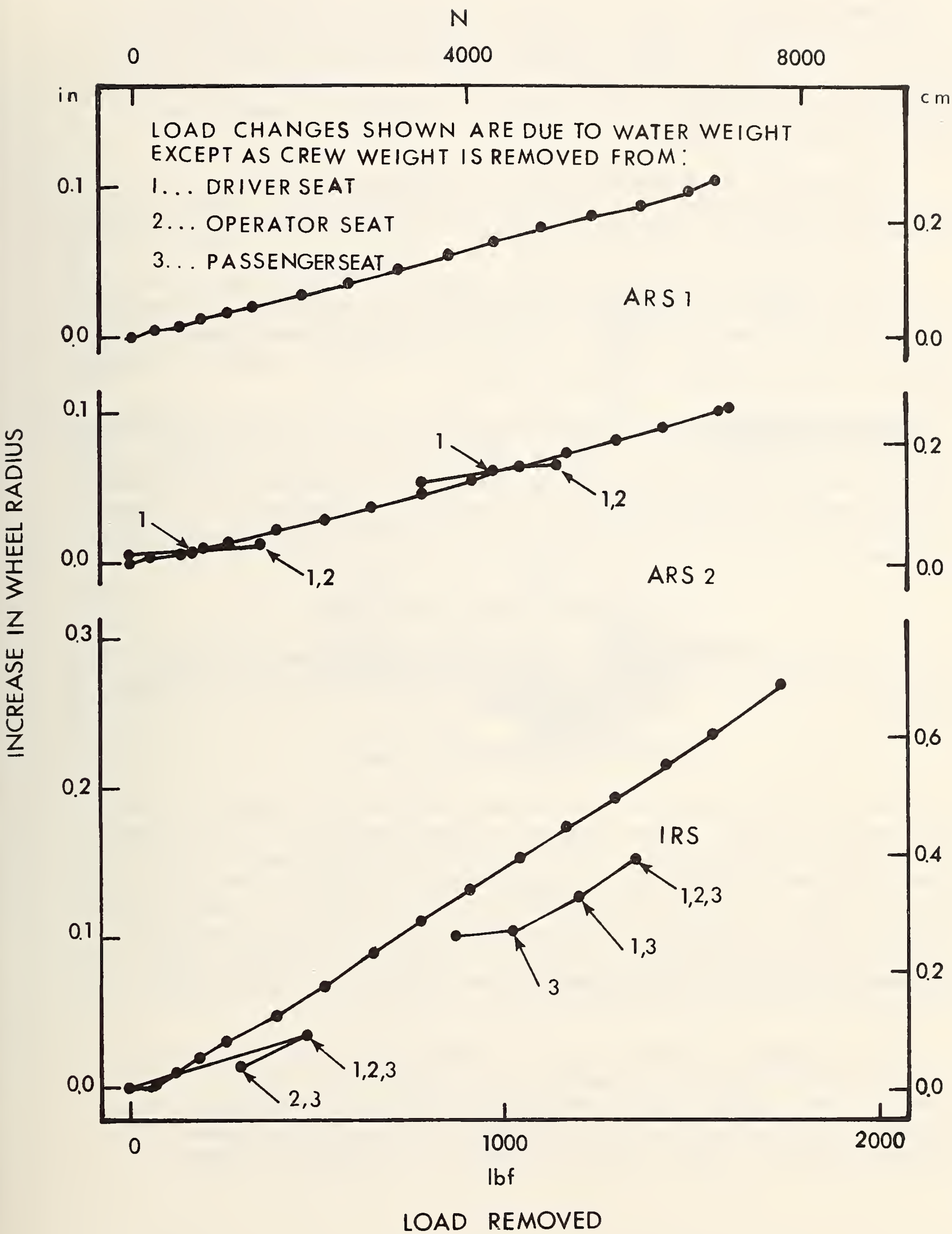

Figure 3. Change in tow vehicle rear wheel radius with load.

Speed subsystems of ARS 1, ARS 2, and the IRS were adjusted on the measured mile and then checked against the IRS stationary radar system (fig. 4). The tests showed agreement between the radar and the vehicle speed subsystems within 0.5 mph (0.8 km/h) at speeds of 20, 40, and 60 mph (32, 64, and 97 km/h). The results of a check at about 40 mph (64 km/h) are shown in figure 5.

A compatibility of measured mile calibrations and radar was thus confirmed. After the initial adjustment of each vehicle, further use of the measured mile was left to the discretion of the vehicle operators.

The EFTC measured mile facility is on a 7.5 mile (12 km) one-way oval track. Because measured mile procedures on this track were difficult and time-consuming, use of the radar for speed checks saved many man-hours. The saving allowed speed checks to be made frequently, which helped to assure accurate readout on board.

During dynamic correlation, checks were made in the same speed range as the subsequent skid tests. Each vehicle's speed subsystem was compared to the radar before each morning or afternoon session and whenever the speed range changed during a session. In addition, the radar was used to independently record the speed of each vehicle during each skid test.

2.5. Pavement Wetting Subsystem

The pavement wetting subsystem was tested for water flow rate, uniformity of water distribution, and width of the water trace on the pavement.

2.5.1. Flow Rate Measurement

The new ARS trailers are fitted with turbine flow sensors of the type used in the IRS. These provide on-board capability for measuring flow rate during skid tests. The ARS sensors were shipped to NBS in advance and were calibrated by the Fluid Meters Section. The calibrations relate the electrical pulse rate of the sensors to water flow. The results were provided to EFTC before the trailers were completed. The final turbine calibration reports are shown in Appendix A. ARS instrumentation converts the sensor pulse train to an analog signal for display on a channel of the ARS strip chart recorder.

The IRS sensor combined with its readout instrumentation has been calibrated as a complete flowmeter in the Fluid Meters Section. This flowmeter uses digital signal processing which is intrinsically free from the offset and gain drifts associated with analog equipment. It provides numerical readout with resolution of 0.1 gpm (0.4 l/min).

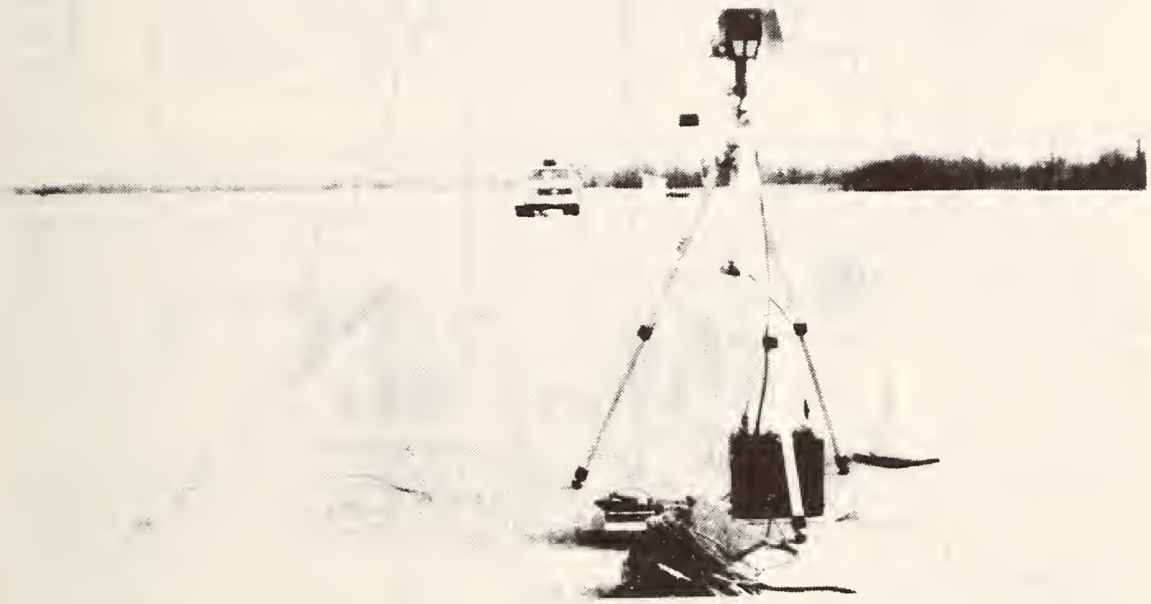

Figure 4. Radar check of vehicle speed.

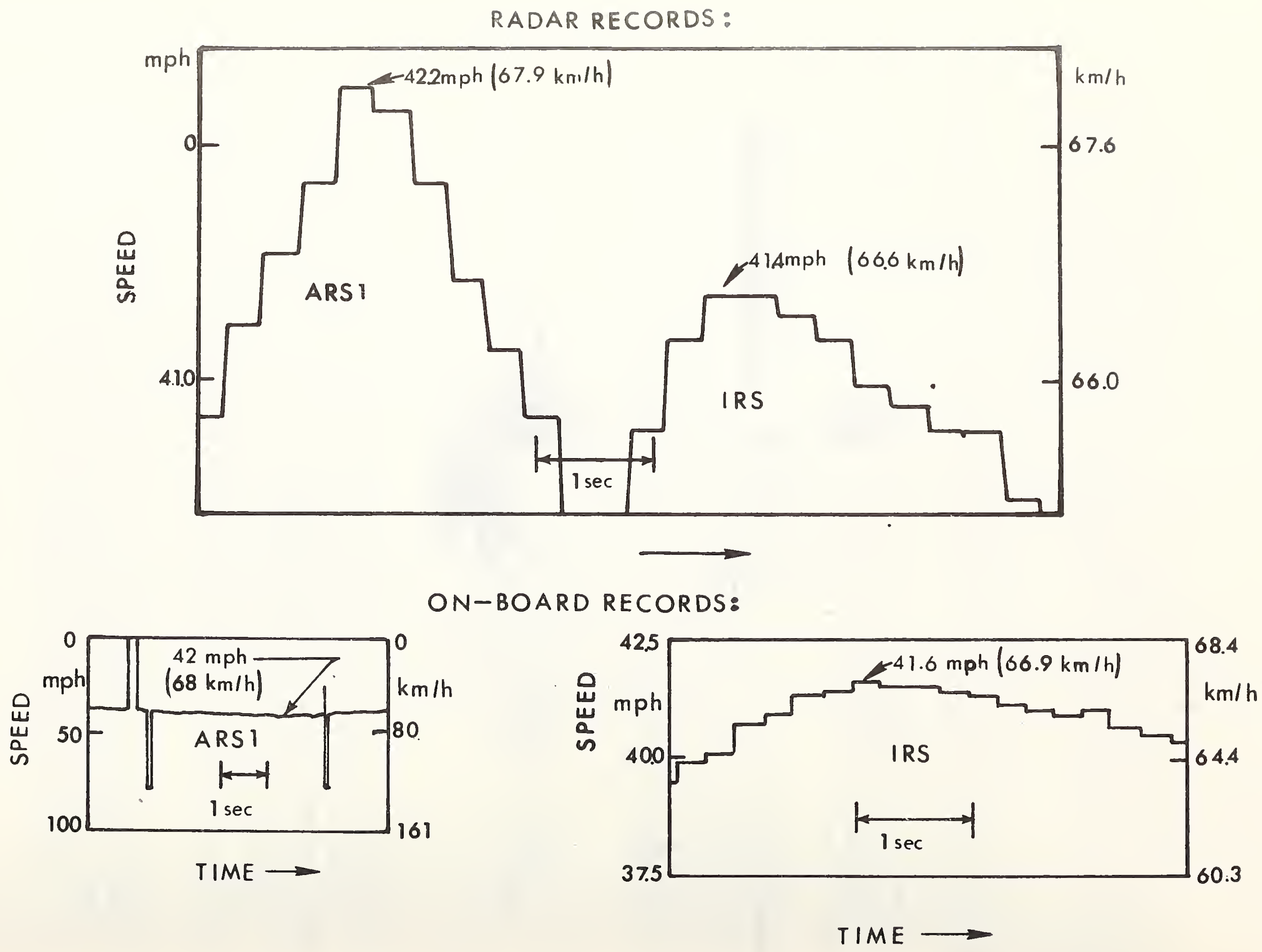

Figure 5. Simultaneous speed data recorded by the stationary radar and the ARS 1 and IRS tow vehicles in motion (fifth wheels).

The offset and gain adjustments of the ARS flow instrumentation can be checked and set at any time by comparing the analog readout with the sensor pulse rate. Had this been done by EFTC personnel, their settings would have been checked by direct comparison with the IRS flowmeter. Unfortunately, the ARS circuit had only one connector so that either the readout or a pulse rate counter could be connected to the sensor, but not both simultaneously. It is recommended that this circuit be modified to permit such simultaneous measurements so that full use can be made of the calibration data.

Since the needed simultaneous measurements could not be made, comparisons between the readouts of the IRS and the ARS were used to make the primary adjustment. The pipe section containing the IRS flow sensor was connected by flexible hose in tandem with the ARS sensor as shown in figure 6. Simultaneous readings were taken at various flow rates. Adjustments were made to bring the ARS readout into agreement with the IRS flowmeter.

It would have been desirable to bring the readout of each ARS into agreement with the reference flowmeter at two flow rates within the upper and lower limits of the useful range. The flow sensor manufacturer specifies linear operation between 3.7 and 60 gpm (14 and 230 l/min) for this model, and the desired operating range is approximately 10 to 50 gpm (40 to 190 l/min). However, EFTC personnel chose to use zero flow as one set point. The positive value was chosen in the upper half of the operating range.

The ARS recording range was 0 to 50 gpm (0 to 190 l/min) in 50 scale divisions, each 0.8 mm wide. The width of the line drawn by the pen was equivalent to about 0.5 gpm (2 l/min). EFTC personnel used a 7X lens to read the record with 0.1 gpm (0.4 l/min) precision.

The comparison results, in this case, were satisfactory after adjustments to the ARS. Calibration signals generated by the ARS instrumentation were determined to have these equivalent values:

ARS 1,	46.5 gpm	(179 l/min);
ARS 2,	46.3 gpm	(175 l/min);
ARS 3,	46.5 gpm	(176 l/min).

These values were provided to the ARS crews for the purpose of readout scaling during the skid tests. The crews used the readouts to trim and monitor flow rates.

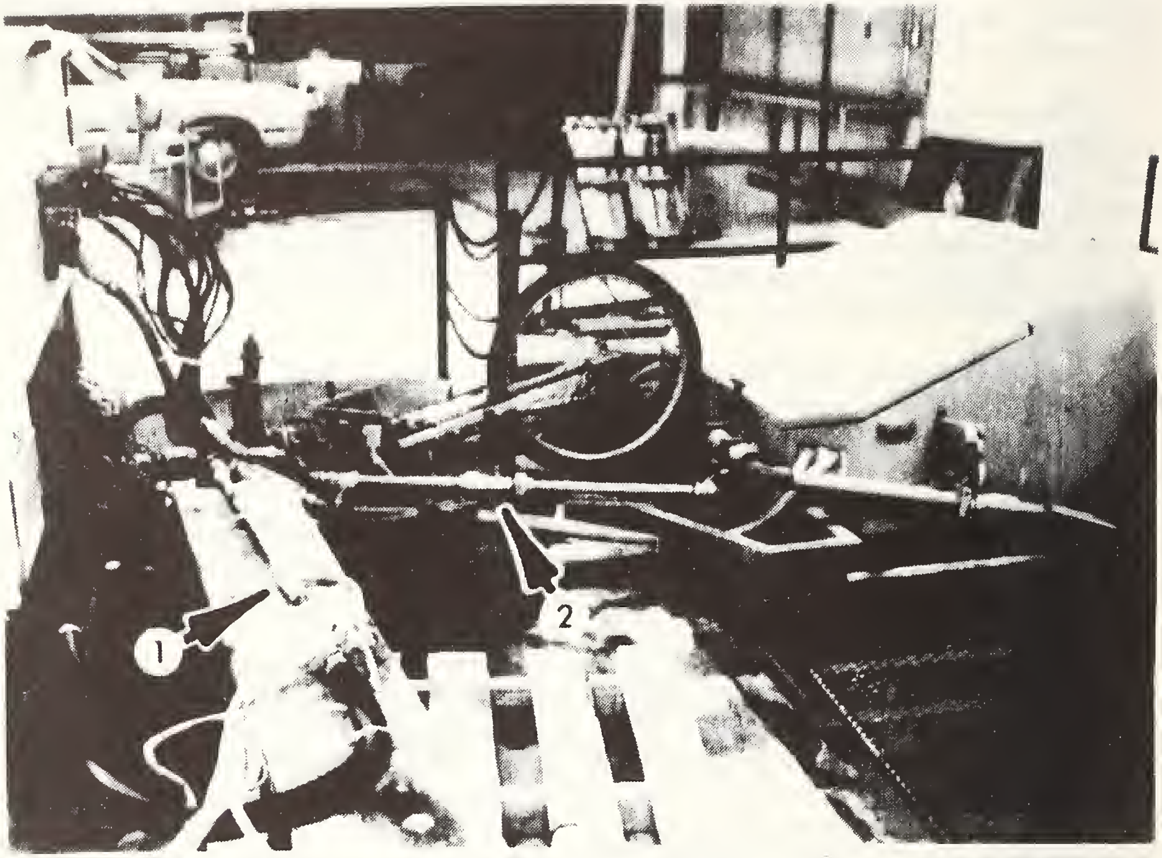

1 = IRS FLOW SENSOR
2 = ARS FLOW SENSOR

Figure 6. Tandem arrangement for comparison of flow rate measurements.

2.5.2. Water Distribution

Distributions measured on the static distribution gage (SDG) have been shown previously [6, sec. 2.5][7, sec. 2.5], both for the type of nozzle used on the new ARS systems and for the flow channel of the IRS. During this testing period, SDG distributions were measured for ARS 1 and the IRS. Later, distribution measurements were also obtained for ARS 2 and ARS 3. Representative examples of distributions at 40 mph (64 km/h) flow rates are shown in figures 7, 8, 9, and 10.

2.5.3. Wetted Width Measurement

To lay the desired water film thickness, the flow rate must be adjusted as a function of the width of the water trace at the leading edge of the tire-pavement interface. A satisfactory method for direct measurement of the width under dynamic conditions is not available. Techniques used during these tests included measurement of stream width pumped while the vehicle remained stationary, measurement of the trace left on the pavement after the vehicle passed, and measurement from photographs taken under dynamic conditions.

ARS pavement wetting nozzles were of the "Penn State" diverging stream type. The orifices were typically centered 3.25 inches (8.3 cm) above the pavement with a 25° angle between the pavement and the top nozzle surface. ARS wetted widths were measured for these conditions.

In the method favored by EFTC, a ruler was used to measure stream width from the stationary vehicle at the level where the stream normally impacts on the pavement. For ARS 1, this measurement was performed over pavement at the approximate flow rate for 40 mph (64 km/h) (fig. 11) and EFTC personnel considered the result to agree with characteristic values for this type of nozzle. They estimated the characteristic value for 20 mph (32 km/h) to be 6-1/4 to 6-1/2 inches (15.9 to 16.5 cm) and for 60 mph (97 km/h) to be 7-3/4 to 7-7/8 inches (19.7 to 20.0 cm). Later, for ARS 2, they performed the measurement over the SDG basin at flow rates corresponding to 20, 40, and 60 mph (32, 64, and 97 km/h). The water passed into the vanes of the basin without actual impact. The method neglects the effects of impact and divergence (shown for the static case in fig. 12) which affect the stream width encountered by the tire.

The measured widths at the level of impact are included in table 2. The results of similar measurements for the non-divergent IRS flow channel are also included, where the level of impact is taken as 1/4 inch (0.6 cm) below the lip of the channel.

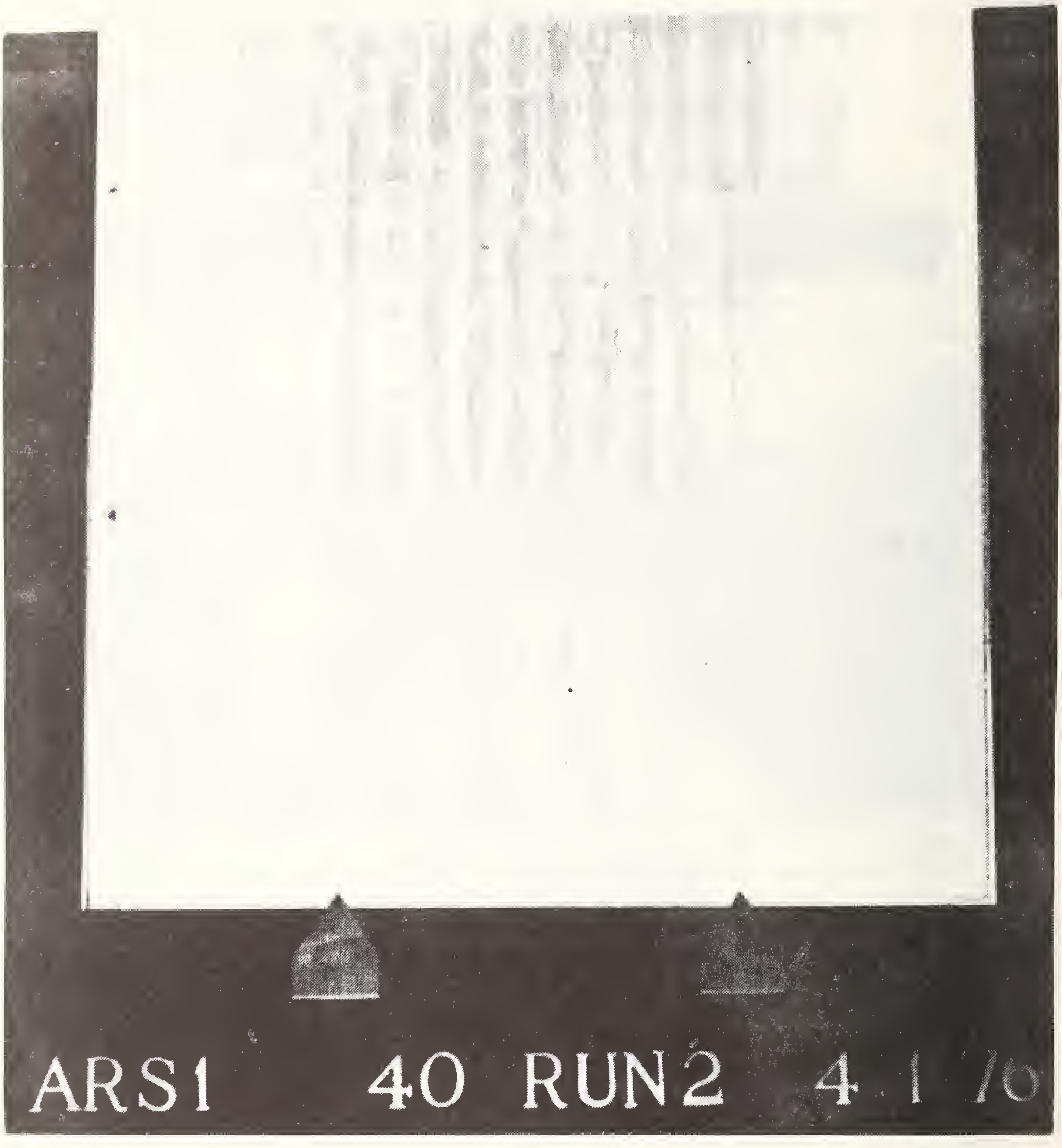

Figure 7. ARS 1 static water distribution at 40 mph (64 km/h).

Figure 8. ARS 2 static water distribution at 40 mph (64 km/h).

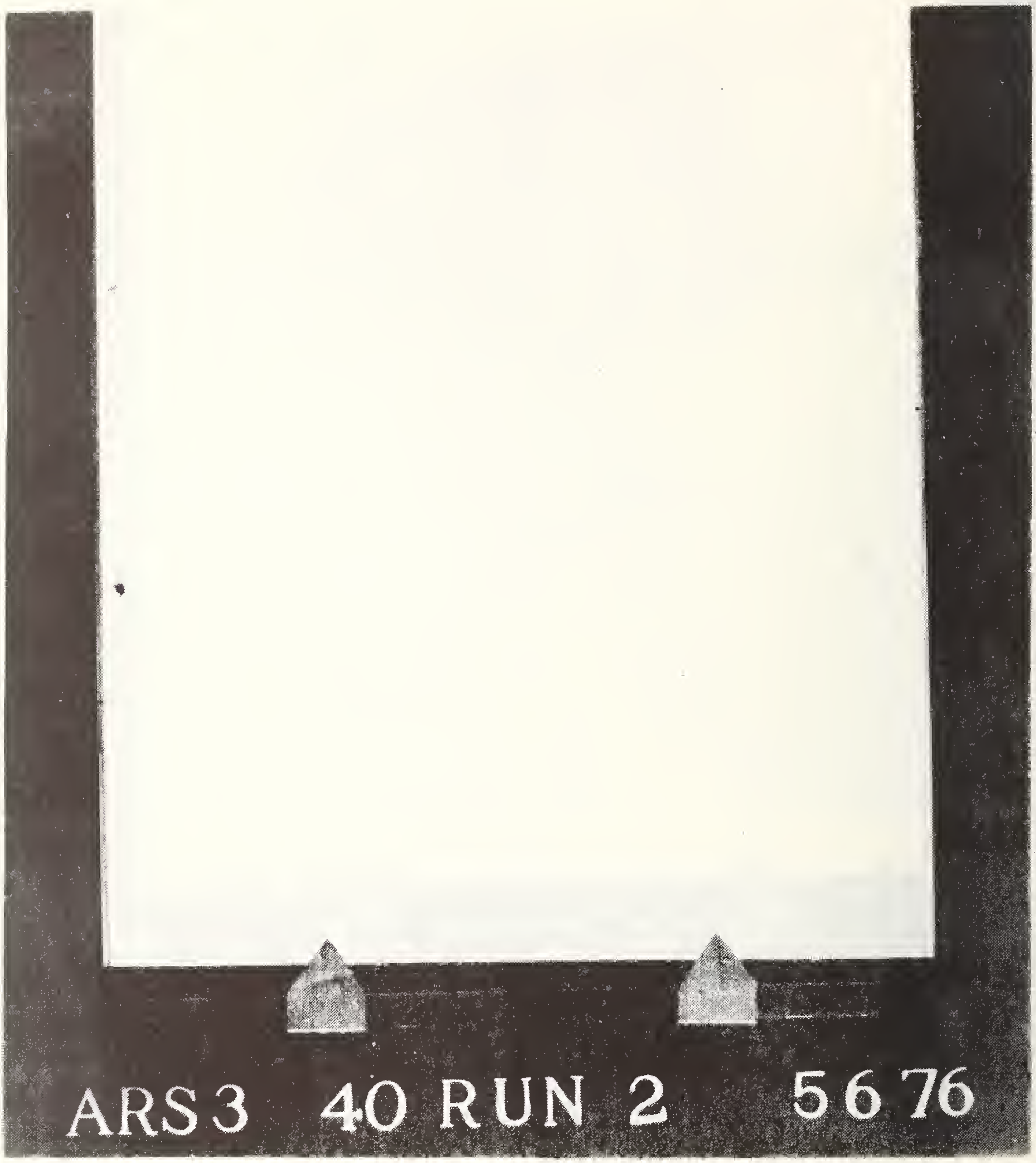

Figure 9. ARS 3 static water distribution at 40 mph (64 km/h).

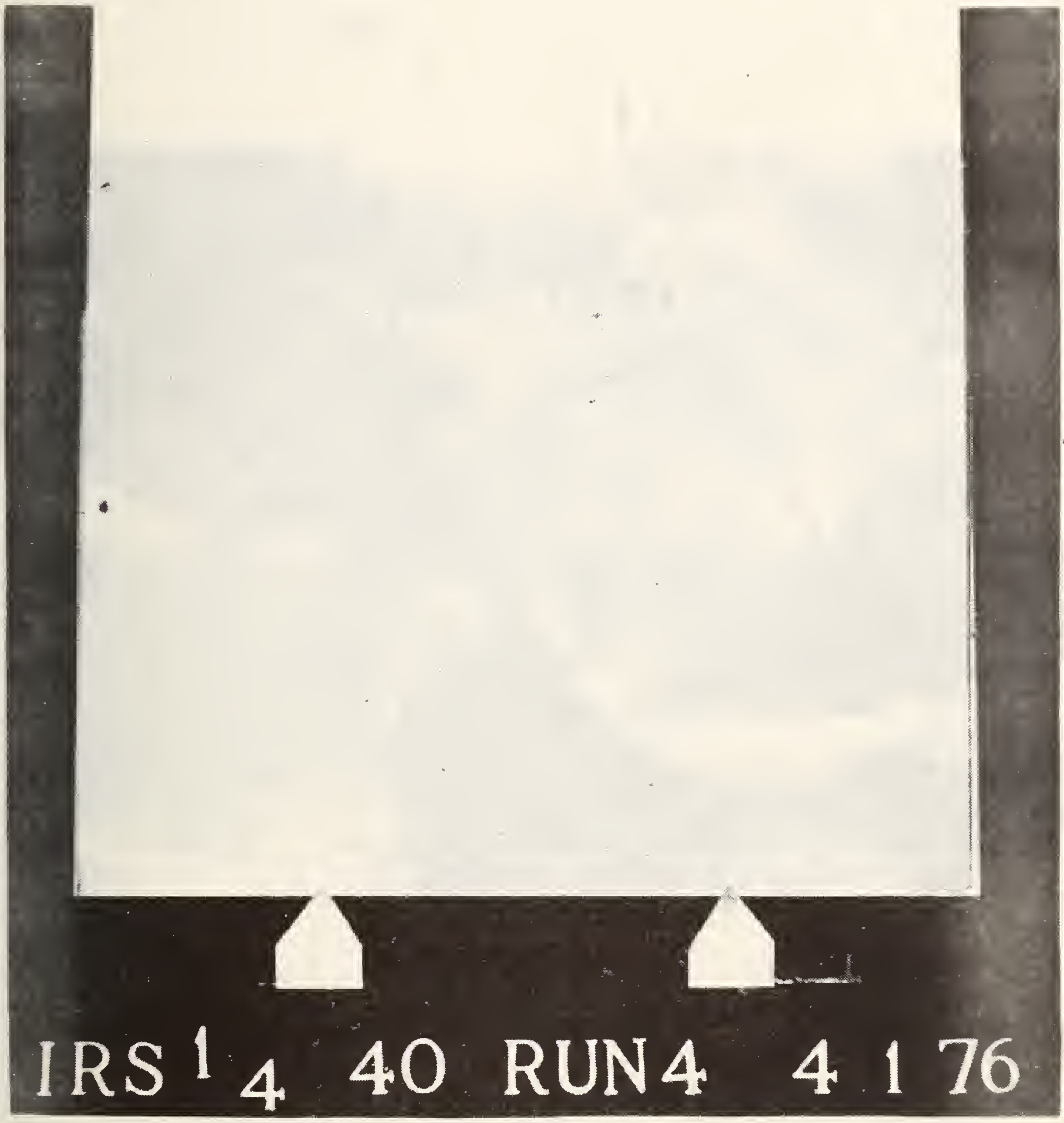

Figure 10. IRS static water distribution at 40 mph (64 km/h).

Figure 11: Measurement of the stream width from an ARS nozzle at the level of impact: The flow rate corresponds to 40 mph (64 km/h):

Figure 12. Impact on the pavement of the stream from a stationary ARS nozzle. The flow rate corresponds to 40 mph (64 km/h). The trailer wheel has been extended to avoid interference with the stream.

Table 2. Wetted width measurements

Speed	Unit	Flow rate	Method	Wetted width
mph[a]		gpm[b]		in[c]
20	ARS 2	13.5	Level of impact	5.8
20	ARS 1	13	Pavement	9.4
20	ARS 1	13	Photo	[d]10 to 13
20	IRS	14.7	Level of impact	7.8
20	IRS	14	Pavement	8.9
20	IRS	14	Photo	8
40	ARS 1	--	Level of impact	7.2
40	ARS 2	25.8	Level of impact	7.2
40	ARS 1	26	Pavement	9.8
40	ARS 1	26	Photo	[d]13 to 14
40	IRS	28.9	Level of impact	7.9
40	IRS	29	Pavement	10.4
40	IRS	29	Photo	14
60	ARS 2	39.0	Level of impact	8.2
60	ARS 1	39	Pavement	[d]20 to 37
60	ARS 1	39	Photo	13
60	IRS	44.1	Level of impact	8.1
60	IRS	44	Pavement	[d]11.6 to 16
60	IRS	44	Photo	17

[a] 1 mph = 1.609 km/h.

[b] 1 gpm = 3.8 l/min.

[c] 1 in = 2.54 cm.

[d] While most water is concentrated within the smaller width, spray can be seen extending to the larger width.

The adjusted flow rate values set by the ARS crews during skid testing were calculated by EFTC personnel from the ASTM E 274-70 quantity specification using the widths they considered characteristic of this method. IRS flow rate settings were based on E 274-70 and the flow channel orifice width, 8 inches (20 cm).

Trace widths left on the pavement by the streams under dynamic conditions were measured for ARS 1 and the IRS. The test wheels of the trailers were extended beyond the water trace (fig. 13). The pavement wetting outlets remained in their normal position. This arrangement was chosen to minimize the change of the aerodynamic disturbance of the stream and the disturbance due to the tire running in the trace. The brake was not applied. Several measurements were made of each trace with increasing delay times to allow extrapolation back to the moment of passage. The data are plotted in figure 14. The lines for 60 mph (97 km/h) relate to the wettest part of the trace rather than the total width. At this speed, spray enlarged the total width to about 37 inches (94 cm) for the ARS 1 trace and about 16 inches (41 cm) for the IRS trace.

Generally the water trace on the pavement spreads in the first minute after the trailer passes. In the case of the ARS, the 60 mph (97 km/h) trace width decreased. Apparently the water was so thin that evaporation overcame spreading. Uncertainties in the use of this method include measurement between the indistinct boundaries of the trace and the validity of linear extrapolation.

Downward views of the water laid by ARS 1 and the IRS were photographed by a high speed camera from mountings on the test trailers. Again, the test wheels were extended. After processing, the photographic images were measured to obtain stream widths at the normal position of the tire-pavement interface. The photographs also give some information about the coupling of water to the pavement: streaks indicate water in contact with the pavement, while the remainder of the stream is in the air and moving almost as fast as the trailer. A wave or pulse effect prominent in ARS 1 streams, is visible in figure 15 as lateral bands. Note also the inboard drift of the stream.

A comparison of the results of these methods, all listed in table 2, illustrates the difficulty in assigning a "wetted width" with confidence.

Figure 13. Measurement of water trace width after the trailer has passed. A 20 mph (32 km/h) run by ARS 1 is shown.

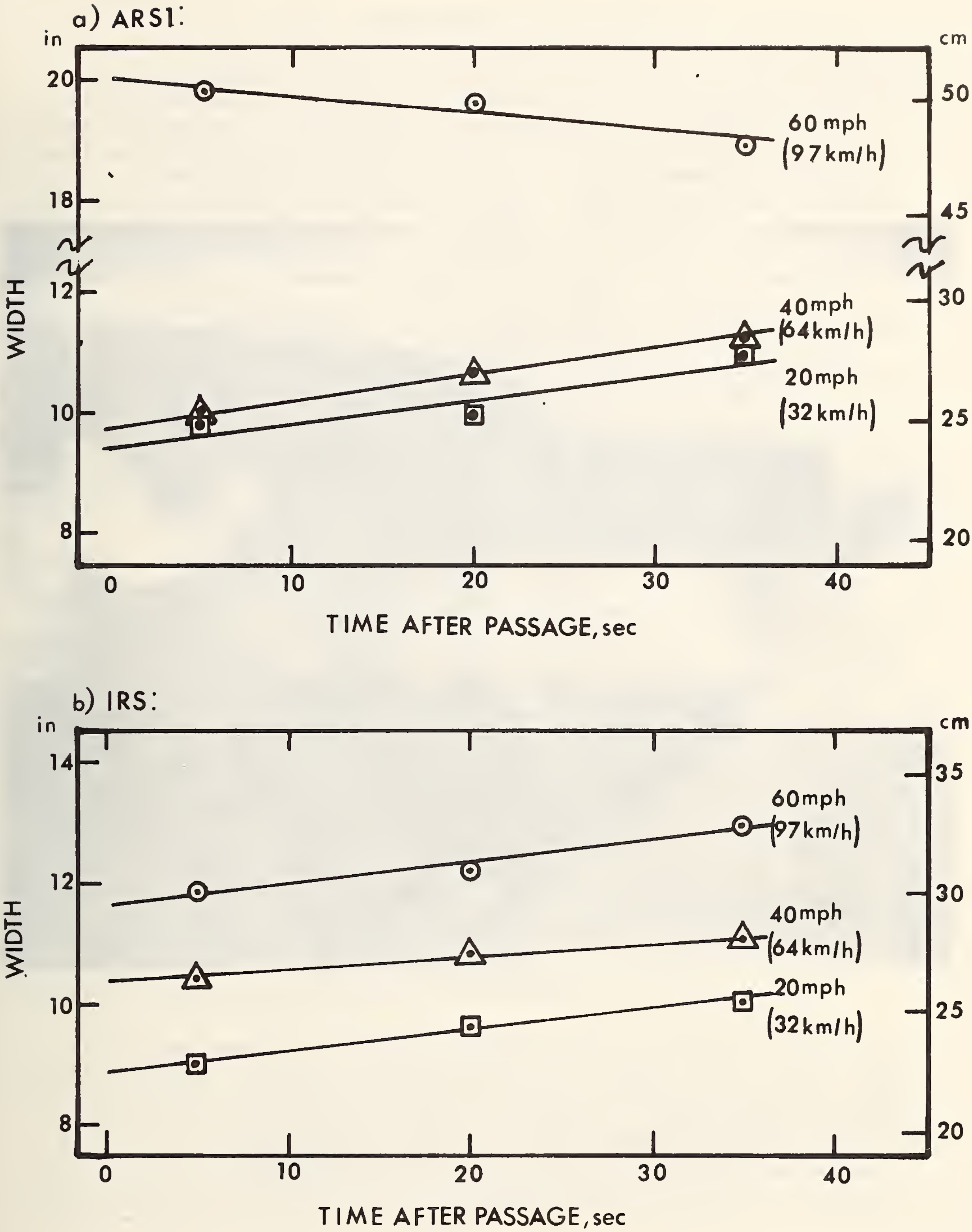

Figure 14. Wetted width by delayed measurement on pavement.

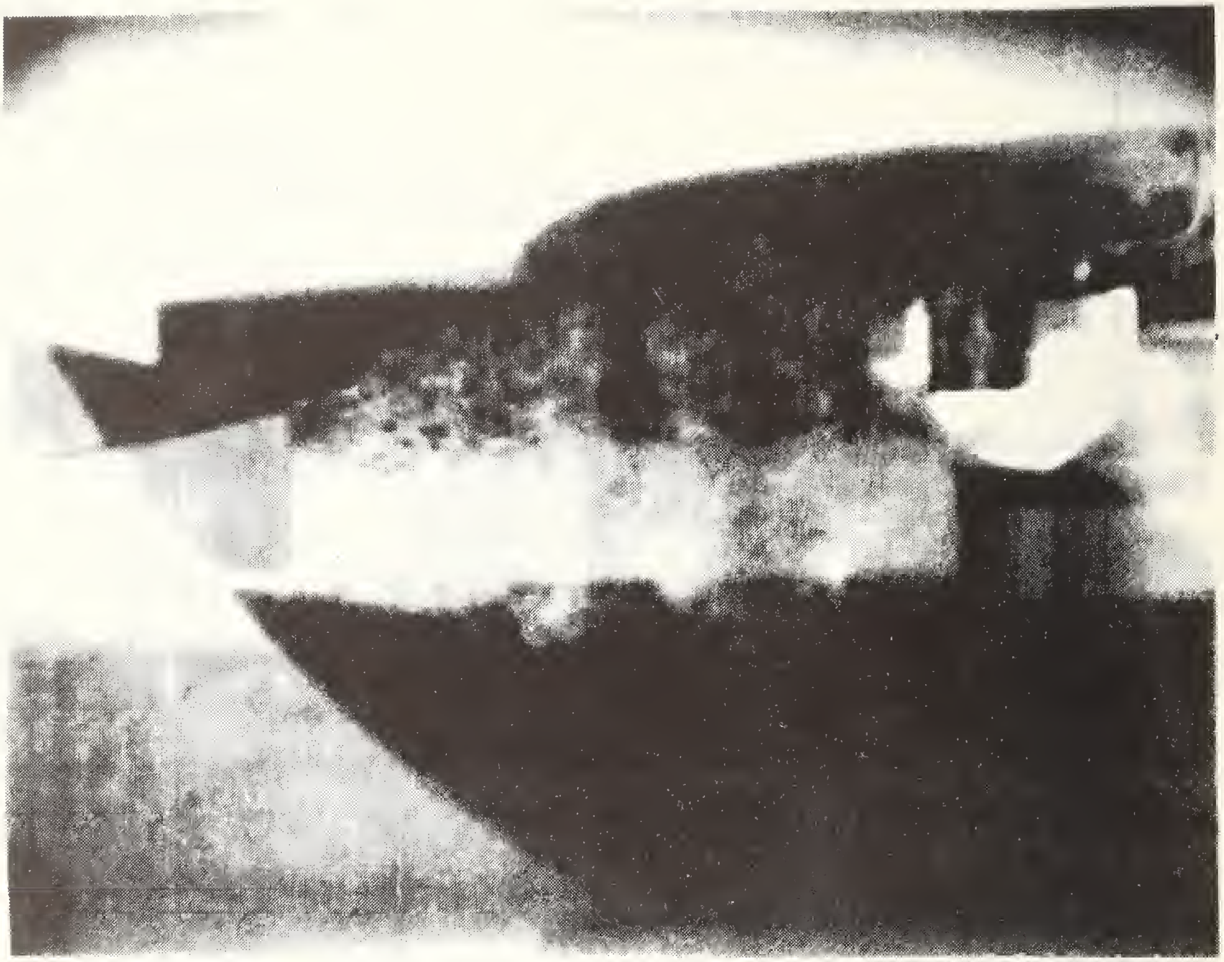

Figure 15. ARS 1 pavement wetting at 40 mph (64 km/h).

2.6. Force Measuring Subsystem

The transducer of the force measuring subsystem is located inboard on the trailer axle, remote from the force it is to measure at the tire-pavement interface. The force at the interface is equivalent to a moment and force acting along vectors in three-dimensional space with respect to the centroid of the transducer. Displacements occurring within the system may alter these vectors. Many effects due to these displacements are minimized by using the tow vehicle and trailer system as a fixture for calibrating the transducer "in situ". Known forces are applied at the tire-pavement interface by means of an air-bearing force plate and calibration box. A locked test wheel is shown on a force plate in figure 16. However, some effects are not accounted for, such as the lateral force at the tire-pavement interface and the yawing orientation of the trailer usually present during skid testing. Displacements of the interface are larger when the tire is "hot" as in a running condition. The tests described here were conducted with the tires at room temperature. However, the tires were previously broken in with approximately 200 miles (320 km) of use, which provides some additional flexibility.

2.6.1. Orientation of the Transducer

The transducer measures a load and traction component of force. To reduce the effects of any cross-axis misalinement, the hitch height was changed until the removal and application of the static vertical load had a minimal effect on the traction channel output. The hitch height found to satisfy this condition is given for each system in table 3. A change of 0.1 in (0.2 cm) in this test is discernible with the on-board tracion instrumentation. This orientation was specified to be maintained during the dynamic measurement program and should be maintained during future trailer use.

2.6.2. Vertical Load Channel Calibration

For wheel transducer vertical calibration, the skid trailer was positioned with the left (test) wheel supported by the IRS air-bearing force plate. Tire inflation pressures were set to 24 psi (165 kPa), and the hitch height was adjusted to the optimum value (sec. 2.6.1).

Force was applied vertically to the trailer body such that the vertical load at the test wheel varied over a range of at least + 230 lbf (1020 N) to - 330 lbf (- 1470 N) from the normal static load (table 1). A force plate test was conducted, using the appropriate on-board amplifier of the system under test for the transducer vertical load signal and an IRS amplifier for the force plate vertical load signal. The outputs were recorded point-by-point, both graphically and numerically.

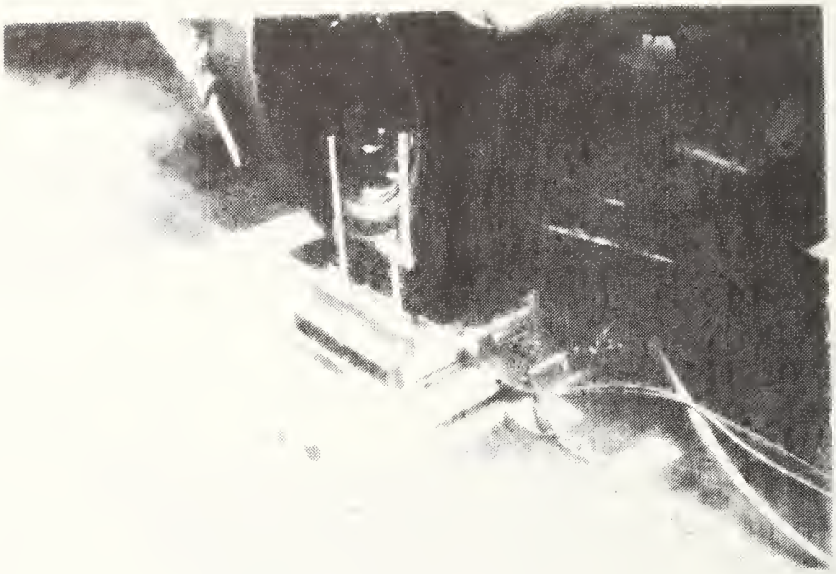

Figure 16. A simulated traction force being applied to a locked test wheel through an air-bearing force plate.

Table 3. Hitch heights for optimum transducer orientation

System	Hitch height[a]
	in[b]
ARS 1	14
ARS 2	12-13/16
ARS 3	14-3/4
IRS	13-7/8

[a] Height is measured from level pavement to center of hitch ball.

[b] 1 in = 2.54 cm.

For all systems, the graphical results verified linear operation of the vertical transducer channel, free from hysteresis. No data point varied by more than 5 lbf (22 N) from the best straight line. Equivalent force values of the on-board calibration signal outputs were calculated from the numerical data by the method of least squares.

2.6.3. Traction Channel Calibration

For traction calibration, the skid trailer was hitched in line with its tow vehicle. The tow vehicle and trailer were put in normal operating condition. Specifically, tire inflation pressures were set, hitch height was adjusted to the optimum value, and crew weights were simulated in the tow vehicle. A 150 to 175 lb (70 to 80 kg) deadweight was placed in each seat. The left (test) wheel of the trailerwas supported by the IRS air-bearing force plate.

Traction force was applied to the test tire through the force plate over the range from zero to 800 lbf (3560 N). A force plate test was conducted, using the appropriate on-board amplifier of the system under test for the transducer traction signal and an IRS amplifier for the force plate traction signal. The outputs were recorded point-by-point, both graphically and numerically.

For all systems, the graphical results verified linear operation of the traction transducer channel. No data point varied by more than 5 lbf (22 N) from the best straight line. For ARS 1, hysteresis between increasing and decreasing traction values resulted in a difference of 10 lbf (44 N) or less. For ARS 2 and ARS 3, the difference was 5 lbf (22 N) or less. The decreasing values were the lower. The IRS transducer traction signal was free of hysteresis. Equivalent force values of the on-board calibration signal outputs were calculated from the numerical data (including both increasing and decreasing values) by the method of least squares.

2.6.4. On-Board Calibration System Equivalent Values

To adjust the gain and offset of the transducer instrumentation, two known values are required for each channel. In each ARS, means were provided to generate one reference output signal for each channel. Zero load served as the other value. A series of signals was available for each channel in the IRS.

The equivalent force values represented by these signals, as calculated from the numerical calibration data, are given in table 4.

Table 4. On-board calibration values

System	Transducer[a] serial number	Force channel	Value
			lbf[b]
ARS 1	80	Vertical	338
		Traction	831
ARS 2	77	Vertical	339
		Traction	910
ARS 3	76	Vertical	337
		Traction	828
IRS	--	Vertical:	
		400	396
		300	296
		200	196
		100	98
		-100	-100
		-200	-199
		-300	-298
		-400	-397
		Traction:	
		100	99
		200	200
		300	301
		400	401
		500	501
		600	600
		700	700
		800	802
		900	903

[a] Installed in the left side of the trailer.

[b] 1 lbf = 4.448N.

2.6.5. Experimental Determination of the Effective Unloading Constant

The vertical force on the test wheel of a towed two-wheeled skid trailer is reduced as the traction force at the tire-pavement interface is increased. This reduction in vertical force can be described in terms of an effective unloading constant [5] which can then be experimentally determined. The reduction in vertical force is given by:

$$F_{WL_z} = F_{WL_{z_o}} \quad F_{WL_x}\left(\frac{H}{L}\right) ,$$

where F_{WL_z} = the total vertical force on the left (test) wheel acting at the tire-pavement interface, $F_{WL_{z_o}}$ = the vertical force on the left wheel acting at the tire-pavement interface when the applied traction is zero, F_{WL_x} = the traction force on the left wheel, and $\frac{H}{L}$ = the effective vertical force unloading constant where H is the hitch height and L is the length from the hitch to the center line of the trailer axle.

There is an uncertainty in the definitions of H and L because of the finite size and shape of the hitch ball.

The determination of the effective vertical force unloading constant for each system was made by using the same set-up of trailer and tow vehicle that was used for traction channel calibration. Vertical and traction outputs were recorded point-by-point, both graphically and numerically, while the traction was varied over the range from 0 to 800 lbf (3560 N). Graphical results confirmed the linear reduction of vertical force with increasing traction for each system. No data point varied by more than 5 lbf (22 N) from the best straight line. Hysteresis differences between rising and falling values did not exceed 5 lbf (22 N). The method of least squares was applied to the numerical results to calculate the effective unloading constant for each system. The values were:

ARS 1; H/L = 0.117,
ARS 2; H/L = 0.108,
ARS 3; H/L = 0.126,
IRS; H/L = 0.125.

2.7. Suspension Subsystem

The measurement of pavement skid resistance at normal traffic speeds is a dynamic test. While data reduction is to occur during a period of steady state friction, the fact is that transient oscillations dominate the entire trace. Trailer motions introduce transient dynamic forces into the system and vice versa. The effective dynamic characteristics of the suspension subsystems need to be measured and reported in analytical form in order that dynamic analyses of the system can be performed for comparison with experimental results and for use in design parameter studies. Further, measurements made by systems of similar or even the same design differ. Consequently, in an attempt to document the dynamic characteristics that might affect measuring performance and account for these differences, the effective spring rates, natural frequencies, Coulomb and viscous friction of the suspension systems were determined. Measurements of certain static displacements were also made as the traction force at the tire-pavement interface was increased to approximately 800 lbf (3560 N) and then decreased to zero.

The dynamic characteristics of the trailer suspensions were obtained while the trailers were connected to a ball hitch on a stationary fixture. The displacements of the trailer under static traction load were measured with the trailer alined and connected to the tow vehicle with the tow vehicle drive wheels and trailer test wheel locked. Consequently, part of the motion occurring under traction force is due to motion between the hitch point and the tow vehicle tire-pavement interface.

Dynamic characteristics were measured for the IRS, ARS 1, and ARS 2, but time permitted static traction tests on ARS 2 only. Its static performance can be compared to previous tests of IRS and other units [6, sec. 2.7][7, sec 2.7].

2.7.1. Trailer Displacements due to Static Traction

a. Displacement of the Test Wheel Hub

The test wheel hub moves back due to static traction loading. This displacement is the resultant of motions throughout the system. Tow vehicle tire and suspension deflections, trailer suspension deflections, and trailer yaw contribute.

The component of hub displacement along the direction of the initial alinement of the ARS 2 tow vehicle and trailer was measured with respect to the floor. The measured displacement is plotted in figure 17. At 800 lbf (3560 N) the ARS hub was displaced 0.32 in (0.81 cm) to the rear. At the same loading, the axle was observed to shift 0.25 in (0.64 cm) to the right, and to yaw to the left by 13 minutes of arc.

b. Displacement of the Test Tire Interface

As the tire of the locked test wheel distorts under static traction loading, the interface of the tire and the force plate moves with respect to the test wheel hub.

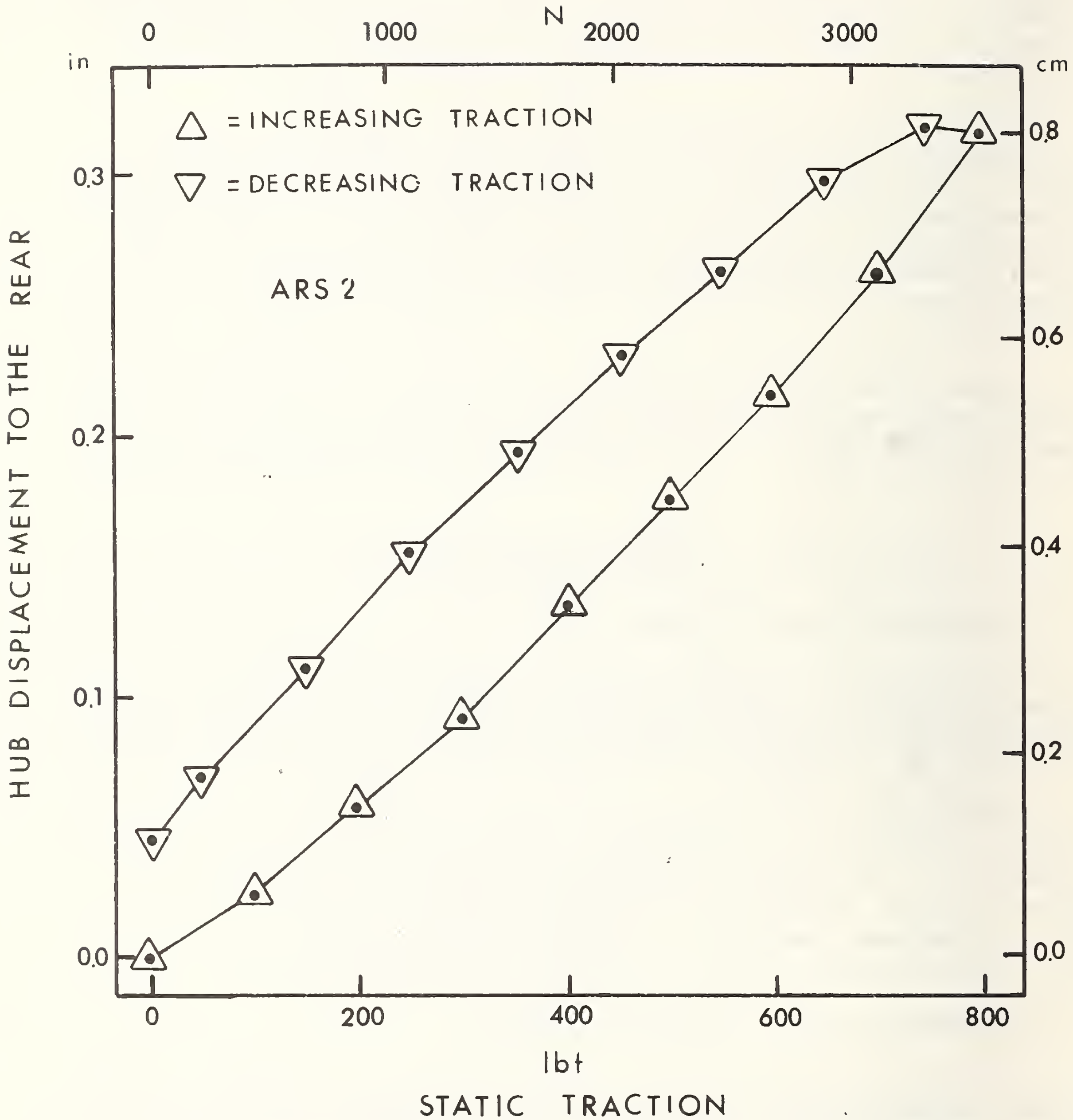

Figure 17. Displacement of the test wheel hub due to static traction.

The rearward displacement of the force plate was measured with respect to the ARS hub. No slippage of the tire on the force plate friction surface was noted. Displacement at 800 lbf (3560 N) was 0.32 in (0.81 cm) to the rear.

c. Displacement of the Trailer Body through Roll Axis Rotation

The body of a two wheeled skid trailer may roll about a longitudinal axis during skid testing. The suspension and tires of the trailer respond to asymmetric forces developed by test wheel traction loading.

Roll displacements of the ARS 2 trailer are shown in figure 18. The displacements were measured with respect to the floor by two sensors applied vertically to the rear corners of the trailer body. Lateral separation of the sensors was 48.5 in (123 cm).

At 800 lbf (3560 N) static traction loading, the ARS trailer body fell 0.10 in (0.25 cm) on the left (test wheel) side and fell 0.02 in (0.05 cm) on the right side, corresponding to a roll axis rotation of 6 minutes of arc. Roll continued to increase as unloading began, peaking at 10 minutes of arc as traction fell to 500 lbf (2220 N). The static friction of the suspension held the ARS body near its peak roll position after the traction loading was removed.

d. Displacement of the Trailer Body through Pitch Axis Rotation

The average of the displacements measured by the two trailer body roll sensors represents the vertical displacement of the center of the trailer body at the rear with respect to the floor. This, combined with the vertical displacement measured by a third sensor at the trailer hitch, yields trailer body pitch.

The pitch displacements for ARS 2 are plotted in figure 19. The longitudinal separation of the front and rear sensors was 156 in (396 cm).

At 800 lbf (3560 N) static traction loading, the ARS trailer body remained unmoved at the hitch and fell 0.09 in (0.23 cm) at the rear corresponding to a pitch axis rotation of 2 minutes of arc. Pitch continued to increase as unloading began, peaking at 3 minutes of arc at 500 lbf (2220 N). The static friction of the suspension held the ARS body near the peak pitch angle after traction loading was removed.

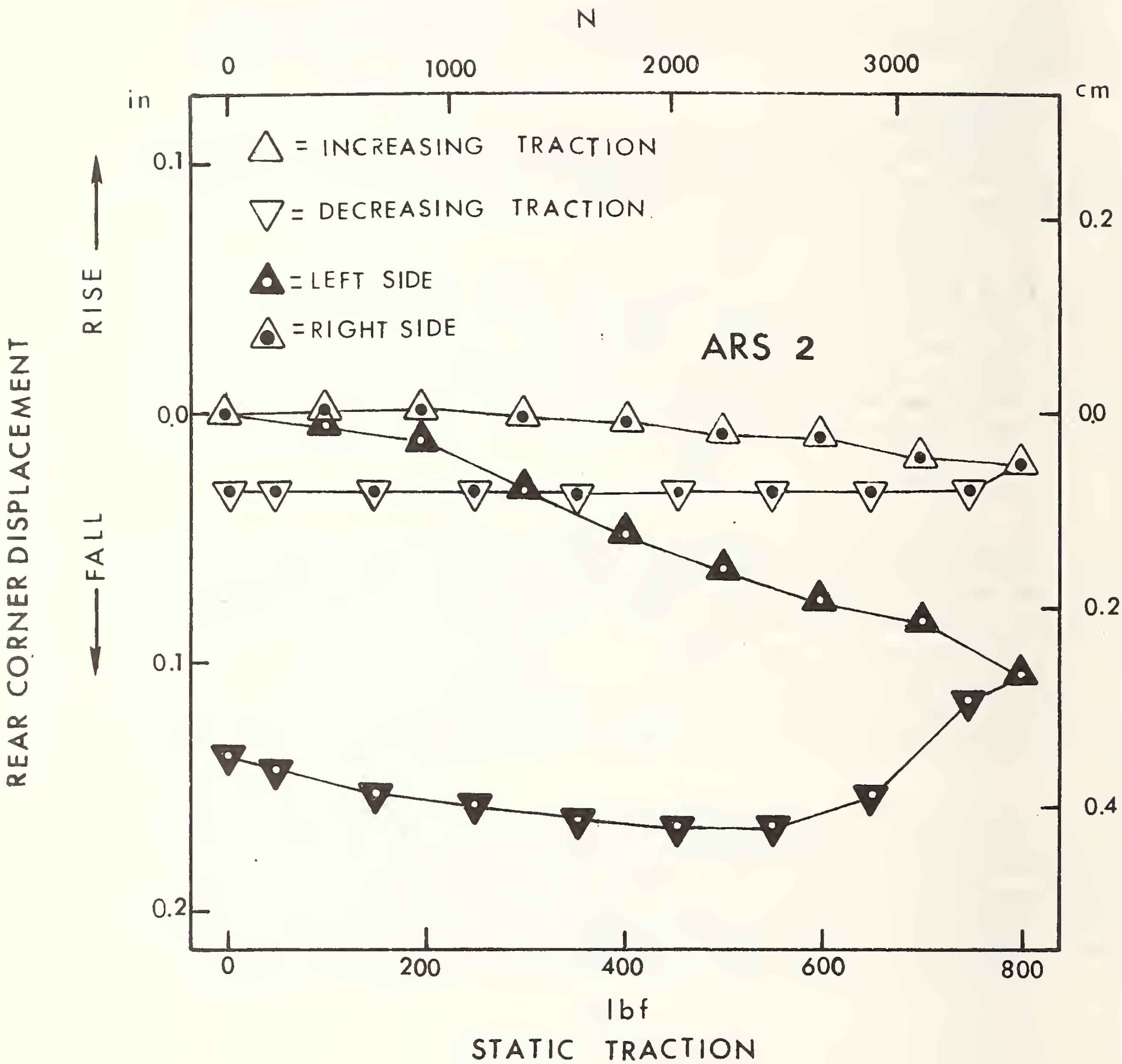

Figure 18. Roll displacement of the trailer body due to static traction.

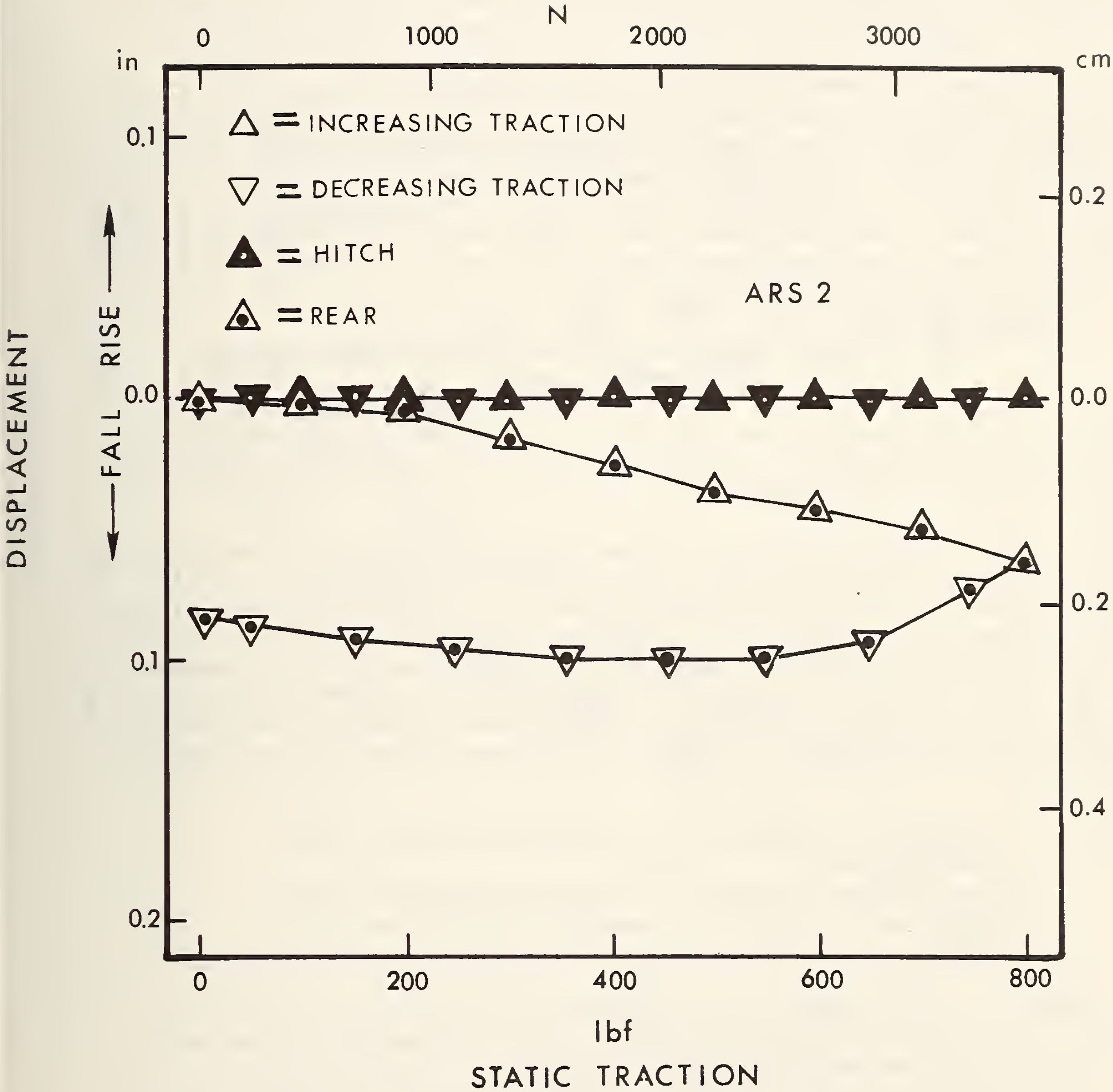

Figure 19. Pitch displacement of the trailer body due to static traction.

e. Displacement of the Trailer Body through Yaw Axis Rotation

Yaw displacements of the ARS 2 trailer are shown in figure 20. The displacements were measured with respect to the floor by two sensors applied horizontally at the hitch and at a rear corner of the trailer body. Longitudinal separation of the sensors was 160 in (406 cm).

At 800 lbf (3560 N) static traction loading, the hitch moved 0.07 in (0.18 cm) to the left and the rear of the body moved 0.39 in (0.99 cm) to the right, corresponding to yaw axis rotation of 10 minutes of arc to the left. Yaw increased slightly as traction was reduced to 750 lbf (3340 N), but diminished to less than 2 minutes of arc when traction was removed. The nearly equal yaw of axle (sec. 2.7.1.a) and body show that the major yaw displacement originated within the right trailer tire rather than the suspension of the ARS.

2.7.2. Suspension Characteristics under Transient Loading

The effective dynamic characteristics of the trailer suspension can be measured in terms of natural frequencies, Coulomb (sliding) friction, spring rates, and damping factors.

There are three natural frequencies of interest. One, arising from flexing of the trailer tires, can be seen under conditions of small variations in vertical load where there is no relative movement within the suspension subsystem. The axle and the body are free to rotate in a vertical plane about the hitch within a small range of displacement of the tires. The other two natural frequencies occur under conditions of larger variations in vertical load where there is relative movement within the suspension subsystem. In this case, there are two degrees of freedom:

a) the body can rotate in a vertical plane about the hitch, while
b) the axle can rotate in a vertical plane about the trailing arm hinge (in designs of the ARS and IRS type).

There is a mode of operation associated with each degree of freedom. Each mode may be produced independently by starting the system oscillation under the proper initial conditions. A dynamic analysis of the trailing arm suspension design of the IRS revealed two dynamic tests which are easy to conduct and which approximate the independent modes such that the measurement of each natural frequency is enhanced. The enhancement is more evident under the condition that the shock absorbers are deactivated.

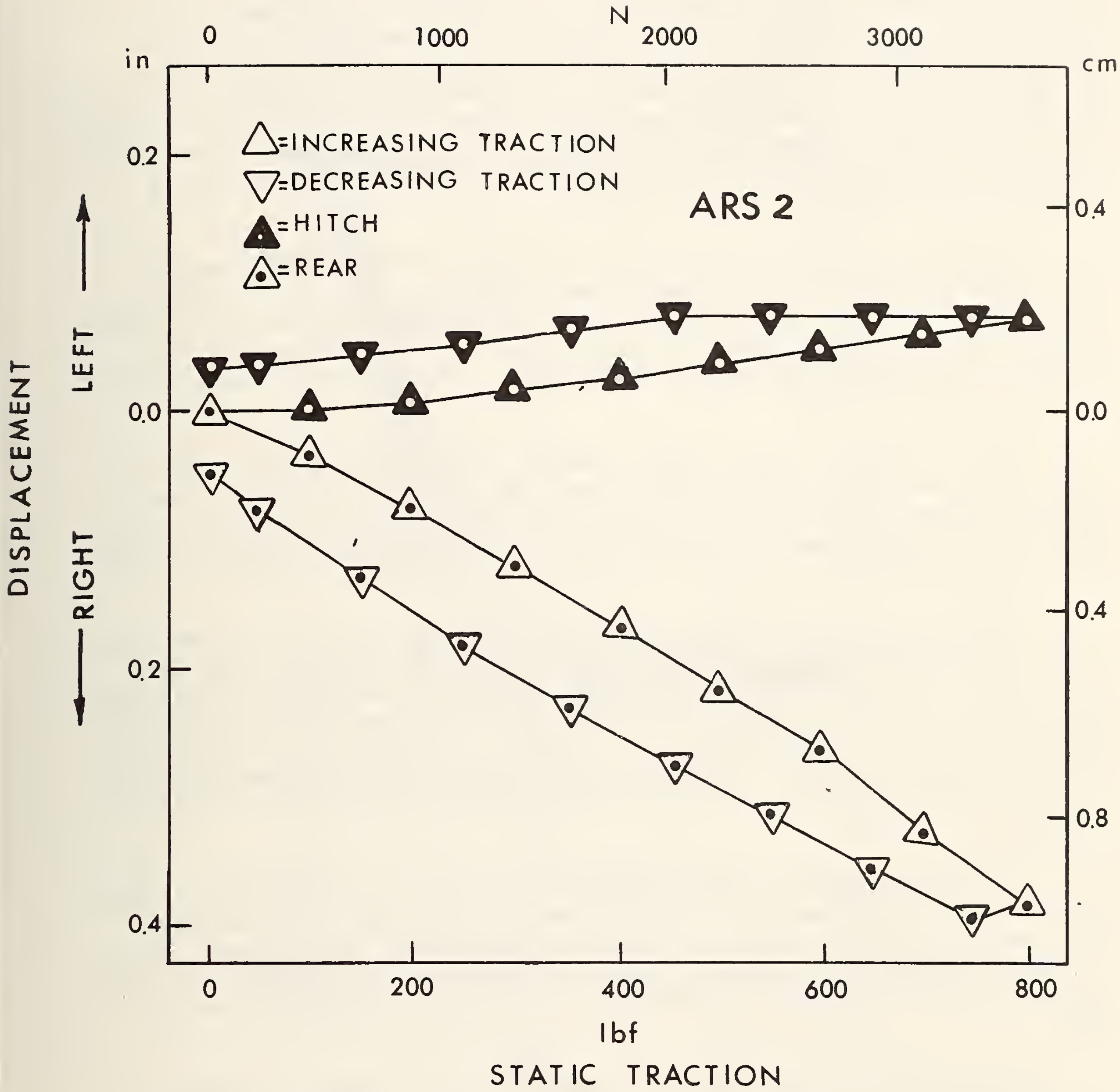

Figure 20. Yaw displacement of the trailer body due to static traction.

The first test is to raise the trailer by a point on the body, allowing it to pivot about the hitch, and to drop it abruptly. With this initial condition, an oscillation occurs where the angular displacements of the body and axle trailing arms are out of phase. In this mode, the vibration which has the lower frequency is enhanced. The second test is to raise the trailer at the axle and drop it abruptly. With this initial condition, an oscillation occurs where the angular displacements of the body and axle trailing arms are in phase. In this mode, the higher frequency is enhanced. After the transient decays such that there is no further relative movement in the suspension, the oscillation of the trailer on the tires persists because there is little damping in the tires.

Trailer response to these tests was measured by an air-bearing force plate under the left trailer wheel and by linear potentiometer displacement sensors operating between the pavement surface, the trailer axle, and the trailer body. The force and displacement signals were plotted versus time, using X - Y recorders. Tests were conducted on ARS 1, ARS 2, and the IRS.

The frequencies found using tests of the first type were 3 Hz for both ARS 1 and ARS 2, and 2 Hz for the IRS. The second type of test gave frequencies of 13 Hz for ARS 1, 12 Hz for ARS 2, and 13 Hz for the IRS. For all systems, a value of about 4 Hz was observed for the small amplitude tire oscillation.

Temporary disconnection of the shock absorbers, which are the major source of viscous damping, aids in determining the amount of Coulomb friction in the suspension. With viscous damping eliminated, the amplitude of the vertical force transient exhibits a linear decay which is a measure of the Coulomb friction. The value of Coulomb friction in the left side of the trailer suspension was determined by this method to be 5 lbf (22 N) for ARS 1, 7 lbf (31 N) for ARS 2, and 10 lbf (44 N) for the IRS.

The change in force and displacement from their equilibrium values is a measure of spring rate. Simultaneously recorded force and displacement data gave values for the effective spring rate between the trailer body and the pavement surface of 1500 lbf/in (260 kN/m) for ARS 1, 1000 lbf/in (175 kN/m) for ARS 2, and 260 lbf/in (45 kN/m) for the IRS.

When the shock absorbers are connected, the transient is damped by both Coulomb and viscous friction, and the decay is non-linear. A non-dimensional family of curves which can be used to estimate the amount of damping in systems represented by a second degree differential equation is shown in figure 21 [8]. The recorded transient decay can be compared to the curves to estimate the effective damping factor, ζ. The curves

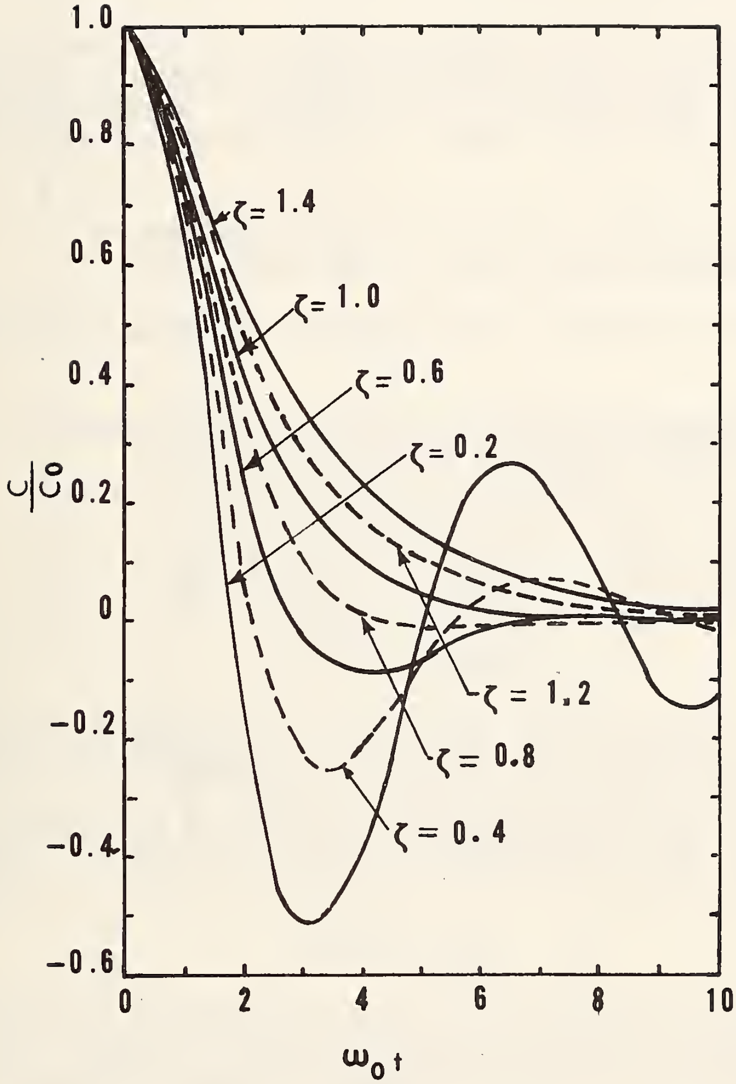

Figure 21. Effect of different damping factors on second-order linear systems.

also indicate that a system with a damping factor of 0.8 nears equilibrium before a system with a damping factor of either 0.6 or 1.0. A more optimum value (not shown) is 0.7. A measuring system which is subject to disturbing transients will measure the near-equilibrium value more often with a damping factor of 0.7.

The effective damping factors observed for ARS 1 and ARS 2 were 0.4. The IRS, which has been provided with extra shock absorbers, exhibited an effective damping factor of 0.6.

There is evidence that the shock absorbers used provide effective damping in one direction only. From figure 22, it can be seen that upward deflection of the trailer axle in undamped. It may be possible to increase the damping factor simply by installation of double-acting shock absorbers.

3. THE DYNAMIC SKID RESISTANCE MEASUREMENT OF SELECTED SURFACES AND ARS-IRS CORRELATIONS

The purpose of the dynamic skid resistance measurement test program was:

a) to measure selected surfaces at the EFTC, and to compare the results with those from a previous program,
b) to measure the consistency and precision in the measure ments of ARS 1, ARS 2, ARS 3 and the IRS, and
c) to interrelate and correlate the degree of match in the measurements between the IRS and the three ARS.

3.1. Surfaces Selected

The surfaces selected were a 100 ft (30.5 m) longitudinal section of lanes 1 through 7 of surfaces identified as 2 and 3 at the EFTC. So that the reduced data would all be within the same 100 ft (30.5 m) section at all test speeds, pylons were set out where the operator would start the automatic skid test sequence for each test speed. These are the same sections of surfaces 2 and 3 measured in a previous program [6].

3.2. Tests Planned

The test program is designed to yield the following information:

a) skid resistance, SN, of a surface as a function of test speed,
b) skid resistance - test speed gradient, Θ, as a function of test speed,
c) skid resistance - test tire inflation pressure gradient at 40 mph (64 km/h),

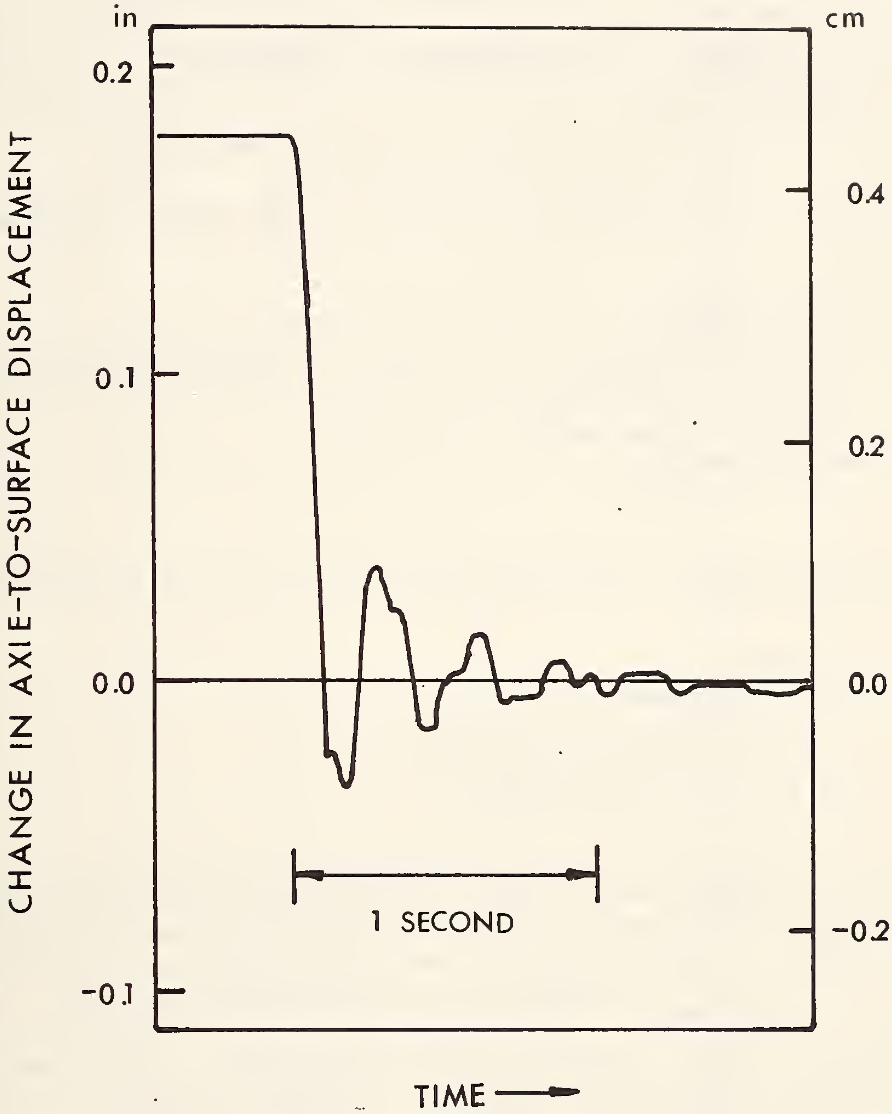

Figure 22. ARS 1 axle-to-surface transient response. Damping is evident only on downward motion.

d) skid resistance - water depth gradient at 40 mph (64 km/h),
e) variability in SN with choice of test tire,
f) variability in SN with choice of lane within the surface, and
g) variation in SN with drying time between tests.

The test plan includes the control of the following operating variables:

a) hitch height,
b) inflation pressure of the tow vehicle rear tires,
c) inflation pressure of the IRS air spring shock absorbers,
d) surface cleanliness,
e) surface minimum degree-of-dryness,
f) test speed, and
g) water flow rate.

The test plan includes the measurement of the following uncontrolled variables:

a) weather,
b) surface temperature,
c) test tire inflation pressure,
d) test tire lock-up position, and
e) IRS test tire tread depth.

The planned test program is contained in table 5. It consists of two main exercises. In the first, occupying time periods 1 through 6, each skid resistance measuring system measures the two surfaces at three nominal speeds. Variation of $\pm$ 2 mph ($\pm$ 3.2 km/h) about the nominal speeds are introduced to measure the local speed gradients. The second exercise, time periods 7 and 8, re-measures the two surfaces to detect variation of SN over the term of the test program. Also, variations are introduced about the normal test tire inflation pressure and about the normal pavement wetting flow rates to determine the effect of changes in these variables on the SN measurement.

3.3. The Test Matrix

The test program consists of a number of measurements of the steady state friction force on a locked test wheel as it is dragged over a wetted pavement surface under known load and at a constant speed. The test is used by others to measure the difference in skid resistance between various designs of tires. The test is used by a majority of state highway departments to inventory and rank the condition of the highways according to skid resistance. In the latter case, a standardized, but special purpose, full-scale automotive tire is mounted on the

Table 5. Test plan sequence

Time Period #1
First Day

Measurement System IRS	1	2	3	Surface	Lane	Test Speed	Tire
x				2	2	40	A1
	x			2	3	40	B1
x				2	4	42	A1
	x			2	5	42	B1
x				2	1	38	A1
	x			2	2	38	B1
		x		3	2	40	A2
			x	3	3	40	B4
		x		3	4	42	A2
			x	3	5	42	B4
		x		3	1	38	A2
			x	3	2	38	B4
	x			2	4	38	D1
x				2	3	38	C1
	x			2	7	42	D1
x				2	6	42	C1
	x			2	5	40	D1
x				2	4	40	C1
			x	3	4	38	D4
		x		3	3	38	C2
			x	3	7	42	D4
		x		3	6	42	C2
			x	3	5	40	D4
		x		3	4	40	C2
x				2	6	40	E1
	x			2	7	40	F1
x				2	5	38	E1
	x			2	2	42	F1
x				2	1	42	E1
	x			2	6	38	F1
		x		3	6	40	E2
			x	3	7	40	F4
		x		3	5	38	E2
			x	3	2	42	F4
		x		3	1	42	E2
			x	3	6	38	F4
x				2	7	38	G1
x				2	3	42	G1
x				2	1	40	G1
		x		3	7	38	G2
		x		3	3	42	G2
		x		3	1	40	G2

Table 5. Test plan sequence - continued

Time Period #1
Second Day

Measurement System				Surface	Lane	Test Speed	Tire
1	IRS	3	2				
x				2	2	40	A1
	x			2	3	40	B1
x				2	4	42	A1
	x			2	5	42	B1
x				2	1	38	A1
	x			2	2	38	B1
		x		3	2	40	A4
			x	3	3	40	B2
		x		3	4	42	A4
			x	3	5	42	B2
		x		3	1	38	A4
			x	3	2	38	B2
	x			2	4	38	D1
x				2	3	38	C1
	x			2	7	42	D1
x				2	6	42	C1
	x			2	5	40	D1
x				2	4	40	C1
			x	3	4	38	D2
		x		3	3	38	C4
			x	3	7	42	D2
		x		3	6	42	C4
			x	3	5	40	D2
		x		3	4	40	C4
x				2	6	40	E1
	x			2	7	40	F1
x				2	5	38	E1
	x			2	2	42	F1
x				2	1	42	E1
	x			2	6	38	F1
		x		3	6	40	E4
			x	3	7	40	F2
		x		3	5	38	E4
			x	3	2	42	F2
		x		3	1	42	E4
			x	3	6	38	F2
x				2	7	38	G1
x				2	3	42	G1
x				2	1	40	G1
		x		3	7	38	G4
		x		3	3	42	G4
		x		3	1	40	G4

Table 5. Test plan sequence - continued

Time Period #2
First Day

Measurement System IRS	1	2	3	Surface	Lane	Test Speed	Tire
x				3	2	40	A4
	x			3	3	40	B2
x				3	4	42	A4
	x			3	5	42	B2
x				3	1	38	A4
	x			3	2	38	B2
		x		2	2	40	A3
			x	2	3	40	B3
		x		2	4	42	A3
			x	2	5	42	B3
		x		2	1	38	A3
			x	2	2	38	B3
	x			3	4	38	D2
x				3	3	38	C4
	x			3	7	42	D2
x				3	6	42	C4
	x			3	5	40	D2
x				3	4	40	C4
			x	2	4	38	D3
		x		2	3	38	C3
			x	2	7	42	D3
		x		2	6	42	C3
			x	2	5	40	D3
		x		2	4	40	C3
x				3	6	40	E4
	x			3	7	40	F2
x				3	5	38	E4
	x			3	2	42	F2
x				3	1	42	E4
	x			3	6	38	F2
		x		2	6	40	E3
			x	2	7	40	F3
		x		2	5	38	E3
			x	2	2	42	F3
		x		2	1	42	E3
			x	2	6	38	F3
x				3	7	38	G4
x				3	3	42	G4
x				3	1	40	G4
		x		2	7	38	G3
		x		2	3	42	G3
		x		2	1	40	G3

Table 5. Test plan sequence - continued

Time Period #2
Second Day

Measurement System				Surface	Lane	Test Speed	Tire
1	IRS	3	2				
x				3	2	40	A2
	x			3	3	40	B4
x				3	4	42	A2
	x			3	5	42	B4
x				3	1	38	A2
	x			3	2	38	B4
		x		2	2	40	A3
			x	2	3	40	B3
		x		2	4	42	A3
			x	2	5	42	B3
		x		2	1	38	A3
			x	2	2	38	B3
	x			3	4	38	D4
x				3	3	38	C2
	x			3	7	42	D4
x				3	6	42	C2
	x			3	5	40	D4
x				3	4	40	C2
			x	2	4	38	D3
		x		2	3	38	C3
			x	2	7	42	D3
		x		2	6	42	C3
			x	2	5	40	D3
		x		2	4	40	C3
x				3	6	40	E2
	x			3	7	40	F4
x				3	5	38	E2
	x			3	2	42	F4
x				3	1	42	E2
	x			3	6	38	F4
		x		2	6	40	E3
			x	2	7	40	F3
		x		2	5	38	E3
			x	2	2	42	F3
		x		2	1	42	E3
			x	2	6	38	F3
x				3	7	38	G2
x				3	3	42	G2
x				3	1	40	G2
		x		2	7	38	G3
		x		2	3	42	G3
		x		2	1	40	G3

Table 5. Test plan sequence - continued

Time Period #3
First Day

Measurement System				Surface	Lane	Test Speed	Tire
IRS	1	2	3				
x				2	2	20	A1
	x			2	3	20	B1
x				2	4	22	A1
	x			2	5	22	B1
x				2	1	18	A1
	x			2	2	18	B1
		x		3	2	20	A2
			x	3	3	20	B4
		x		3	4	18	A2
			x	3	5	22	B4
		x		3	1	18	A2
			x	3	2	18	B4
	x			2	4	18	D1
x				2	3	18	C1
	x			2	7	22	D1
x				2	6	22	C1
	x			2	5	20	D1
x				2	4	20	C1
			x	3	4	18	D4
		x		3	3	18	C2
			x	3	7	22	D4
		x		3	6	22	C2
			x	3	5	20	D4
		x		3	4	20	C2
x				2	6	20	E1
	x			2	7	20	F1
x				2	5	18	E1
	x			2	2	22	F1
x				2	1	22	E1
	x			2	6	18	F1
		x		3	6	20	E2
			x	3	7	20	F4
		x		3	5	18	E2
			x	3	2	22	F4
		x		3	1	22	E2
			x	3	6	18	F4
x				2	7	18	G1
x				2	3	22	G1
x				2	1	20	G1
		x		3	7	18	G2
		x		3	3	22	G2
		x		3	1	20	G2

Table 5. Test plan sequence - continued

Time Period #3
Second Day

Measurement System				Surface	Lane	Test Speed	Tire
1	IRS	3	2				
x				2	2	20	A1
	x			2	3	20	B1
x				2	4	22	A1
	x			2	5	22	B1
x				2	1	18	A1
	x			2	2	18	B1
		x		3	2	20	A4
			x	3	3	20	B2
		x		3	4	22	A4
			x	3	5	22	B2
		x		3	1	18	A4
			x	3	2	18	B2
	x			2	4	18	D1
x				2	3	18	C1
	x			2	7	22	D1
x				2	6	22	C1
	x			2	5	20	D1
x				2	4	20	C1
			x	3	4	18	D2
		x		3	3	18	C4
			x	3	7	22	D2
		x		3	6	22	C4
			x	3	5	20	D2
		x		3	4	20	C4
x				2	6	20	E1
	x			2	7	20	F1
x				2	5	18	E1
	x			2	2	22	F1
x				2	1	22	E1
	x			2	6	18	F1
		x		3	6	20	E4
			x	3	7	20	F2
		x		3	5	18	E4
			x	3	2	22	F2
		x		3	1	22	E4
			x	3	6	18	F2
x				2	7	18	G1
x				2	3	22	G1
x				2	1	20	G1
		x		3	7	18	G4
		x		3	3	22	G4
		x		3	1	20	G4

Table 5. Test plan sequence - continued

Time Period #4
First Day

Measurement System IRS	1	2	3	Surface	Lane	Test Speed	Tire
x				3	2	20	A4
	x			3	3	20	B2
x				3	4	22	A4
	x			3	5	22	B2
x				3	1	18	A4
	x			3	2	18	B2
		x		2	2	20	A3
			x	2	3	20	B3
		x		2	4	22	A3
			x	2	5	22	B3
		x		2	1	18	A3
			x	2	2	18	B3
	x			3	4	18	D2
x				3	3	18	C4
	x			3	7	22	D2
x				3	6	22	C4
	x			3	5	20	D2
x				3	4	20	C4
			x	2	4	18	D3
		x		2	3	18	C3
			x	2	7	22	D3
		x		2	6	22	C3
			x	2	5	20	D3
		x		2	4	20	C3
x				3	6	20	E4
	x			3	7	20	F2
x				3	5	18	E4
	x			3	2	22	F2
x				3	1	22	E4
	x			3	6	18	F2
		x		2	6	20	E3
			x	2	7	20	F3
		x		2	5	18	E3
			x	2	2	22	F3
		x		2	1	22	E3
			x	2	6	18	F3
x				3	7	18	G4
x				3	3	22	G4
x				3	1	20	G4
		x		2	7	18	G3
		x		2	3	22	G3
		x		2	1	20	G3

Table 5. Test plan sequence - continued

Time Period #4
Second Day

Measurement System				Surface	Lane	Test Speed	Tire
1	IRS	3	2				
x				3	2	20	A2
	x			3	3	20	B4
x				3	4	22	A2
	x			3	5	22	B4
x				3	1	18	A2
	x			3	2	18	B4
		x		2	2	20	A3
			x	2	3	20	B3
		x		2	4	22	A3
			x	2	5	22	B3
		x		2	1	18	A3
			x	2	2	18	B3
	x			3	4	18	D4
x				3	3	18	C2
	x			3	7	22	D4
x				3	6	22	C2
	x			3	5	20	D4
x				3	4	20	C2
			x	2	4	18	D3
		x		2	3	18	C3
			x	2	7	22	D3
		x		2	6	22	C3
			x	2	5	20	D3
		x		2	4	20	C3
x				3	6	20	E2
	x			3	7	20	F4
x				3	5	18	E2
	x			3	2	22	F4
x				3	1	22	E2
	x			3	6	18	F4
		x		2	6	20	E3
			x	2	7	20	F3
		x		2	5	18	E3
			x	2	2	22	F3
		x		2	1	22	E3
			x	2	6	18	F3
x				3	7	18	G2
x				3	3	22	G2
x				3	1	20	G2
		x		2	7	18	G3
		x		2	3	22	G3
		x		2	1	20	G3

Table 5. Test plan sequence - continued

Time Period #5
First Day

Measurement System				Surface	Lane	Test Speed	Tire
IRS	1	2	3				
x				2	2	60	A1
	x			2	3	60	B1
x				2	4	62	A1
	x			2	5	62	B1
x				2	1	58	A1
	x			2	2	58	B1
		x		3	2	60	A2
			x	3	3	60	B4
		x		3	4	62	A2
			x	3	5	62	B4
		x		3	1	58	A2
			x	3	2	58	B4
	x			2	4	58	D1
x				2	3	58	C1
	x			2	7	62	D1
x				2	6	62	C1
	x			2	5	60	D1
x				2	4	60	C1
			x	3	4	58	D4
		x		3	3	58	C2
			x	3	7	62	D4
		x		3	6	62	C2
			x	3	5	60	D4
		x		3	4	60	C2
x				2	6	60	E1
	x			2	7	60	F1
x				2	5	58	E1
	x			2	2	62	F1
x				2	1	62	E1
	x			2	6	58	F1
		x		3	6	60	E2
			x	3	7	60	F4
		x		3	5	58	E2
			x	3	2	62	F4
		x		3	1	62	E2
			x	3	6	58	F4
x				2	7	58	G1
x				2	3	62	G1
x				2	1	60	G1
		x		3	7	58	G2
		x		3	3	62	G2
		x		3	1	60	G2

Table 5. Test plan sequence - continued

Time Period #5
Second Day

Measurement System 1	IRS	3	2	Surface	Lane	Test Speed	Tire
x				2	2	60	A1
	x			2	3	60	B1
x				2	4	62	A1
	x			2	5	62	B1
x				2	1	58	A1
	x			2	2	58	B1
		x		3	2	60	A4
			x	3	3	60	B2
		x		3	4	62	A4
			x	3	5	62	B2
		x		3	1	58	A4
			x	3	2	58	B2
	x			2	4	58	D1
x				2	3	58	C1
	x			2	7	62	D1
x				2	6	62	C1
	x			2	5	60	D1
x				2	4	60	C1
			x	3	4	58	D2
		x		3	3	58	C4
			x	3	7	62	D2
		x		3	6	62	C4
			x	3	5	60	D2
		x		3	4	60	C4
x				2	6	60	E1
	x			2	7	60	F1
x				2	5	58	E1
	x			2	2	62	F1
x				2	1	62	E1
	x			2	6	58	F1
		x		3	6	60	E4
			x	3	7	60	F2
		x		3	5	58	E4
			x	3	2	62	F2
		x		3	1	62	E4
			x	3	6	58	F2
x				2	7	58	G1
x				2	3	62	G1
x				2	1	60	G1
		x		3	7	58	G4
		x		3	3	62	G4
		x		3	1	60	G4

Table 5. Test plan sequence - continued

Time Period #6
First Day

Measurement System IRS	1	2	3	Surface	Lane	Test Speed	Tire
x				3	2	60	A4
	x			3	3	60	B2
x				3	4	62	A4
	x			3	5	62	B2
x				3	1	58	A4
	x			3	2	58	B2
		x		2	2	60	A3
			x	2	3	60	B3
		x		2	4	62	A3
			x	2	5	62	B3
		x		2	1	58	A3
			x	2	2	58	B3
	x			3	4	58	D2
x				3	3	58	C4
	x			3	7	62	D2
x				3	6	62	C4
	x			3	5	60	D2
x				3	4	60	C4
			x	2	4	58	D3
		x		2	3	58	C3
			x	2	7	62	D3
		x		2	6	62	C3
			x	2	5	60	D3
		x		2	4	60	C3
x				3	6	60	E4
	x			3	7	60	F2
x				3	5	58	E4
	x			3	2	62	F2
x				3	1	62	E4
	x			3	6	58	F2
		x		2	6	60	E3
			x	2	7	60	F3
		x		2	5	58	E3
			x	2	2	62	F3
		x		2	1	62	E3
			x	2	6	58	F3
x				3	7	58	G4
x				3	3	62	G4
x				3	1	60	G4
		x		2	7	58	G3
		x		2	3	62	G3
		x		2	1	60	G3

Table 5. Test plan sequence - continued

Time Period #6
Second Day

Measurement System 1	IRS	3	2	Surface	Lane	Test Speed	Tire
x				3	2	60	A2
	x			3	3	60	B4
x				3	4	62	A2
	x			3	5	62	B4
x				3	1	58	A2
	x			3	2	58	B4
		x		2	2	60	A3
			x	2	3	60	B3
		x		2	4	62	A3
			x	2	5	62	B3
		x		2	1	58	A3
			x	2	2	58	B3
	x			3	4	58	D4
x				3	3	58	C2
	x			3	7	62	D4
x				3	6	62	C2
	x			3	5	60	D4
x				3	4	60	C2
			x	2	4	58	D3
		x		2	3	58	C3
			x	2	7	62	D3
		x		2	6	62	C3
			x	2	5	60	D3
		x		2	4	60	C3
x				3	6	60	E2
	x			3	7	60	F4
x				3	5	58	E2
	x			3	2	62	F4
x				3	1	62	E2
	x			3	6	58	F4
		x		2	6	60	E3
			x	2	7	60	F3
		x		2	5	58	E3
			x	2	2	62	F3
		x		2	1	62	E3
			x	2	6	58	F3
x				3	7	58	G2
x				3	3	62	G2
x				3	1	60	G2
		x		2	7	58	G3
		x		2	3	62	G3
		x		2	1	60	G3

Table 5. Test plan sequence - continued

Time Period #7
First Day

Measurement System IRS	1	2	3	Surface	Lane	Test Speed	Δ15% Water Flow Rate	Tire Inflation Pressure	Tire
x				2	1	40	-	24	A1
	x			2	2	40	-	24	B1
x				2	4	40	+	24	A1
	x			2	5	40	+	24	B1
		x		3	1	40	-	24	A2
			x	3	2	40	-	24	B4
		x		3	4	40	+	24	A2
			x	3	5	40	+	24	B4
x				2	1	40	Normal	20	A1
	x			2	2	40	Normal	20	B1
x				2	4	40	Normal	28	A1
	x			2	5	40	Normal	28	B1
		x		3	1	40	Normal	20	A2
			x	3	2	40	Normal	20	B4
		x		3	4	40	Normal	28	A2
			x	3	5	40	Normal	28	B4
x				2	3	40	-	24	C1
	x			2	4	40	-	24	D1
x				2	6	40	+	24	C1
	x			2	7	40	+	24	D1
		x		3	3	40	-	24	C2
			x	3	4	40	-	24	D4
		x		3	6	40	+	24	C2
			x	3	7	40	+	24	D4
x				2	3	40	Normal	20	C1
	x			2	4	40	Normal	20	D1
x				2	6	40	Normal	28	C1
	x			2	7	40	Normal	28	D1
		x		3	3	40	Normal	20	C2
			x	3	4	40	Normal	20	D4
		x		3	6	40	Normal	28	C2
			x	3	7	40	Normal	28	D4
x				2	5	40	-	24	E1
	x			2	2	40	+	24	F1
x				2	1	40	+	24	E1
	x			2	6	40	-	24	F1
		x		3	5	40	-	24	E2
			x	3	2	40	+	24	F4
		x		3	1	40	+	24	E2
			x	3	6	40	-	24	F4

Table 5. Test plan sequence - continued

Time Period #7
Second Day

Measurement System IRS	1	2	3	Surface	Lane	Test Speed	Δ15% Water Flow Rate	Tire Inflation Pressure	Tire
x				2	5	40	Normal	20	E1
	x			2	2	40	Normal	28	F1
x				2	1	40	Normal	28	E1
	x			2	6	40	Normal	20	F1
		x		3	5	40	Normal	20	E2
			x	3	2	40	Normal	28	F4
		x		3	1	40	Normal	28	E2
			x	3	6	40	Normal	20	F4
x				2	7	40	-	Normal	G1
x				2	3	40	+	Normal	G1
		x		3	7	40	-	Normal	G2
		x		3	3	40	+	Normal	G2
x				2	7	40	Normal	20	G1
x				2	3	40	Normal	28	G1
		x		3	7	40	Normal	20	G2
		x		3	3	40	Normal	28	G2
			x	3	7	40	-	Normal	G4
			x	3	3	40	+	Normal	G4
	x			2	7	40	-	Normal	G1
	x			2	3	40	+	Normal	G1
			x	3	7	40	Normal	20	G4
			x	3	3	40	Normal	28	G4
	x			2	7	40	Normal	20	G1
	x			2	3	40	Normal	28	G1
	x			2	1	40	-	Normal	A1
x				2	2	40	-	Normal	B1
	x			2	4	40	+	Normal	A1
x				2	5	40	+	Normal	B1
			x	3	1	40	-	Normal	A4
		x		3	2	40	-	Normal	B2
			x	3	4	40	+	Normal	A4
		x		3	5	40	+	Normal	B2
	x			2	1	40	Normal	20	A1
x				2	2	40	Normal	20	B1
	x			2	4	40	Normal	28	A1
x				2	5	40	Normal	28	B1
			x	3	1	40	Normal	20	A4
		x		3	2	40	Normal	20	B2
			x	3	4	40	Normal	28	A4
		x		3	5	40	Normal	28	B2

Table 5. Test plan sequence - continued

Time Period #7
Third Day

Measurement System IRS	1	2	3	Surface	Lane	Test Speed	Δ15% Water Flow Rate	Tire Inflation Pressure	Tire
	x			2	3	40	-	Normal	C1
x				2	4	40	-	Normal	D1
	x			2	6	40	+	Normal	C1
x				2	7	40	+	Normal	D1
			x	3	3	40	-	Normal	C4
		x		3	4	40	-	Normal	D2
			x	3	6	40	+	Normal	C4
		x		3	7	40	+	Normal	D2
	x			2	3	40	Normal	20	C1
x				2	4	40	Normal	20	D1
	x			2	6	40	Normal	28	C1
x				2	7	40	Normal	28	D1
			x	3	3	40	Normal	20	C4
		x		3	4	40	Normal	20	D2
			x	3	6	40	Normal	28	C4
		x		3	7	40	Normal	28	D2
	x			2	5	40	-	Normal	E1
x				2	2	40	+	Normal	F1
	x			2	1	40	+	Normal	E1
x				2	6	40	-	Normal	F1
			x	3	5	40	-	Normal	E4
		x		3	2	40	+	Normal	F2
			x	3	1	40	+	Normal	E4
		x		3	6	40	-	Normal	F2
	x			2	5	40	Normal	20	E1
x				2	2	40	Normal	28	F1
	x			2	1	40	Normal	28	E1
x				2	6	40	Normal	20	F1
			x	3	5	40	Normal	20	E4
		x		3	2	40	Normal	28	F2
			x	3	1	40	Normal	28	E4
		x		3	6	40	Normal	20	F2

Table 5. Test plan sequence - continued

Time Period #8
First Day

Measurement System IRS	1	2	3	Surface	Lane	Test Speed	Δ15% Water Flow Rate	Tire Inflation Pressure	Tire
x				3	1	40	-	Normal	A4
	x			3	2	40	-	Normal	B2
x				3	4	40	+	Normal	A4
	x			3	5	40	+	Normal	B2
		x		2	1	40	-	Normal	A3
			x	2	2	40	-	Normal	B3
		x		2	4	40	+	Normal	A3
			x	2	5	40	+	Normal	B3
x				3	1	40	Normal	20	A4
	x			3	2	40	Normal	20	B2
x				3	4	40	Normal	28	A4
	x			3	5	40	Normal	28	B2
		x		2	1	40	Normal	20	A3
			x	2	2	40	Normal	20	B3
		x		2	4	40	Normal	28	A3
			x	2	5	40	Normal	28	B3
x				3	3	40	-	Normal	C4
	x			3	4	40	-	Normal	D2
x				3	6	40	+	Normal	C4
	x			3	7	40	+	Normal	D2
		x		2	3	40	-	Normal	C3
			x	2	4	40	-	Normal	D3
		x		2	6	40	+	Normal	C3
			x	2	7	40	+	Normal	D3
x				3	3	40	Normal	20	C4
	x			3	4	40	Normal	20	D2
x				3	6	40	Normal	28	C4
	x			3	7	40	Normal	28	D2
		x		2	3	40	Normal	20	C3
			x	2	4	40	Normal	20	D3
		x		2	6	40	Normal	28	C3
			x	2	7	40	Normal	28	D3
x				3	5	40	-	Normal	E4
	x			3	2	40	+	Normal	F2
x				3	1	40	+	Normal	E4
	x			3	6	40	-	Normal	F2
		x		2	5	40	-	Normal	E3
			x	2	2	40	+	Normal	F3
		x		2	1	40	+	Normal	E3
			x	2	6	40	-	Normal	F3

Table 5. Test plan sequence - continued

Time Period #8
Second Day

Measurement System				Surface	Lane	Test Speed	Δ15% Water Flow Rate	Tire Inflation Pressure	Tire
IRS	1	2	3						
x				3	5	40	Normal	20	E4
	x			3	2	40	Normal	28	F2
x				3	1	40	Normal	28	E4
	x			3	6	40	Normal	20	F2
		x		2	5	40	Normal	20	E3
			x	2	2	40	Normal	28	F3
		x		2	1	40	Normal	28	E3
			x	2	6	40	Normal	20	F3
x				3	7	40	-	Normal	G4
x				3	3	40	+	Normal	G4
		x		2	7	40	-	Normal	G3
		x		2	3	40	+	Normal	G3
x				3	7	40	Normal	20	G4
x				3	3	40	Normal	28	G4
		x		2	7	40	Normal	20	G3
		x		2	3	40	Normal	28	G3
	x			3	7	40	-	Normal	G2
	x			3	3	40	+	Normal	G2
			x	2	7	40	-	Normal	G3
			x	2	3	40	+	Normal	G3
	x			3	7	40	Normal	20	G2
	x			3	3	40	Normal	28	G2
			x	2	7	40	Normal	20	G3
			x	2	3	40	Normal	28	G3
	x			3	1	40	-	Normal	A2
x				3	2	40	-	Normal	B4
	x			3	4	40	+	Normal	A2
x				3	5	40	+	Normal	B4
			x	2	1	40	-	Normal	B3
		x		2	2	40	-	Normal	A3
			x	2	4	40	+	Normal	B3
		x		2	5	40	+	Normal	A3
	x			3	1	40	Normal	20	A2
x				3	2	40	Normal	20	B4
	x			3	4	40	Normal	28	A2
x				3	5	40	Normal	28	B4
			x	2	1	40	Normal	20	B3
		x		2	2	40	Normal	20	A3
			x	2	4	40	Normal	28	B3
		x		2	5	40	Normal	28	A3

Table 5. Test plan sequence - continued

Time Period #8
Third Day

Measurement System IRS	1	2	3	Surface	Lane	Test Speed	Δ15% Water Flow Rate	Tire Inflation Pressure	Tire
	x			3	3	40	-	Normal	C2
x				3	4	40	-	Normal	D4
	x			3	6	40	+	Normal	C2
x				3	7	40	+	Normal	D4
			x	2	3	40	-	Normal	C3
		x		2	4	40	-	Normal	D3
			x	2	6	40	+	Normal	C3
		x		2	7	40	+	Normal	D3
	x			3	3	40	Normal	20	C2
x				3	4	40	Normal	20	D4
	x			3	6	40	Normal	28	C2
x				3	7	40	Normal	28	D4
			x	2	3	40	Normal	20	C3
		x		2	4	40	Normal	20	D3
			x	2	6	40	Normal	28	C3
		x		2	7	40	Normal	28	D3
	x			3	5	40	-	Normal	E2
x				3	2	40	+	Normal	F4
	x			3	1	40	+	Normal	E2
x				3	6	40	-	Normal	F4
			x	2	5	40	-	Normal	E3
		x		2	2	40	+	Normal	F3
			x	2	1	40	+	Normal	E3
		x		2	6	40	-	Normal	F3
	x			3	5	40	Normal	20	E2
x				3	2	40	Normal	28	F4
	x			3	1	40	Normal	28	E2
x				3	6	40	Normal	20	F4
			x	2	5	40	Normal	20	E3
		x		2	2	40	Normal	28	F3
			x	2	1	40	Normal	28	E3
		x		2	6	40	Normal	20	F3

test wheel to enhance the sensitivity of the measurement to differences in surface characteristics. One purpose of this program is to correlate the measurement performance of different systems. However, variations in the test results occur which are not due to differences in the measuring system. The test tire is subject to wear and the surface over which it is dragged has nonuniform skid resistance characteristics. To measure the effect of the different operating variables and to account for some of the disagreement between measuring systems, the nonuniformities of standard tires and test surfaces need to be identified. Accordingly, the test program employs, as a building block, a test matrix which allows a measure of the difference between test tires and the difference between the lanes comprising the test surface to be determined while the significance of a given variable is being tested. A sample test matrix is shown below:

Time Period ________
Surface ________

	Tires						
Speed	A	B	C	D	E	F	G
$S - \Delta S$	1	2	3	4	5	6	7
S	2	3	4	5	6	7	1
$S + \Delta S$	4	5	6	7	1	2	3

Letters A thru G designate 7 tires while numbers 1 through 7 identify the 7 lanes comprising the surface [7]. The nominal test speed is S, while ΔS is an incremental change in the speed. Since ΔS is small, the slope over the range $2\Delta S$ approaches the speed gradient at S.

Twenty-one skid resistance measurements are made in one matrix, using seven tires, over seven lanes of the surface, with three values of the test variable being studied. The mean of the twenty-one test values represents the skid resistance of the surface measured during the time period using the "average" tire, over the "average" lane at the "average" value of the test variable. The novelty of the test matrix is that it yields a skid resistance-test variable gradient for the surface as well as an indication of the dispersion due to choice of tire or lane. The operating variables planned for study using test matrices were test speed, water depth, and test tire inflation pressure. The test matrix is explained further in Appendix B.

Twenty-eight test tires were used by the four systems in the conduct of the test program.

3.4. Tests Accomplished

The accomplishment of the full program requires eighteen days of dynamic testing. Since some unsuitable weather was expected, the tests which would allow comparison of results with those of the previous program were scheduled to be conducted first. The weather conditions at the test site are given in figure 23 for the March 30 to April 8, 1976 period and in figure 24 for the April 19 to April 29 period. Correlation testing did not occur on March 31, April 1, 2, 3, 4, 19, 21, or 25. By April 28, the first six time periods of two days each had been completed. With one more day available for testing a supplemental period 7 was designed (table 6) for additional direct comparisons between the skid measuring systems. These comparisons did not include all the combinations of tires and lanes used in the earlier tests. Table 7 summarizes the comparisons between systems.

3.5. Control of Operating Variables

Previous experiments with the IRS had shown that the operating variables listed in section 3.2 required control.

Variations in hitch height, as expected, change the unloading constant of the test wheel vertical load. Variations in hitch height which also rotate the force transducer cause a shift in the zero of the traction channel and change the unloading constant, as measured by the vertical load channel, from the expected value. Two-axis force transducers are used on the IRS and the three ARS units. The static tests (sec. 2.3) had demonstrated the changes of hitch height resulting from variation of water load.

Variations in the inflation pressure of the tow vehicle rear tires change the water laying system pump rate with test speed. The test crews controlled the inflation pressure of the tow vehicle rear tires.

The IRS trailer suspension system utilizes air-adjustable shock absorbers. Variations in shock absorber inflation pressure result in a shift in trailer body orientation which changes the static vertical test wheel load. The IRS shock absorber pressure was controlled by the IRS crew.

In a previous IRS - Western (WARS) test program it was noted that the average skid number values measured, in each of seven two-day pairs of test conducted with both systems, on the second day were lower than the average skid numbers measured on the first day [7, sec. 3.10]. It

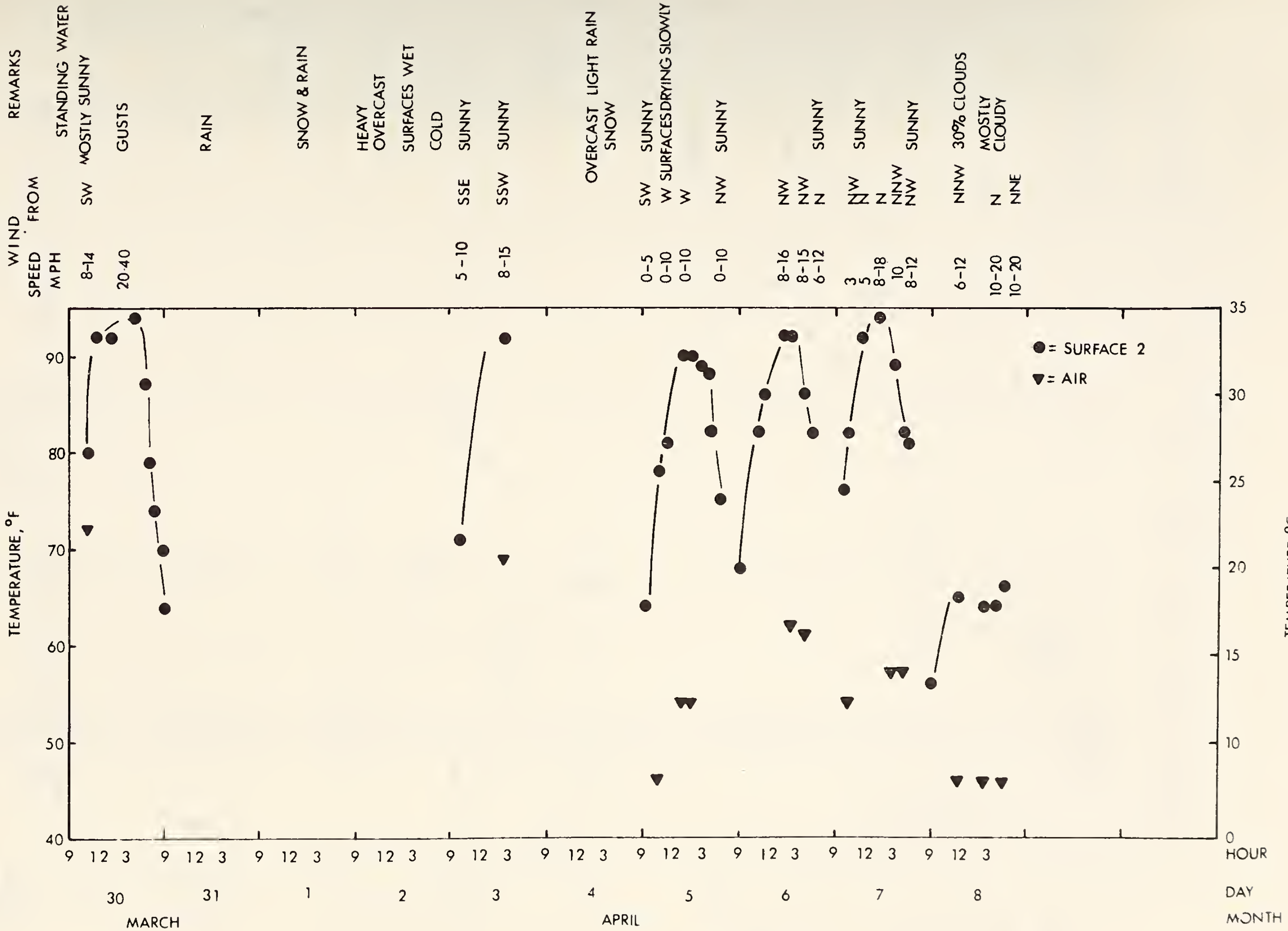

Figure 23. Weather conditions during dynamic tests, March 30 - April 8, 1976.

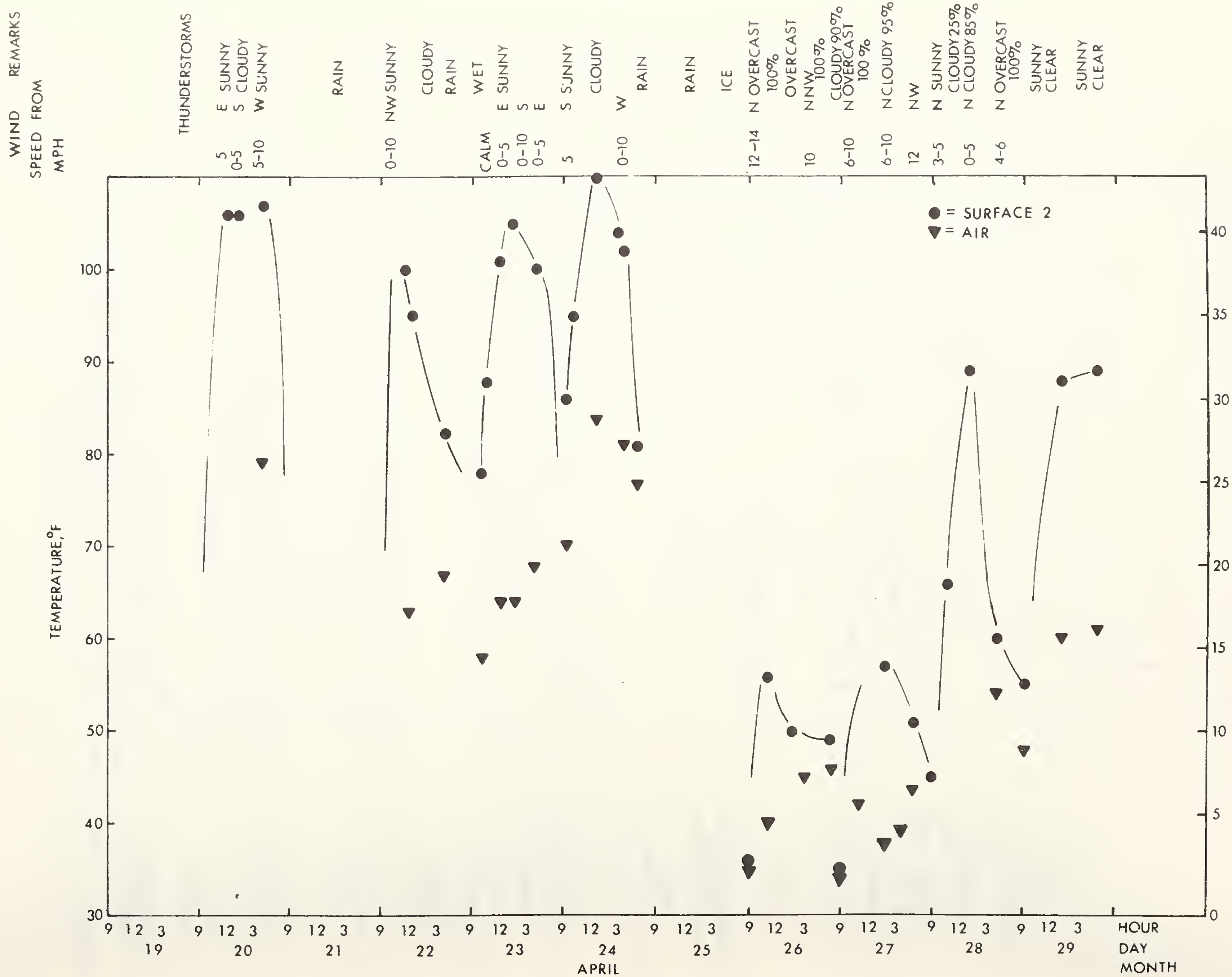

Figure 24. Weather conditions during dynamic tests, April 19 - April 29, 1976.

Table 6. Supplementary test plan sequence

Time Period #7
One Day

Measurement System IRS	1	2	3	Surface	Lane	Test Speed	Tire
x				2	2	20	D2
		x		2	3	20	B2
x				2	4	40	D2
		x		2	5	40	B2
x				2	1	60	D2
		x		2	2	60	B2
			x	3	2	20	F2
	x			3	3	20	A2
			x	3	4	40	F2
	x			3	5	40	A2
			x	3	1	60	F2
	x			3	2	60	A2
x				2	4	20	F2
			x	2	3	20	A2
x				2	7	40	F2
			x	2	6	40	A2
x				2	5	60	F2
			x	2	4	60	A2
x				3	4	20	B2
		x		3	3	20	D2
x				3	7	40	B2
		x		3	6	40	D2
x				3	5	60	B2
		x		3	4	60	D2
			x	2	6	20	F2
	x			2	7	20	A2
			x	2	5	40	F2
	x			2	2	40	A2
			x	2	1	60	F2
	x			2	6	60	A2
x				3	6	20	A2
	x			3	7	20	F2
x				3	5	40	A2
	x			3	2	40	F2
x				3	1	60	A2
	x			3	6	60	F2

Table 6. Supplementary test plan sequence - continued

Time Period #7
One Day (continued)

Measurement System IRS 1	2	3	Surface	Lane	Test Speed	Tire
	x		2	2	20	D2
x			2	3	20	B2
	x		2	4	40	D2
x			2	5	40	B2
	x		2	1	60	D2
x			2	2	60	B2
		x	3	2	20	D2
	x		3	3	20	B2
		x	3	4	40	D2
	x		3	5	40	B2
		x	3	1	60	D2
	x		3	2	60	B2

Table 7. Summary of direct comparisons between skid measurement systems

Speed	Time period	Surface 2	Surface 3
mph[a]			
20	3	[b]IRS /ARS 1	ARS 2/ARS 3
	4	ARS 2/ARS 3	IRS /ARS 1
40	1	IRS /ARS 1	ARS 2/ARS 3
	2	ARS 2/ARS 3	IRS /ARS 1
60	5	IRS /ARS 1	ARS 2/ARS 3
	6	ARS 2/ARS 3	IRS /ARS 1
20, 40, 60	7	IRS /ARS 2	ARS 1/ARS 3
		IRS /ARS 3	IRS /ARS 2
		ARS 1/ARS 3	IRS /ARS 1
		ARS 1/ARS 2	ARS 2/ARS 3

[a] 1 mph = 1.609 km/h.

[b] This notation means that the two systems were tested alternately on lanes of the same surface.

was suspected that the power-broom sweeping of the surfaces at the beginning of each test day was not adequate to remove the rubber deposited on the surfaces by tire wear. In this test program the surfaces were flooded with pressurized water from a tank truck the evening before a test day.

The degree-of-dryness of the test surfaces was controlled such that any wetness was not visible in the lane immediately before a skid test. The test plan sequence was ordered to facilitate control of the degree-of-dryness. Testing was also delayed as necessary to allow a longer time for the lane to dry.

Test speed on-board recorded values and driver visual aids were checked against the IRS stationary differential radar system at least once each day. The resolution of the system is 0.1 mph (0.2 km/h). Variations from the planned speed occurring during a test run were recorded by the radar system. These recorded values were used in the data reduction for all systems.

Water flow rate was recorded in all systems. The records were used to trim the flow rate to predetermined values corresponding to the different test speeds.

In all previous test programs in which the IRS participated, both an instrumentation operator and a driver were in the tow vehicle. The operator would zero the instrumentation as necessary immediately before each skid test. The operator was not made available for this test program. The instrumentation was zeroed, however, at the beginning of the morning and afternoon test periods. IRS traction force, vertical load, and flow rate signals were recorded on board in both digital and analog form. The digital data was transferred to a ground station where it was scaled into engineering units and filed on a magnetic tape. In order to utilize the available time most effectively, only minimal data reduction was carried out while the tests were being conducted. Only two or three tests were processed by the ground station each day. As a result, it was not until the third time period that drift in the vertical load signal of the IRS was detected by inspection of the ground station plots. Experiments then verified a vertical signal drift due to temperature changes at the IRS wheel transducer. Immediate steps were taken to control this effect by re-zeroing the force signals of the IRS just prior to each test. The problem would have been avoided had a full-time instrumentation operator been available to carry out the normal procedures.

3.6. Measurement of Uncontrolled Variables

The weather conditions around the test site and the surface temperature of surface 2 have been given in figures 23 and 24. The surface temperature of the base material on which surface 2 was constructed was the same within ± 4 °F (2 °C). The temperature was measured with a sensor located in the northwest corner of the surface. The temperature sensitive area of the sensor was placed in contact with the top of the aggregate. A conductive grease was used to provide thermal contact between the sensor, the sides of the protruding aggregate, and the binder of the surface. The surface temperatures ranged from 35 °F to 110 °F (2 °C to 43 °C) during the testing period.

Wind speeds were measured at the site, approximately 5 feet (1.5 m) above the surface. It was noted that the wind speed dropped by approximately half within a foot (0.3 m) of the surface.

Test tire inflation pressure was measured after a five mile warm-up drive and before each skid test.

The test wheel lock-up position was noted by an observer during each test. When mounted on the IRS, the tread depth at each groove across the width of the tire at the lock-up position was measured and recorded after the skid. The tire tread surface temperature, higher where the skid occurred, was a further guide in locating the lock-up position.

The type of tire wear measured on these surfaces was reported previously [6, sec. 3.6].

3.7. The Correlation Test Plan

A purpose of the dynamic skid test program listed previously is to correlate the degree to which the measurement results from the three ARS units and the IRS match. The correlation is degraded by three sources of dispersion:

a) different times at which the measurements are made,
b) any nonuniformity between test tires, and
c) any nonuniformity between lanes of the test surface.

The correlation test plan is designed to measure these sources of dispersion. If their existance can be proven and quantified, their effect on the results can be taken into account to yield a more precise correlation. Knowledge of the bounds of these sources of dispersion can be used to establish an uncertainty band around the correlation result.

Statistical confidence in the results can be improved by running a sufficiently large number of tests. Confidence in the correlation of equipments is enhanced by finding consistency both in the magnitude of the results at a point, and in the first derivative of the results with respect to a test variable through that point. Confidence in the measurement results in enhanced when the data points are found to be within small intervals of variation.

The number of tests planned was based on the degree of precision previously reached by the IRS and anticipated for the ARS units, under controlled test procedures. Tests of the sensitivity of SN to water flow rate and test tire inflation pressure were planned for 40 mph (64 km/h) since this is the more usual test speed. The test plan contained 182 skid measurement tests for each participating skid measurement system.

3.8. Test Matrix Results

The skid resistance measurement results are given in terms of a mean value at the nominal test speed, the measured skid resistance-test speed gradient through that mean value, and a 99 percent confidence interval about the mean value.

As noted in section 3.5, drift affected the dynamic vertical load measurements made by the IRS during the first three time periods. Consequently, for consistency, all SN results have been calculated using test wheel load reductions derived from the experimentally determined effective unloading constants. Preliminary comparisons were made between SN results calculated this way and those calculated on the basis of dynamically measured vertical loads (excluding the drifted data). The comparisons showed agreement between the two methods with 2 SN. The unloading constant method yielded higher values for two systems (ARS 1 and the IRS) and lower values for the other two systems, on both surfaces.

Each curve (SN_c) shown by dashed lines in figures 25 and 26 represents a least squares fit to all the measurements made by one skid measurement system on one surface during the first six time periods.

The measurements were clustered about the three nominal test speeds; V = 20, 40, and 60 mph (32, 64, and 97 km/h). The slope of the curve obtained from all the measurements (Θ_c, the calculated skid resistance-test speed gradient) has been used to adjust the value of each measurement to correspond exactly to its nominal speed. The means of the adjusted values are shown (SN_{20}, SN_{40}, and SN_{60}) and the 99 percent confidence interval (L) is shown for each mean. A straight line segment is shown through each mean, representing the speed gradients (Θ_{20}, Θ_{40}, and Θ_{60}) measured using the incremental speeds of the test plan. The numerical values for the plots of figures 25 and 26 are given in tables 8 and 9.

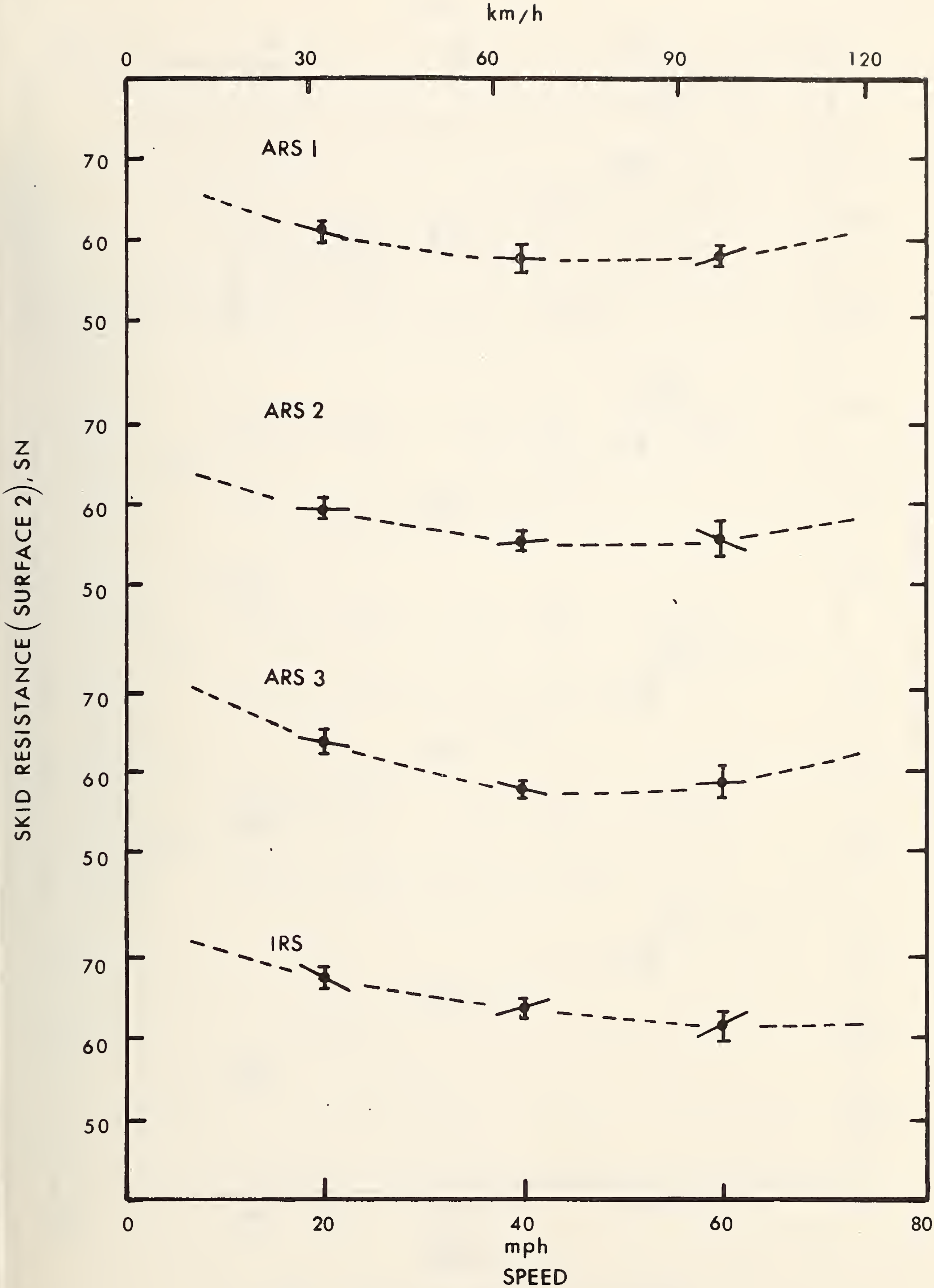

Figure 25. Test matrix results, surface 2.

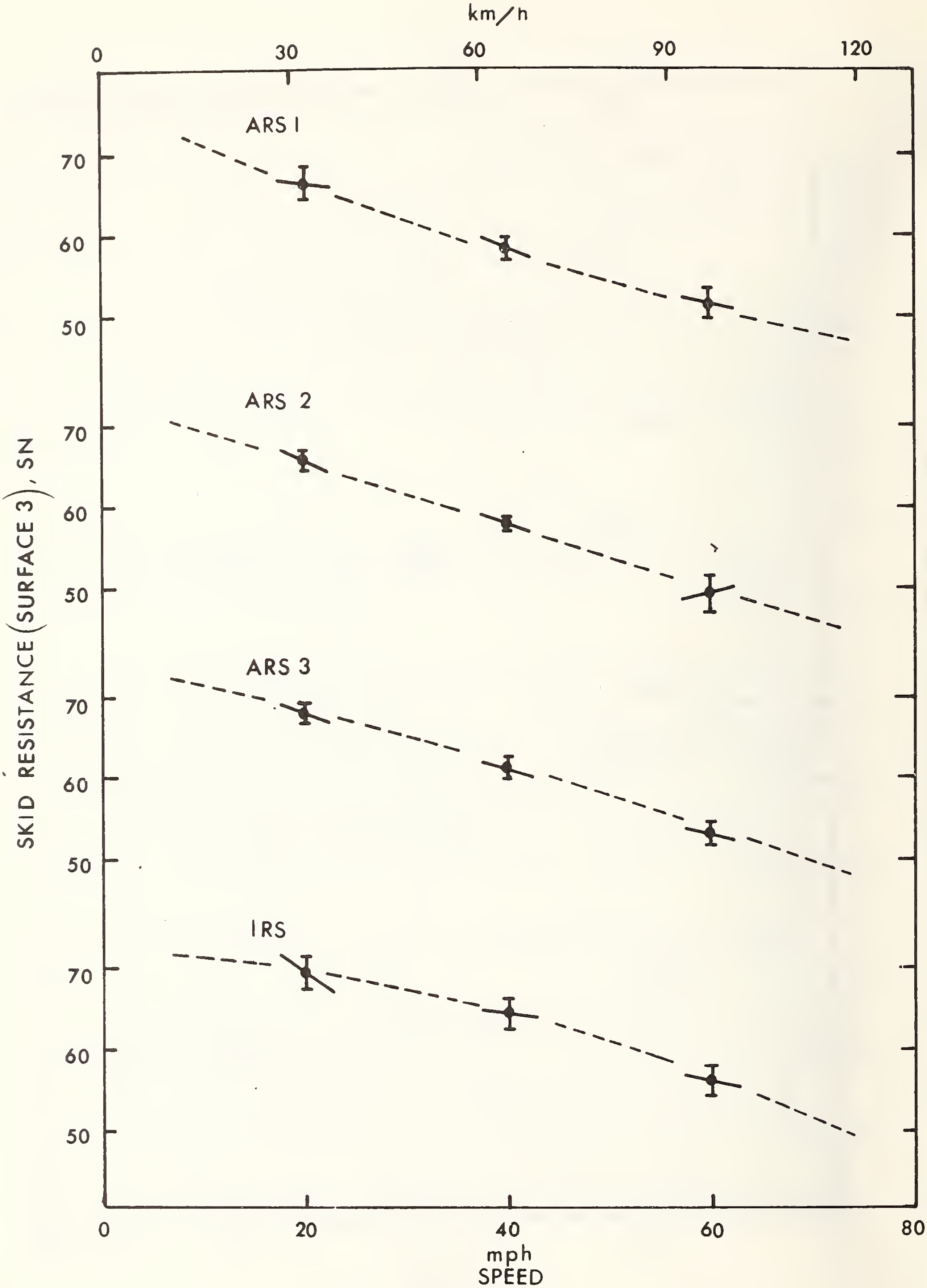

Figure 26. Test matrix results, surface 3.

Table 8. Test matrix results, surface 2

ARS 1	$SN_{20} = 61.36$	$\Theta_{20} = -0.30$	$L = \pm 1.5$
	$SN_{40} = 57.61$	$\Theta_{40} = -0.05$	$L = \pm 1.6$
	$SN_{60} = 58.04$	$\Theta_{60} = +0.39$	$L = \pm 1.4$
	$SN_c = 69.66 - 0.53\ V + 0.006\ V^2$		
	$\Theta_c = -\ 0.53 + 0.011\ V$		
ARS 2	$SN_{20} = 59.56$	$\Theta_{20} = -0.03$	$L = \pm 1.4$
	$SN_{40} = 55.21$	$\Theta_{40} = +0.04$	$L = \pm 1.3$
	$SN_{60} = 55.63$	$\Theta_{60} = -0.54$	$L = \pm 2.1$
	$SN_c = 67.96 - 0.54\ V + 0.006\ V^2$		
	$\Theta_c = -\ 0.54 + 0.011\ V$		
ARS 3	$SN_{20} = 63.63$	$\Theta_{20} = -0.20$	$L = \pm 1.6$
	$SN_{40} = 57.83$	$\Theta_{40} = -0.29$	$L = \pm 1.0$
	$SN_{60} = 58.54$	$\Theta_{60} = +0.02$	$L = \pm 1.8$
	$SN_c = 75.46 - 0.75\ V + 0.008\ V^2$		
	$\Theta_c = -\ 0.75 + 0.015\ V$		
IRS	$SN_{20} = 67.82$	$\Theta_{20} = -0.58$	$L = \pm 1.4$
	$SN_{40} = 63.72$	$\Theta_{40} = +0.34$	$L = \pm 1.1$
	$SN_{60} = 61.43$	$\Theta_{60} = +0.59$	$L = \pm 1.6$
	$SN_c = 74.95 - 0.42\ V + 0.003\ V^2$		
	$\Theta_c = -\ 0.42 + 0.007\ V$		

Table 9. Test matrix results, surface 3

ARS 1	$SN_{20} = 66.20$	$\Theta_{20} = -0.12$	$L = \pm 1.8$
	$SN_{40} = 57.87$	$\Theta_{40} = -0.51$	$L = \pm 1.3$
	$SN_{60} = 50.94$	$\Theta_{60} = -0.27$	$L = \pm 1.7$
	$SN_c = 76.27 - 0.55\ V + 0.002\ V^2$		
	$\Theta_c = -\ 0.55 + 0.004\ V$		
ARS 2	$SN_{20} = 65.38$	$\Theta_{20} = -0.59$	$L = \pm 1.5$
	$SN_{40} = 57.60$	$\Theta_{40} = -0.43$	$L = \pm 1.0$
	$SN_{60} = 48.87$	$\Theta_{60} = +0.28$	$L = \pm 2.0$
	$SN_c = 73.54 - 0.41\ V + 0.0001\ V^2$		
	$\Theta_c = -\ 0.41 + 0.0001\ V$		
ARS 3	$SN_{20} = 67.81$	$\Theta_{20} = -0.46$	$L = \pm 1.2$
	$SN_{40} = 60.95$	$\Theta_{40} = -0.36$	$L = \pm 1.3$
	$SN_{60} = 53.03$	$\Theta_{60} = -0.30$	$L = \pm 1.4$
	$SN_c = 73.89 - 0.28\ V - 0.001\ V^2$		
	$\Theta_c = -\ 0.28 - 0.002\ V$		
IRS	$SN_{20} = 69.11$	$\Theta_{20} = -0.88$	$L = \pm 1.9$
	$SN_{40} = 64.14$	$\Theta_{40} = -0.14$	$L = \pm 1.6$
	$SN_{60} = 55.86$	$\Theta_{60} = -0.25$	$L = \pm 1.6$
	$SN_c = 72.37 - 0.09\ V - 0.003\ V^2$		
	$\Theta_c = -\ 0.09 - 0.006\ V$		

According to the test plan, each skid measuring system made a matrix of SN measurements on a given surface, at each nominal speed, using a group of seven tires. The test matrix was used to calculate the deviation of the SN measurements made by each tire from the mean of all the measurements in the matrix. In the first six time periods, each tire group was included in six matrices (two systems measuring one surface at three nominal speeds). The exceptions were tire C of group 1, with five matrices completed, and all the tires of group 2, with five matrices completed. The deviations for each tire, as calculated from the several matrices, were then averaged to obtain the overall measurement deviation for each tire. These overall deviations are shown in figure 27 for the tire groups used to measure surface 2 and in figure 28 for the tire groups used to measure surface 3.

Six of the twenty-eight tires (identified by asterisks in the figures) made SN measurements that deviated significantly from the measurements made by the "average tire" of their particular group.

The SN measurements also form a matrix for each system on a given surface, at each nominal speed, for seven lanes of the surface. The matrix was used to calculate the deviation of the SN measurements made on each lane from the mean of all the measurements in the matrix. In the first six time periods, the lanes of surfaces 2 and 3 were included in twelve matrices (four systems measuring each surface at three nominal speeds). The twelve calculated deviations were then averaged to obtain the overall measurement deviation for each lane. These overall deviations are shown in figure 29.

The outside lanes 1 and 7 of surface 2 were found to yield a significantly higher SN than the surface average, while center lanes 4 and 5 measured significantly lower. On surface 3, lane 2 measured significantly higher than the average.

The bounds of the deviations due to tires and lanes were approximately $\pm$ 2 SN. No significant deviations attributable to time of day, surface temperature or variations of test tire inflation were detected.

3.9. Ranking of the Sources of Dispersion

The calculated deviations have been used to rank the sources of dispersion in the skid number measurement. The ranking of SN dispersions attributed to tires and surfaces is shown for the four measuring systems separately in tables 10, 11, 12, and 13.

When the deviations are pooled without regard to system, the overall ranking is obtained, as shown in table 14. Tire dispersions are slightly higher than surface dispersions.

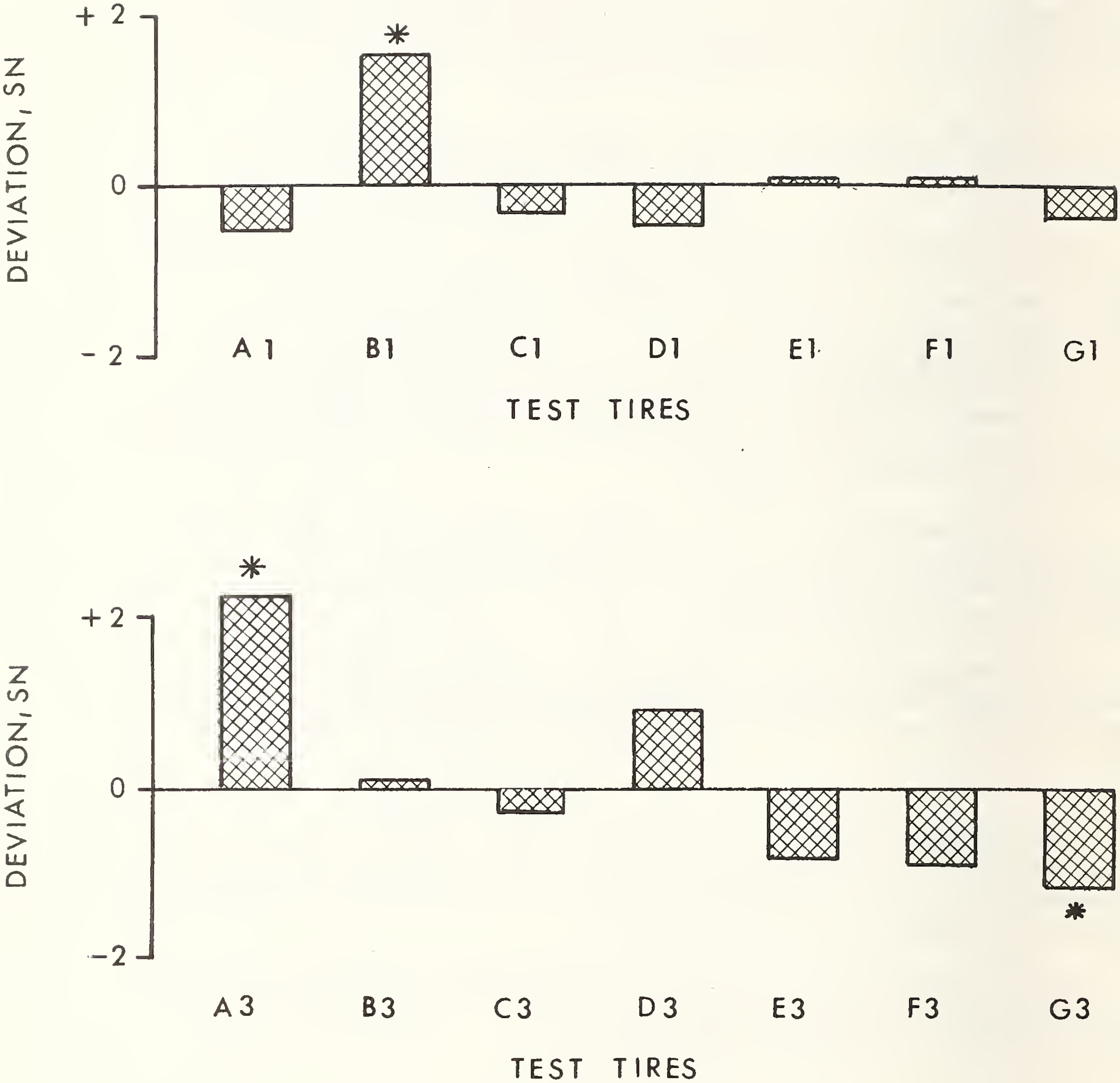

Figure 27. Deviations from the mean skid number observed for tires of groups 1 and 3, from skid resistance measurements on surface 2. Deviations marked with an asterisk are considered large enough to be statistically significant.

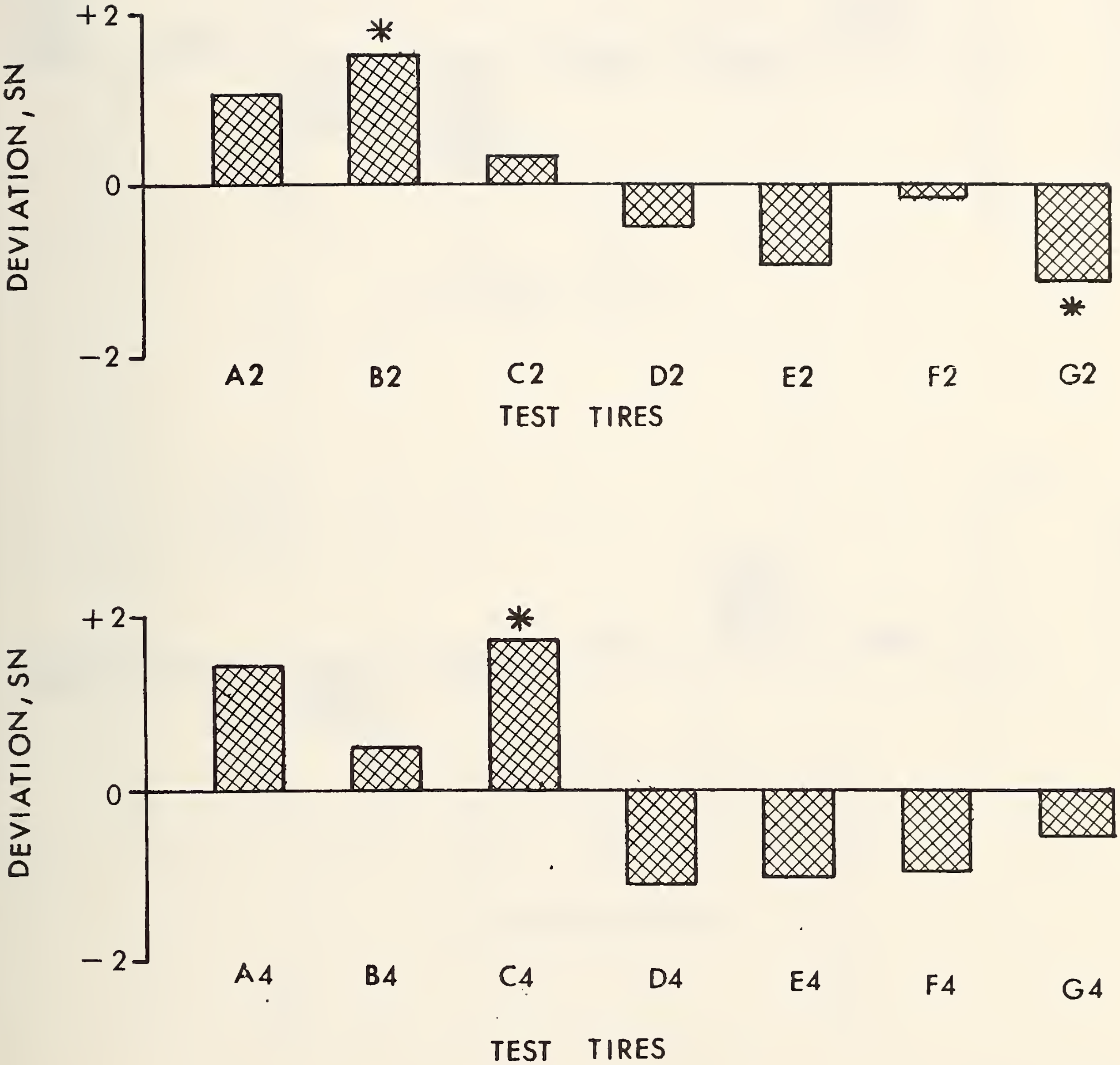

Figure 28. Deviations from the mean skid number observed for tires of groups 2 and 4, from skid resistance measurements on surface 3. Deviations marked with an asterisk are considered large enough to be statistically significant.

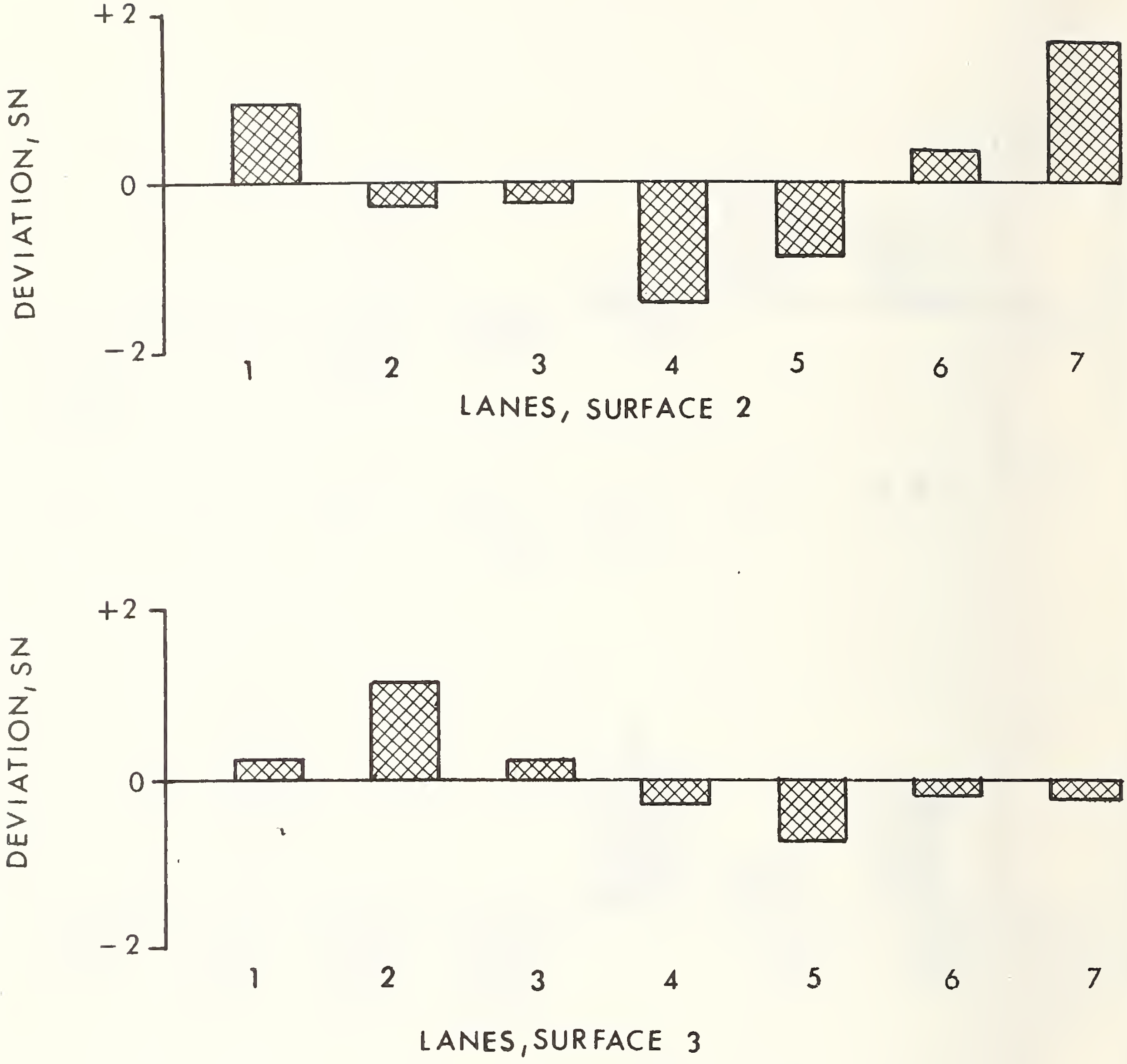

Figure 29. Deviations from the mean skid number observed for the lanes of surfaces 2 and 3.

Table 10. Ranking of possible sources of dispersion in ARS 1 results

Rank	Possible source of dispersion	Sample standard deviation	Subrank	Surface	Speed	Sample standard deviation
					mph[a]	
1	Tire group 2 (7 tires)	1.93	A	3	20	2.24
			B	3	60	2.08
			C	3	40	1.76
2	Surface 2 (7 lanes)	1.53	A	2	40	1.93
			B	2	60	1.62
			C	2	20	1.19
3	Surface 3 (7 lanes)	1.47	A	3	60	1.91
			B	3	40	1.46
			C	3	20	1.18
4	Tire group 1 (7 tires)	1.35	A	2	60	1.82
			B	2	20	1.44
			C	2	40	0.71

[a] 1 mph = 1.609 km/h.

Table 11. Ranking of possible sources of dispersion in ARS 2 results

Rank	Possible source of dispersion	Sample standard deviation	Subrank	Surface	Speed	Sample standard deviation
					mph[a]	
1	Tire group 3 (7 tires)	2.29	A	2	60	3.15
			B	2	40	2.02
			C	2	20	1.89
2	Surface 3 (7 lanes)	1.78	A	3	60	2.39
			B	3	20	1.81
			C	3	40	1.23
3	Surface 2 (7 lanes)	1.61	A	2	20	2.02
			B	2	60	1.73
			C	2	40	1.17
4	Tire group 2 (7 tires)	1.51	A	3	20	1.66
			B	3	40	1.48
			-	3	60	--

[a] 1 mph = 1.609 km/h.

Table 12. Ranking of possible sources of dispersion in ARS 3 results

Rank	Possible source of disperion	Sample standard deviation	Subrank	Surface	Speed	Sample standard deviation
					mph[a]	
1	Surface 2 (7 lanes)	1.75	A	2	60	2.04
			B	2	20	2.00
			C	2	40	1.42
2	Tire group 4 (7 tires)	1.56	A	3	20	1.85
			B	3	40	1.67
			C	3	60	1.37
3	Surface 3 (7 lanes)	1.38	A	3	60	1.83
			B	3	20	1.24
			C	3	40	1.20
4	Tire group 3 (7 tires)	1.35	A	2	60	1.95
			B	2	20	1.43
			C	2	40	0.48

[a] 1 mph = 1.609 km/h.

Table 13. Ranking of possible sources of dispersion in IRS results

Rank	Possible source of dispersion	Sample standard deviation	Subrank	Surface	Speed	Sample standard deviation
					mph[a]	
1	Tire group 4 (7 tires)	1.82	A	3	20	2.15
			B	3	60	1.95
			C	3	40	1.61
2	Tire group 1 (7 tires)	1.64	A	2	60	2.18
			B	2	40	1.52
			C	2	20	1.40
3	Surface 3 (7 lanes)	1.24	A	3	40	1.60
			B	3	60	1.18
			C	3	20	1.07
4	Surface 2 (7 lanes)	0.82	A	2	20	1.05
			B	2	40	0.88
			C	2	60	0.60

[a] 1 mph = 1.609 km/h.

Table 14. Ranking of possible sources of dispersion in the overall results

Rank	Possible source of dispersion	Sample standard deviation
1	Tire group 3 (7 tires)	1.86
2	Tire group 2 (7 tires)	1.75
3	Tire group 4 (7 tires)	1.67
4	Tire group 1 (7 tires)	1.49
5	Surface 3 (7 lanes)	1.45
6	Surface 2 (7 lanes)	1.44

The sample standard deviations of skid number, with the calculated tire and lane dispersions, are listed according to system, surface, and speed in table 15. The standard deviation of the calculated tire and lane dispersion is comparable to or less than the standard deviation of the skid number measurement result in each case.

3.10. Deviation from Desired Test Speeds

The frequent use of nominal speeds in skid number data reduction is justified when actual speeds fall within appropriate limits. Limits are needed because SN is speed-dependent. E 274-70 sets bounds on the allowable deviation: $\pm$ 0.5 mph (0.8 km/h) for test speeds at or below 40 mph (64.4 km/h) and $\pm$ 1 mph (1.6 km/h) at higher speeds. Data reduction can compensate for off-target speeds only when measured speeds and speed gradients are available.

In general, each skid represents a driver's attempt to perform a test as near to a specified speed as possible. For the tests under discussion, speeds of all four vehicles were accurately recorded during all skids. Later, the observed speed for each skid was averaged over the portion of the skid used for skid number calculation. Here we present the dispersion of the averaged speeds about the target values.

Bar graphs illustrate the speed dispersions found for each system (figs. 30, 31, and 32). Specified speeds were 18, 20, and 22 mph (29.0, 32.2, and 35.4 km/h); 38, 40, and 42 mph (61.1, 64.4, and 67.6 km/h); and 58, 60, and 62 mph (93.3, 96.5, and 99.8 km/h). Data is graphed by speed range since the effects of operational conditions such as time available to reach test speed and test wheel traction were clearly associated with slow, moderate, or fast ranges. ARS 1, 2, and 3 were mechanically similar. Crew technique may be considered as a cause of consistent differences seen in ARS speed performance (e.g., wider scatter in speeds of the ARS 2). The IRS differed mechanically from the ARS units.

Test conditions were good: speed subsystems were well calibrated, tests were repetitive, and in comparison to roadway testing, test pavements were good and traffic distractions were minimal. Even so, observed speeds exceeding limits for the three speed ranges totalled 3 (2% of the skids) for ARS 1, 26 (20%) for ARS 2, 16 (12%) for ARS 3, and 4 (3%) for the IRS. It can be seen from the graphs that distributions were not balanced around the desired speed. Slow runs were more numerous in ten of the twelve distributions. The mean values of the distributions are listed in table 16. These fall within the previously quoted limits, however each is derived from approximately 45 tests.

The results underscore the importance of speed measurement. The data analyst must have assurance that the speed system operated suitably close to the desired speed.

Table 15. Dispersion sample standard deviations

		Sample standard deviation											
		ARS 1 results			ARS 2 results			ARS 3 results			IRS results		
Surface	Speed	SN	Tire	Lane	SN	Tire	Lane	SN	Tire	Lane	SN	Tire	Lane
	mph[a]												
2	20	2.39	1.44	1.19	2.32	1.89	2.02	2.55	1.43	2.00	2.22	1.40	1.05
2	40	2.34	0.71	1.93	2.06	2.02	1.17	1.60	0.48	1.42	1.82	1.52	0.88
2	60	2.20	1.82	1.62	3.21	3.15	1.73	2.84	1.95	2.04	2.63	2.18	0.60
3	20	2.87	2.24	1.18	2.48	1.66	1.81	1.88	1.85	1.24	3.00	2.15	1.07
3	40	1.96	1.76	1.46	1.67	1.48	1.23	2.11	1.67	1.20	2.63	1.61	1.60
3	60	2.80	2.08	1.91	2.38	--	2.39	2.26	1.37	1.83	2.65	1.95	1.18

[a] 1 mph = 1.609 km/h.

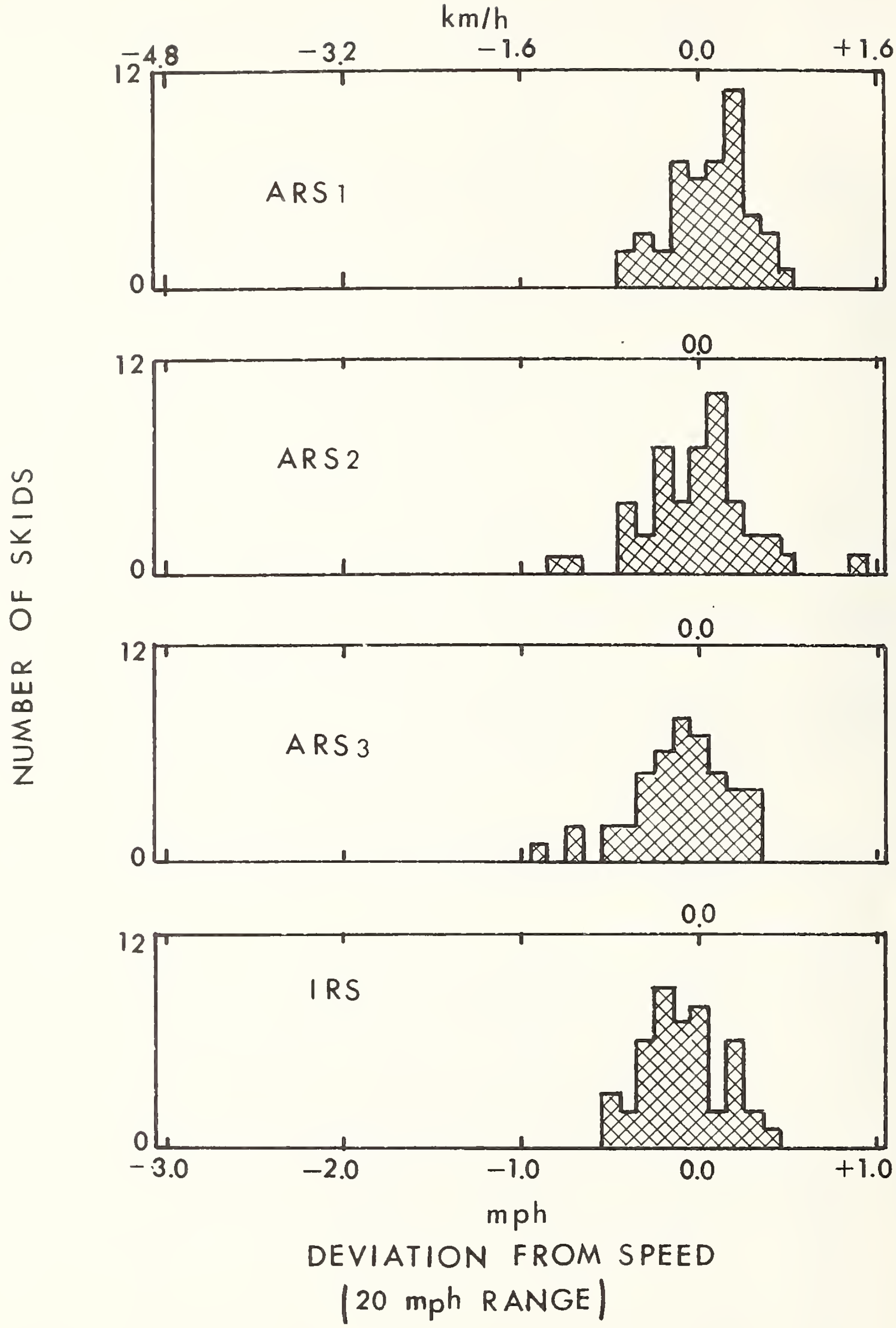

Figure 30. Average deviations from nominal speed observed during skids at 18, 20, and 22 mph (29.0, 32.2, and 35.4 km/h).

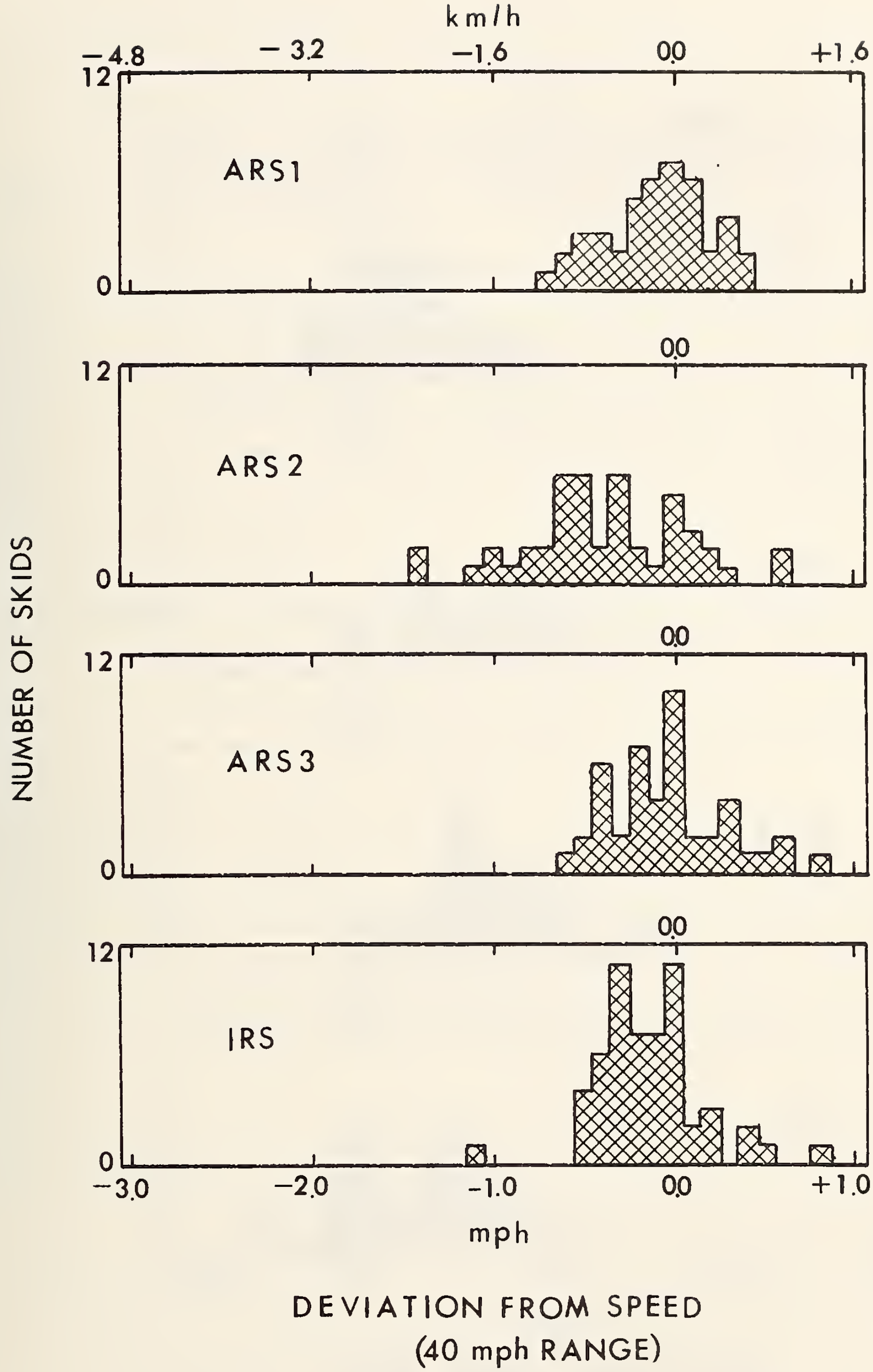

Figure 31. Average deviations from nominal speed observed during skids at 38, 40, and 42 mph (61.1, 64.4, and 67.6 km/h).

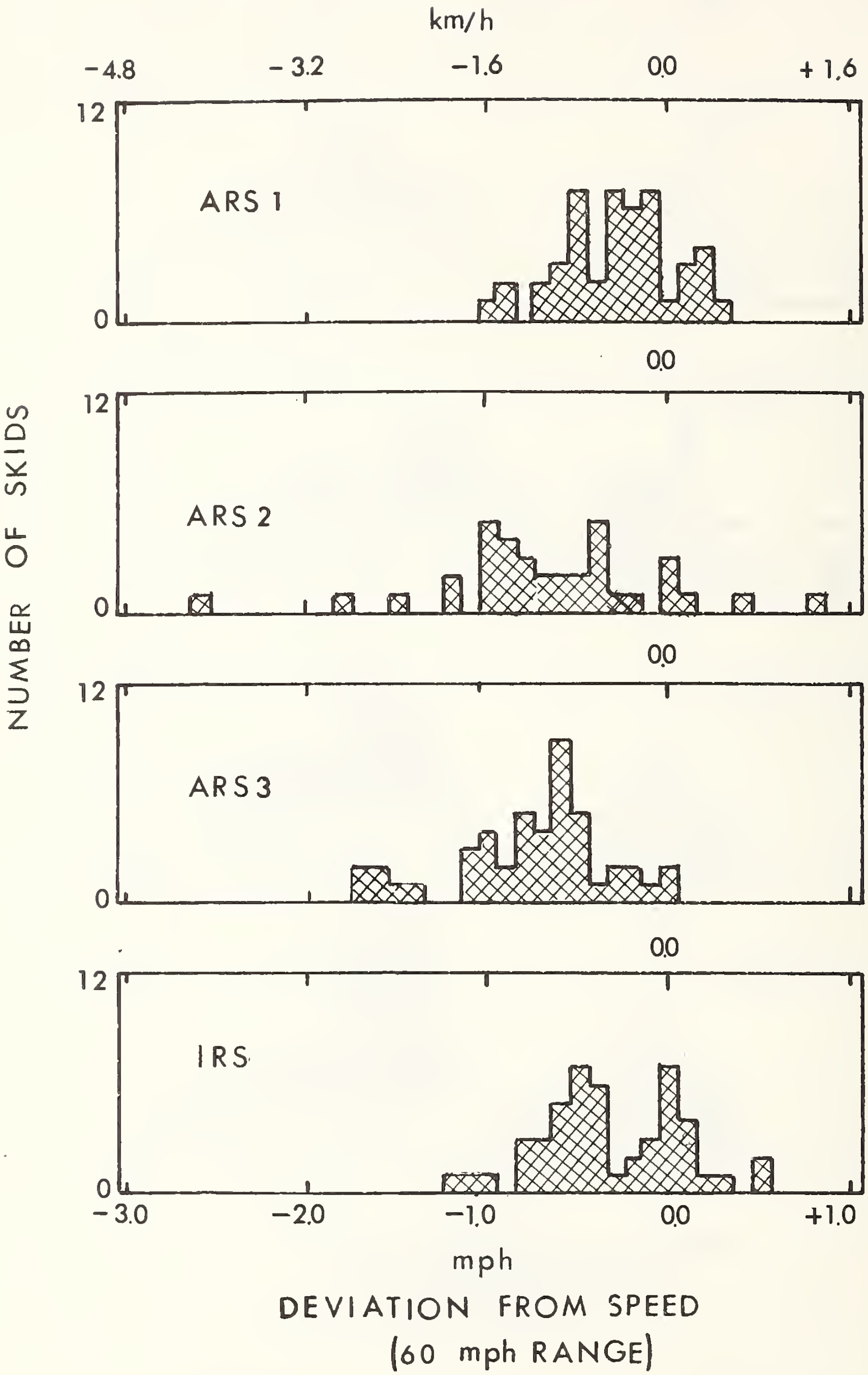

Figure 32. Average deviations from nominal speed observed during skids at 58, 60, and 62 mph (93.3, 96.5, and 99.8 km/h).

Table 16. Mean deviation from nominal speed

Unit	Mean deviation: 20 mph range		40 mph range		60 mph range	
		mph[a]		mph		mph
ARS 1	[b](46)	+0.1	(43)	-0.1	(46)	-0.3
ARS 2	(46)	0.0	(46)	-0.4	(36)	-0.7
ARS 3	(46)	-0.1	(45)	0.0	(46)	-0.8
IRS	(46)	-0.1	(56)	-0.1	(48)	-0.3

[a] 1 mph = 1.609 km/h.

[b] The number of tests considered is shown in parentheses.

3.11. Skid Resistance Speed Gradients

It is known from test data generated at largely different test speeds that pavement skid resistance varies with speed. In this section we show that the skid resistance - test speed gradients measured using the 2 mph (3.2 km/h) differential test speeds, ΔS, of the test matrix, in conjunction with the differential radar system, are generally consistent with the slope of a continuous polynomial expression of skid resistance as a function of test speed.

The synthesis of the polynomial skid resistance expression for a skid measuring system-surface combination at EFTC utilized the results of the respective test matrices of time periods 1 through 6 over the full speed range. Least squares techniques were used to fit the data with an expression of the form:

$$SN_c = A + BV + CV^2$$

where V is the test speed in mph (1 mph = 1.609 km/h).

Differentiation of SN_c produces an expression for calculation of the skid resistance - test speed gradient which is also a function of test speed:

$$\Theta_c = \frac{d(SN_c)}{d(V)} = B + 2CV.$$

The SN_c curves, shown plotted on separate ordinates in section 3.8, are re-plotted with common ordinates in figure 33 to illustrate the agreement obtained between measuring systems. The systems tend to produce similar curves on a surface; that is, the speed gradients characteristic of the system-surface combinations in this experiment appear to be more dependent on the surface than on the choice of measuring system. It can be seen that the SN_c differences between systems on a surface could be largely corrected by an adjustment of the constant term.

For all four systems, the SN_c curve on surface 2 is concave upwards with zero slope (speed gradient) at a point above 40 mph (64 km/h). This agress with measurements previously reported on surface 2 at EFTC [6, sec. 3.8] and on the similar surface 2 at WFTC [7, sec. 3.9].

On surface 3, the SN_c results for the four systems are more linear, and are divided between slightly concave and convex curves. Again, the earlier measruements [6, sec. 3.8][7, sec. 3.9] agree, in that the SN_c results for surface 3 were more linear than for surface 2. Of the curves developed on surface 3 by the IRS, the present measurement is convex while the earlier two were concave.

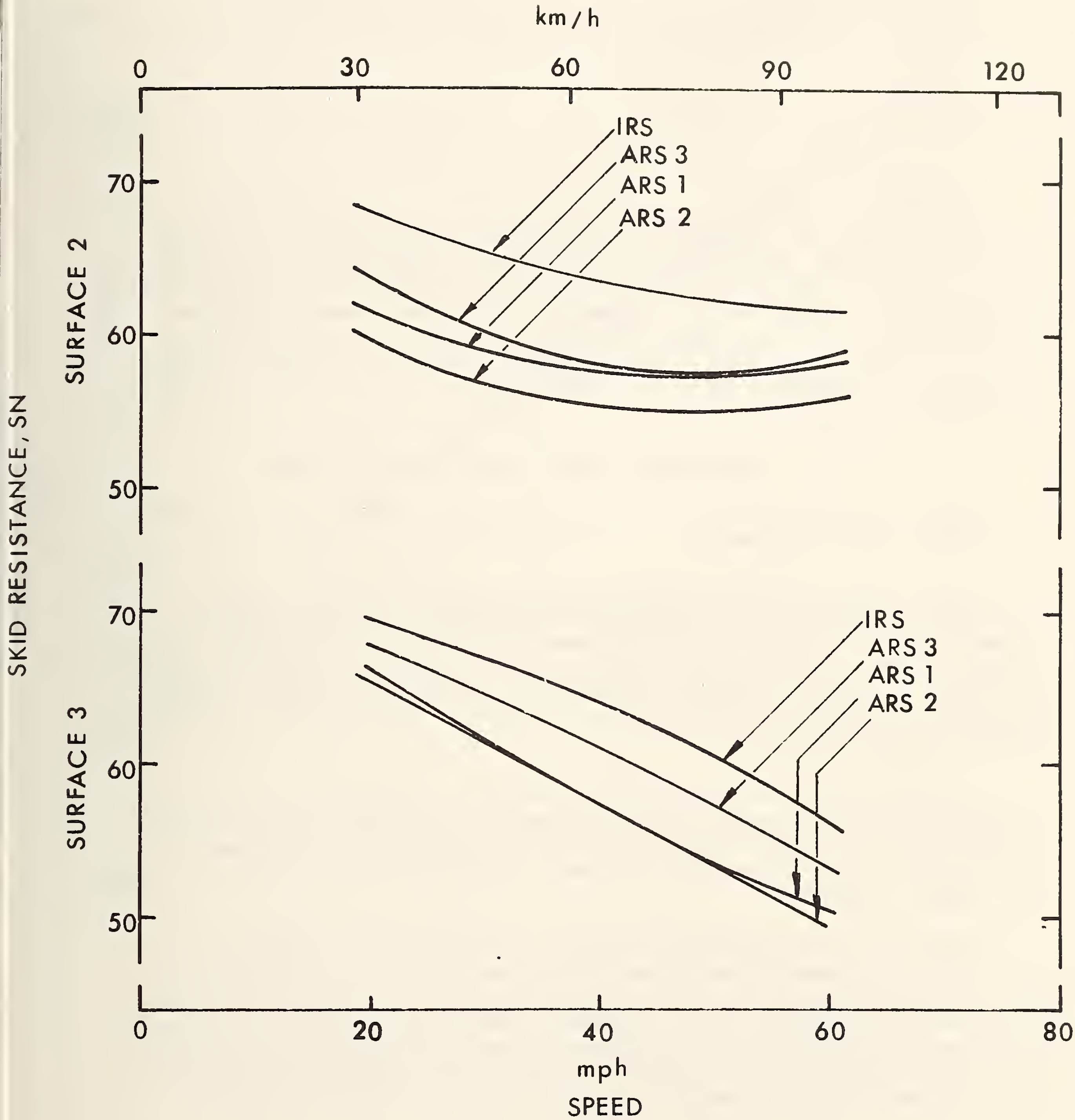

Figure 33. Skid resistance as a function of speed, calculated for surfaces 2 and 3 at EFTC.

The Θ_c results are shown in figure 34 for surface 2 and in figure 35 for surface 3. If the results are taken as system-independent and averaged, the dashed lines in the figures represent the average Θ_c for the respective surfaces. The expressions for the averages are:

$$\text{(surface 2)}\ \Theta_c = -0.557 + 0.0111V$$

and

$$\text{(surface 3)}\ \Theta_c = -0.332 - 0.0010V.$$

Experimental values of the speed gradient, Θ_m, measured using variations about the nominal test speeds, are shown in table 17. Each value of Θ_m is the slope of a least squares line through the group of data points, for the particular system-surface combination, representing skid numbers obtained at radar-measured differential speeds about the nominal speed. The Θ_m values are paired with the Θ_c values for comparison. They can be seen to be generally consistent in sign, and also consistent in magnitude in about half of the comparisons. The averaged magnitudes are more consistent.

3.12. Supplementary Comparisons between Systems

The test plan consists of direct comparisons between ARS 1 and IRS, and between ARS 2 and ARS 3.

Steps were taken in planning to ensure that the pairs of skid resistance measuring systems would indeed measure the same property. Common elements of the measurements made by each pair of systems during a time period included surface, speed range, and tires, with the time span kept as short as possible consistent with surface drying. Drying time and the number of tests required per system per tire precluded a direct four-way comparison.

The test plan provides for measurement of the range of surface variability over the term of the tests and for the measurement of tire variability. If these effects are known, the test results can be extended to interrelate all four systems, using surface and speed as the common elements.

The loss of several test days (sec. 3.4) prevented completion of the final two planned time periods; consequently, surface variability over the testing time was not measured. An estimate is available from previous experiments [7, sec. 3.9] but it was felt worthwhile to use the last remaining test day to make direct comparisons between all pairings of the four systems, even though the number of data points obtainable for each match would be small.

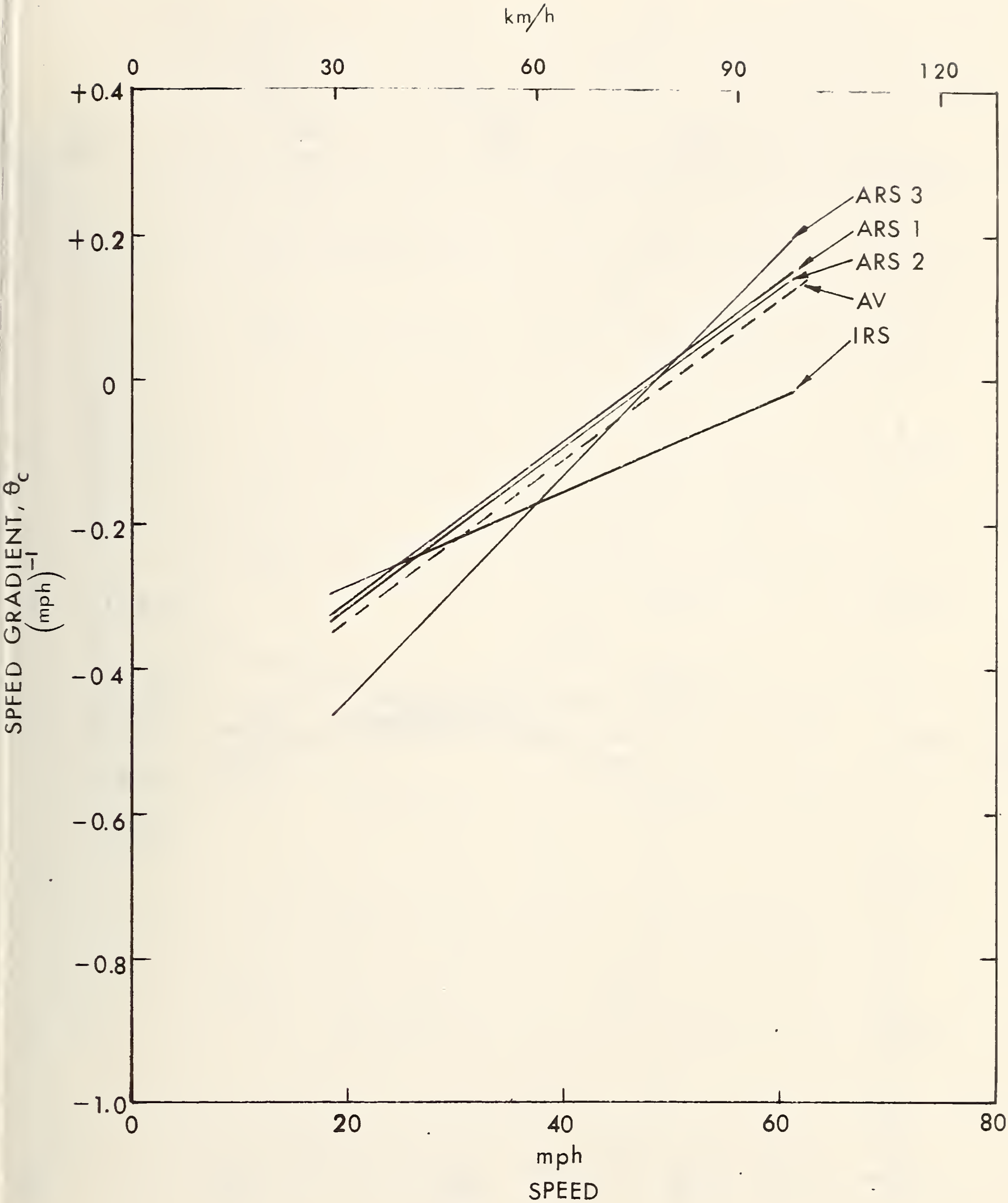

Figure 34. Skid resistance speed gradients calculated from measurements on surface 2 at EFTC.

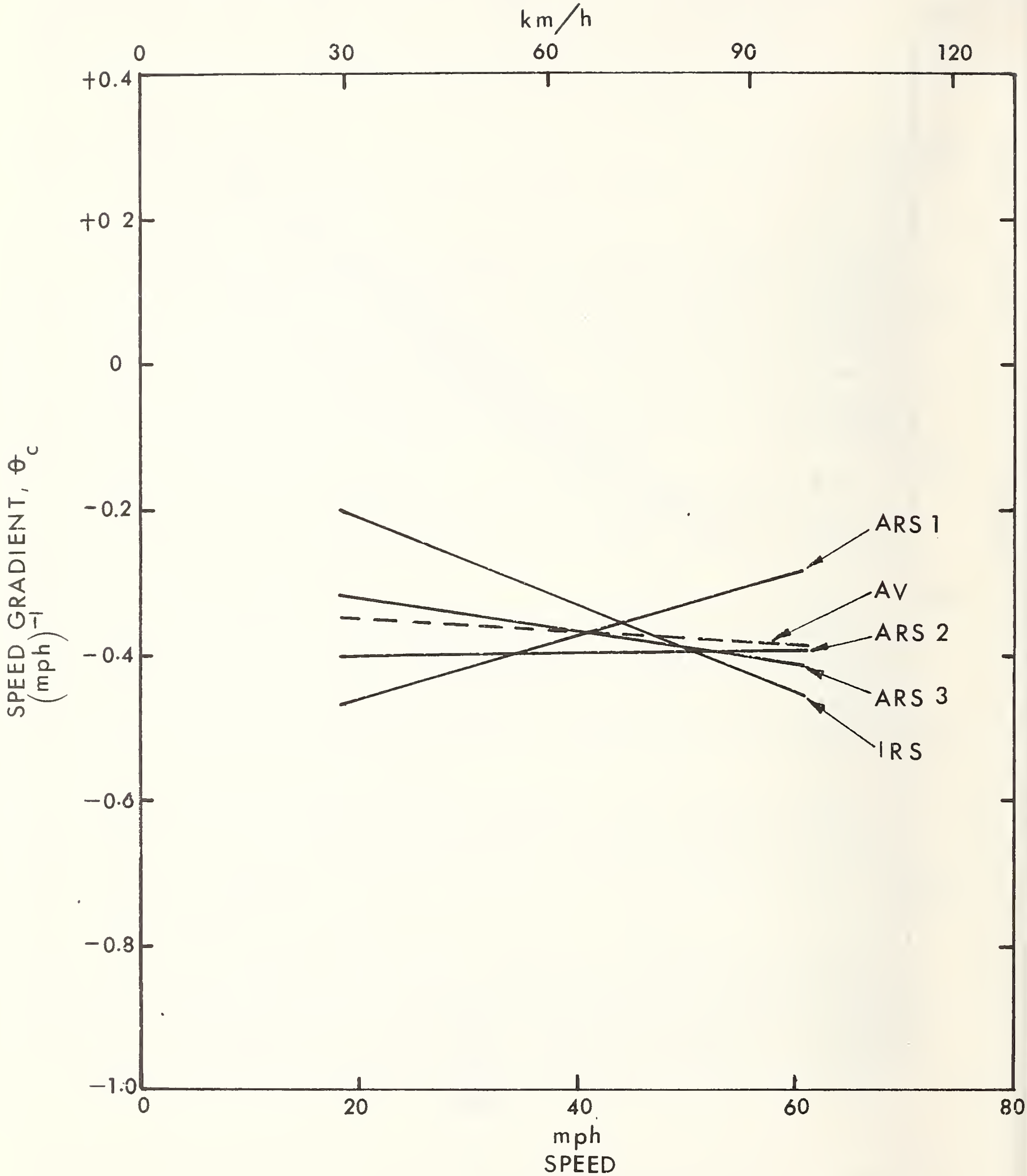

Figure 35. Skid resistance speed gradients calculated from measurements on surface 3 at EFTC.

Table 17. Measured and calculated skid resistance speed gradients

For surface 2:										
Speed	ARS 1		ARS 2		ARS 3		IRS		Average	
	Θ_m	Θ_c	Θ_m	Θ_c	Θ_m	Θ_c	Θ_m	Θ_c	Θ_m	Θ_c
mph[a]										
20	-0.30	-0.30	-0.03	-0.31	-0.20	-0.44	-0.58	-0.29	-0.28	-0.34
40	-0.05	-0.08	+0.04	-0.09	-0.29	-0.13	+0.34	-0.16	+0.01	-0.11
60	+0.39	+0.14	-0.54	+0.13	+0.02	+0.18	+0.59	-0.03	+0.12	+0.11

For surface 3:										
Speed	ARS 1		ARS 2		ARS 3		IRS		Average	
	Θ_m	Θ_c	Θ_m	Θ_c	Θ_m	Θ_c	Θ_m	Θ_c	Θ_m	Θ_c
mph										
20	-0.12	-0.46	-0.59	-0.40	-0.46	-0.32	-0.88	-0.21	-0.51	-0.35
40	-0.51	-0.38	-0.43	-0.40	-0.36	-0.37	-0.14	-0.33	-0.36	-0.37
60	-0.27	-0.29	+0.28	-0.40	-0.30	-0.41	-0.25	-0.45	-0.14	-0.39

[a] 1 mph = 1.609 km/h.

The supplementary test plan sequence shown previously in table 6 was followed. Each system made two measurements at each speed on each surface measured. Tires from tire group 2, which showed the least wear, were used.

The resulting SN values did not compare well with the average SN values from the first six time periods. When the two measurements were corrected for speed deviation and averaged, sixteen of the twenty-four results agreed with the previous averages within limits of two standard deviations, whereas eight were quite far apart. The new results were predominantly lower (table 18).

This large percentage of excessive discrepancies suggests that the SN measurements are still not under statistical control, perhaps due to factors that have not been taken into account.

One procedural change in particular may have contributed to the discrepancy. The tires used in time periods 1 through 6 were each used on only one surface, and so each skid occurred on either virgin tread or tread with the wear pattern characteristic of that surface [6, sec. 3.6]. In the supplementary comparisons, tires which had previously been used only on surface 3 were now used alternately on surfaces 2 and 3. The variations in tread wear texture may have affected the measured SN. It may be desirable in the future to include skids on virgin tread as a control to determine this effect.

Confidence in the supplementary comparisons is clouded by the discrepancies. Least squares fits to the comparison data points are:

$$SN_{ARS\ 1} = 14.9 + 0.703\ SN_{IRS}$$

$$SN_{ARS\ 2} = -15.8 + 1.102\ SN_{IRS}$$

$$SN_{ARS\ 3} = 125.6 - 1.101\ SN_{IRS}$$

$$SN_{ARS\ 2} = 327.3 - 4.682\ SN_{ARS\ 1}$$

$$SN_{ARS\ 3} = 6.3 + 0.985\ SN_{ARS\ 1}$$

$$SN_{ARS\ 3} = 170.0 - 2.140\ SN_{ARS\ 2}$$

These lines and the data points are plotted in figure 36.

Table 18. Difference between two sets of average SN measurements

System	Surface	Speed mph[b]	SN discrepancy[a]	
ARS 2	3	40	-9.5	Exceed 2 std. dev. of the TP 1-6 values
ARS 2	3	20	-8.1	
ARS 1	2	20	-7.4	
IRS	2	20	-5.7	
IRS	2	40	-4.9	
ARS 3	3	40	-4.7	
ARS 2	2	60	-3.4	
ARS 1	2	40	-2.8	
ARS 1	3	40	-1.9	
IRS	3	40	-1.7	
ARS 2	2	40	-1.6	
IRS	3	60	-1.5	
ARS 1	2	60	-1.4	
ARS 1	3	20	-1.2	
ARS 3	2	20	-0.6	
ARS 3	3	20	-0.4	
ARS 1	3	60	-0.1	
ARS 3	2	40	+0.5	
ARS 3	3	60	+0.6	
IRS	2	60	+0.6	
ARS 3	2	60	+1.1	
ARS 2	3	60	+1.9	
ARS 2	2	20	+2.0	
IRS	3	20	+2.6	

[a] For each system-surface-speed combination, the discrepancy is the difference between the average SN measured on the final test day and the average SN measured during time periods 1 through 6.

[b] 1 mph = 1.609 km/h.

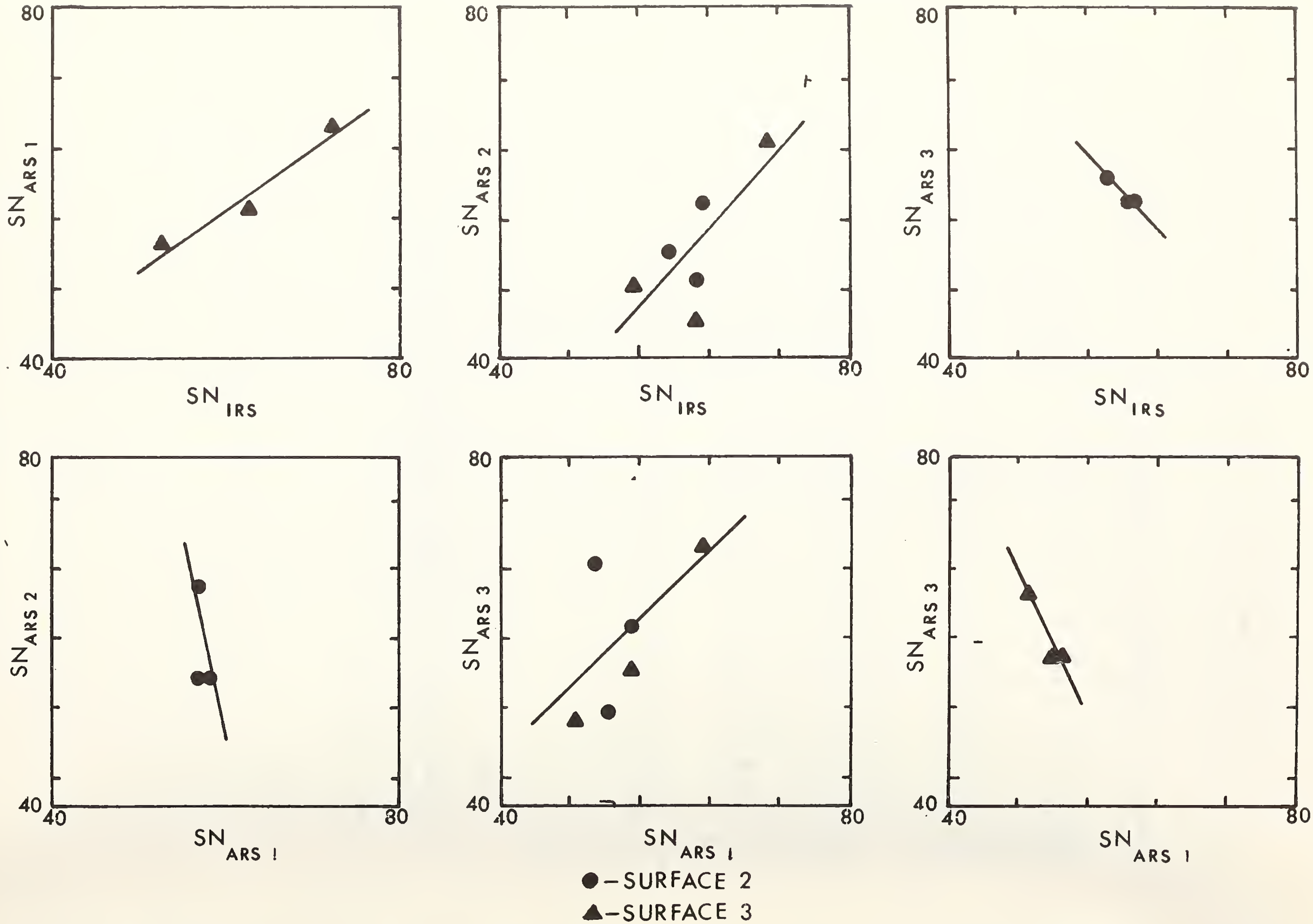

Figure 36. Direct comparisons between systems on the last day of testing.

3.13. The Correlation Equations

A summary of the results of the dynamic skid resistance measurement test program conducted on the two chosen surfaces at the EFTC is given in table 19.

As pointed out in section 3.12, the results include direct comparisons between ARS 1 and the IRS, and between ARS 2 and ARS 3, because these system pairs measured the same surfaces contemporaneously. Comparisons drawn between other combinations of the systems are inferred on the premise that the effects of a few days interval between like measurements can be neglected.

The comparisons are expressed as linear correlation equations. Coefficients for the equations have been calculated by least squares, using the mean SN values, and are listed in table 20.

3.14. Use of the Correlation Equations

Each of the correlation equations results from six measurement pairs. Therefore, to predict a value with 95 percent confidence limits, the standard deviation of predicted values is to be multiplied by 2.78. To predict a value with 90 percent confidence limits, the standard deviation of predicted values is to be multiplied by 2.13.

At present, the national FHWA standard for skid number measurement is the IRS. Field Test Center personnel would presumably like to predict, for ongoing ARS SN measurements, the values that would be obtained by the IRS, using the appropriate correlation equation.

A plot of a representative equation (for ARS 1 and IRS) is shown in figure 37. The lengths of the crosses correspond to the 99 percent confidence intervals, L, of the measured mean skid numbers from which the correlation line was derived, while the curves symmetric to the correlation line represent the 90 percent confidence limits for the predicted values.

Of course, the random error component of the new ARS SN measurements must also be taken into consideration. A graphical procedure is perhaps the easiest way to estimate the total range of uncertainty. With reference to figure 37, the projection of the ARS measurement uncertainty from the 90 percent confidence band to the IRS axis represents the range of uncertainty of the predicted value.

The uncertainty for the correlation line itself is, in a sense, systematic in nature from the ARS point of view, i.e., if an ARS is comparing the SN of two different surfaces, this systematic uncertainty cancels out. However, if an ARS compares its results with another ARS via the correlations with IRS, then the uncertainty of the two correlation lines will have to be taken into consideration.

Table 19. Correlation summary

	Test matrix				Results				
System	Surface	Speed	Tire group	Time period	No. of tests	Mean SN	Gradient Θ_m	Sample std. dev.	99% Confidence interval L, (SN)
		mph[a]							
ARS 1	2	20	1	3	21	61.36	-0.30	2.39	±1.5
	2	40	1	1	18	57.61	-0.05	2.34	±1.6
	2	60	1	5	21	58.04	+0.39	2.20	±1.4
	3	20	2	4	21	66.20	-0.12	2.87	±1.8
	3	40	2	2	20	57.87	-0.51	1.96	±1.3
	3	60	2	6	21	50.94	-0.27	2.80	±1.7
ARS 2	2	20	3	4	21	59.56	-0.03	2.32	±1.4
	2	40	3	2	21	55.21	+0.04	2.06	±1.3
	2	60	3	6	19	55.63	-0.54	3.21	±2.1
	3	20	2	3	21	65.38	-0.59	2.48	±1.5
	3	40	2	1	21	57.60	-0.43	1.67	±1.0
	3	60	2	5	13	48.87	+0.28	2.38	±2.0
ARS 3	2	20	3	4	21	63.63	-0.20	2.55	±1.6
	2	40	3	2	21	57.83	-0.29	1.60	±1.0
	2	60	3	6	21	58.54	+0.02	2.84	±1.8
	3	20	4	3	21	67.81	-0.46	1.88	±1.2
	3	40	4	1	21	60.95	-0.36	2.11	±1.3
	3	60	4	5	21	53.03	-0.30	2.26	±1.4
IRS	2	20	1	3	21	67.82	-0.58	2.22	±1.4
	2	40	1	1	21	63.72	+0.34	1.82	±1.1
	2	60	1	5	21	61.43	+0.59	2.63	±1.6
	3	20	4	4	21	69.11	-0.88	3.00	±1.9
	3	40	4	2	21	64.14	-0.14	2.63	±1.6
	3	60	4	6	21	55.86	-0.25	2.65	±1.6

[a] 1 mph = 1.609 km/h.

Table 20. Correlation equations

		Correlation equation: Y = A + BX + error terms (fitted to 6 pairs of mean SN values)						
Y (SN)	X (SN)	A	B	Residual std. dev.	Predicted value std. dev. SN_{low}	SN_{mean}	SN_{high}	Correlation coefficient
ARS 1	IRS	-5.25	1.0038	1.73	1.5	0.7	1.1	0.951
ARS 2	IRS	-12.22	1.0877	1.91	1.6	0.8	1.2	0.950
ARS 3	IRS	-4.80	1.0223	1.72	1.4	0.7	1.0	0.954
ARS 2	ARS 1	-5.95	1.0736	0.90	0.7	0.4	0.7	0.989
ARS 3	ARS 1	2.07	0.9925	1.22	1.0	0.5	1.0	0.977
ARS 3	ARS 2	7.30	0.9291	0.70	0.5	0.3	0.6	0.992
IRS	ARS 1	10.78	0.9017	1.64	1.3	0.7	1.3	0.951
IRS	ARS 2	16.38	0.8291	1.67	1.3	0.7	1.3	0.950
IRS	ARS 3	10.06	0.8893	1.60	1.2	0.7	1.2	0.954

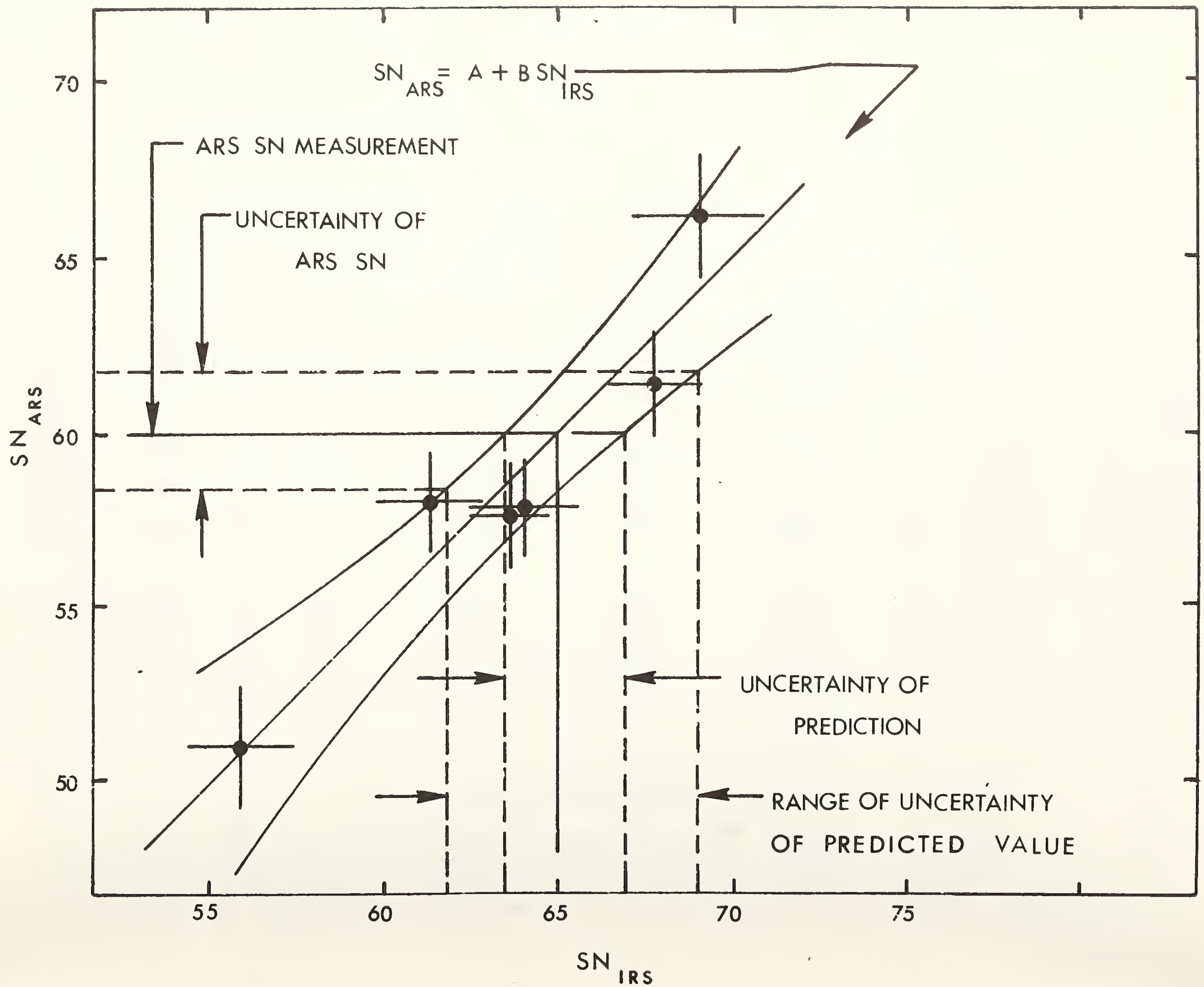

Figure 37. Use of the correlation equations to predict IRS values.

Indeed, it is a consequence of the choice of an artifact standard such as a reference measurement system, rather than a purely procedural standard, that the uncertainty of the relation increases with each comparison step separating a user-level system from the ultimate reference. In the skid resistance case, two comparisons apply, since the user-level skid measurement systems have access to the national reference system only through an area reference system. The uncertainty increase in a two-step correlation is illustrated by figure 38. In order to obtain an acceptable level for the overall uncertainty, great care in measurement is needed at each step to achieve narrow confidence bands on the relations between systems.

4. The IRS Ground Station

The features of the ground station have been described in detail previously [7, sec. 4]. Briefly, the ground station provides a magnetic tape record of the data obtained by the skid test system, automatically calculates SN from the data, plots the data and SN versus location on the test surface, and provides a printed statistical analysis of the SN results. The calculation, plotting, and analysis can be done on site while skid tests proceed or can be done at a later time, using the magnetic tapes. The measurement process is improved in two ways by use of the ground station -- first, the portion of the surface measured is identified, and second, automatic data processing eliminates the subjective judgements of the data analyst as a source of error.

The ground station was developed partly in the expectation that, once its usefulness had been demonstrated, the calculator could be used to process inputs from all skid test vehicles engaged in a correlation. At present, only the IRS has been provided with a digital on-board memory to transfer data to the ground station. The original analog strip-chart recorder remains on the IRS as the primary means of recording data.

During this program of skid resistance measurements, the ground station was operated daily to evaluate its reliability. Examination of ground station plots, as mentioned in section 3.5, first detected the unexpected drift of the IRS vertical load transducer signal.

The ground station functioned well throughout the testing period. The calculator and associated electronics performed reliably. Mechanical difficulties with the start and finish tapeswitch assemblies across the test surfaces caused some loss of ground station data. Data-taking resumed when the assemblies were temporarily bypassed with manually operated switches.

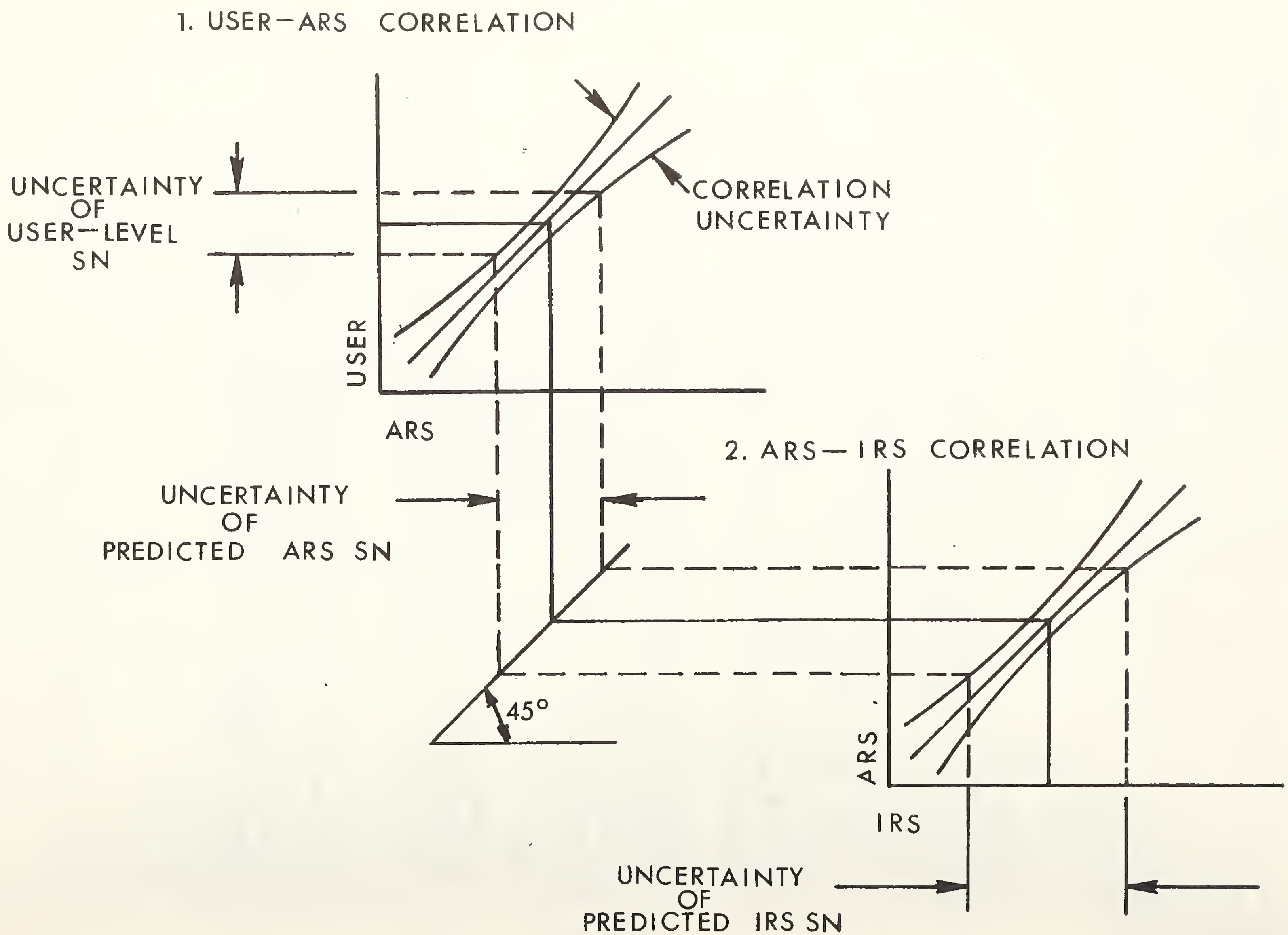

Figure 38. Uncertainty increase in a two-step correlation.

A number of the magnetic data tapes recorded at EFTC have been played back at NBS. The SN results are compatible with the data analyst's interpretation of the corresponding analog strip chart records. Ground station plots made during skid tests at EFTC have been duplicated from the tapes. Because traction, vertical force, speed, etc. are recorded by the ground station as separate data channels, it is possible to vary the calculator program to obtain, for instance, SN in terms of either the quotient of instantaneous traction and vertical load values or the quotient of instantaneous traction and the vertical load values obtained using the H/L unloading constant.

In overall performance, the ground station has been found to be versatile and reliable.

5. RECOMMENDATIONS

To improve the reliability of subsystem evaluation, skid measurement correlation results, and the convenience of conducting the tests, the following recommendations are made:

a) A measured distance for adjusting the fifth wheel subsystem should be established at a place more convenient to the skid test surfaces, where it would be possible to make test runs in both directions, and where extended driving distance would not be required between runs.

b) Drivers assigned to reference skid measuring systems should check the speed record frequently to develop driving techniques for maintaining the specified speed during skids.

c) Means should be provided to increase the sensitivity of ARS recording ranges for speed, flow, vertical force, and traction by a factor of ten or more. A series of reference signals should be provided for each channel to allow linearity checks and to facilitate zero suppression.

d) ARS flow readouts should be adjusted regularly, using the flow sensor calibration results provided by NBS. An additional connector should be installed in each ARS to make this possible.

e) The damping factor of the ARS trailer suspension should be in creased. This might be accomplished by the installation of additional shock absorbers or the use of double-acting shock absorbers.

f) Reference surfaces should be clean when skid tests are con ducted. It is recommended that the surfaces be hosed down with water and allowed to dry prior to each day of testing.

g) The temperature drift of the IRS wheel transducer vertical load channel should be eliminated. Until this is done, an operator should adjust the vertical load channel immediately before each skid test.

During the program conducted by NBS involving correlations at the Field Test Centers, it has become apparent that problems exist in the skid resistance measurement process that require study beyond the scope of the correlation tests. The following recommendations deal with some of those problems:

a) The effects on SN due to changes in pavement wetting variables should be determined. One variable is water layer depth. The nozzles that have been used in these correlations do not produce a uniform water layer. This is largely because the air stream and the speed difference between the water and the pavement violently affect the water as it falls from the nozzle onto the pavement. The wetted width on the pavement and the water distribution across that width are not well formed. As a result, there is presently no satisfactory method for measuring the effective depth of the water layer encountered by the test tire or for determining that the water quantity specification of E 274-70 is met. Another variable is soak time. Pavement wetting serves as a lubricant for the skidding tire and, to some degree, simulates wet weather conditions. Water applied by the nozzle hits the pavement only milliseconds before it is encountered by the tire. In this time span, the pavement may become superficially wet or the water may remain beaded on the dry surface. Actual wet weather persists for an extended time, and the pavement becomes soaked. When the effects of changes in water layer depth and soak time are known, it may be possible to choose optimum values objectively.

b) The effect on SN due to changes in test tire inflation pressure should be determined. Unless the effect of changes such as those that may occur during skid testing is found to be negligible, test tire inflation pressure should be controlled at the specified value. It should be determined whether the inflation pressure specified for the standard tire in E 274-70 results in the best skid resistance consistent with other requirements for an automotive tire such as ride quality and tread life.

c) It should be determined whether the calibration procedures that have been developed for force-sensing skid measurement systems are adaptable to torque-sensing systems and, if they are not, new procedures should be developed for torque.

d) The effect of tread wear texture on SN should be determined. Each skid wears a patch of tread with a texture characteristic of the pavement. At present, a test tire may lock and skid at random on worn or virgin tread. If the effect of wear texture on SN is not shown to be negligible, lock position should be controlled such that each skid measurement is made with virgin tread.

e) It should be determined whether correlations obtained on the reference surfaces are valid on common highway pavements. The present reference surfaces are constructed with epoxy as a binder and, in some cases, as an overcoat. This is not typical of highway construction. Skids on the reference surfaces pro duce unusual wear textures. This suggests that skid resistance is generated differently on these surfaces than on common pave ments.

f) Means should be provided to improve trailer stability. For example, traction force on the locked test wheel of a two-wheeled skid trailer acts at a distance from the trailer center line, causing the trailer to rotate in roll, pitch, and yaw. This results in a deflection of the test wheel that is contrary to a condition of E 274-70 that "its major plane is parallel to its direction of motion and perpendicular to the pavement" while the skid resistance measurement is made. Balanced traction developed by an anti-skid brake on the opposite wheel might be used as a means of preventing trailer roll and yaw, and would also have the desirable effect of eliminating lateral force on the test wheel.

The reference skid measuring system evaluations and correlation results reported here are valid only if no modifications are made and if no changes are made in mechanical and electrical components that affect the results, and if the systems are operated in the same manner as they were at the time of these tests.

It is a pleasure to acknowledge the cooperative participation of personnel of the Federal Highway Administration and the FHWA Field Test Centers in these tests. Special thanks are also due to the following NBS staff members; Dr. Hsien H. Ku, for his contributions and guidance in the statistical treatment of the experiment; Ray Russell, driver of the IRS, for his excellent control of the system despite the inconvenience of a foot injury, and for doubling in operation of the on-board instrumentation; Bill Appleton, IRS instrumentation operator on previous trips, for his contributions to the construction of the system electronic equipment and for preparing it for use in the field; John Hazzard, for aid in mechanical design, drafting, and illustration; John Heine, for additional drafting aid; and Ruth Davenport, for patient and careful reading of the strip chart skid records. Their support has been invaluable to the completion of this complex task.

6. REFERENCES

[1] Standard method of test for skid resistance of paved surfaces using a full-scale tire, ASTM Designation E 274-70, Annual Book of ASTM Standards, Part 11 (American Society for Testing and Materials, Philadelphia, Pa., 1973).

[2] Watson, John R., and Cook, Larry M., A national program to standardize skid resistance measurements, Public Roads, A Journal of Highway Research, 37, No. 3, pp. 7780 (Dec. 1972).

[3] Smith, L. L., and Fuller, S. L., Florida skid correlation study of 1967 - skid testing with trailers, Highway Skid Resistance STP 456 (American Society for Testing and Materials, Philadelphia, Pa., 1969).

[4] Kearns, R. W., and Ward, J. F., A method and means of calibrating an air-bearing force plate for use with a towed pavement friction test trailer, Nat. Bur. Stand. (U.S.), NBSIR 75-738 (Dec. 1974).

[5] Standard specification for standard tire for pavement skid resistance tests, ASTM Designation E 501-73, Annual Book of ASTM Standards, Part 15 (American Society for Testing and Materials, Philadelphia, Pa., 1976).

[6] Kearns, R. W., and Ward, J. F., Skid resistance measurement tests at the FHWA Eastern Field Test Center, Nat. Bur. Stand. (U.S.), NBSIR 75-972 (July 1976).

[7] Kearns, R. W., and Ward, J. F., Skid resistance measurement tests of FHWA reference systems at the Western Field Test Center, Nat. Bur. Stand. (U.S.), NBSIR 76-1133 (Oct. 1976).

[8] Chestnut, H., and Mayer, R. W., Solution of linear differential equations, Chapter 3, Servomechanisms and Regulation System Design, 1 p. 62 (John Wiley and Sons, Inc., New York, N. Y., 1951).

FORM NBS-443
(REV. 12-65)

KRB:plb

U.S. DEPARTMENT OF COMMERCE
NATIONAL BUREAU OF STANDARDS
WASHINGTON, D.C. 20234

213.06/2130440
July 2, 1976

REPORT OF CALIBRATION

OF A TURBINE TYPE FLOW TRANSDUCER

Maker: ITT Barton
Monterey Park, California

Serial: 7101-2567

submitted by

Engineering Mechanics
Mechanics Division
National Bureau of Standards
Washington, D.C. 20234

A calibration has been performed on the meter described above by counting the total pulses generated during discharge of a weighed quantity of water converted to gallons.

As tested, this assembly consisted of upstream tubing 1 inch inside diameter and 28 inches in length preceded by an elbow, the meter, and exit tubing 20 inches in length. The assembly mounted horizontally with the meter pickoff coil in a vertical position was connected by a straight AN nipple to AN - 16 hose. Test temperature and downstream pressure level were 22 ± 4.5°C and 38 psig, respectively, and the pulse frequency was controlled to within one-half percent of the values listed.

The results given in the attached table are the arithmetic means of ten separate observations taken in groups of five successive runs on each of two different days. The reported values of pulses per gallon have an estimated overall uncertainty of ± 0.19 percent based on a standard error of 0.03 percent and an allowance of ± 0.1 percent for possible systematic error.

For the Director,

L. K. Irwin

L. K. Irwin
Acting Chief
Fluid Meters Section
Mechanics Division, IBS

Results of Water Calibration

ITT Barton Turbine Meter, S/N 7101-2567

Pulses/Sec	Pulses/Gal
235	1371.6
460	1367.8
681	1370.9
920	1371.5
1160	1372.4

213.06/2130440
July 2, 1976

FORM NBS-443
(REV. 12-65)

KRB:plb

U.S. DEPARTMENT OF COMMERCE
NATIONAL BUREAU OF STANDARDS
WASHINGTON, D.C. 20234

213.06/2130440
July 2, 1976

REPORT OF CALIBRATION

OF A TURBINE TYPE FLOW TRANSDUCER

Maker: ITT Barton
Monterey Park, California

Serial: 7101-2568

submitted by

Engineering Mechanics
Mechanics Division
National Bureau of Standards
Washington, D.C. 20234

A calibration has been performed on the meter described above by counting the total pulses generated during discharge of a weighed quantity of water converted to gallons.

As tested, this assembly consisted of upstream tubing 1 inch inside diameter and 28 inches in length preceded by an elbow, the meter, and exit tubing 20 inches in length. The assembly mounted horizontally with the meter pickoff coil in a vertical position was connected by a straight AN nipple to AN - 16 hose. Test temperature and downstream pressure level were 24.3 ± 0.8°C and 38 psig, respectively, and the pulse frequency was controlled to within one-half percent of the values listed.

The results given in the attached table are the arithmetic means of ten separate observations taken in groups of five successive runs on each of two different days. The reported values of pulses per gallon have an estimated overall uncertainty of ± 0.19 percent based on a standard error of 0.03 percent and an allowance of ± 0.1 percent for possible systematic error.

For the Director,

L. K. Irwin

L. K. Irwin
Acting Chief
Fluid Meters Section
Mechanics Division, IBS

Results of Water Calibration

ITT Barton 1-in Turbine Meter, S/N 7101-2568

Pulses/Sec	Pulses/Gal
236	1365.4
462	1363.9
684	1366.4
920	1368.2
1151	1368.6

213.06/2130440
July 2, 1976

FORM NBS-443
(REV. 12-65)

KRB:plb

U.S. DEPARTMENT OF COMMERCE
NATIONAL BUREAU OF STANDARDS
WASHINGTON, D.C. 20234

213.06/2130440
July 2, 1976

REPORT OF CALIBRATION

OF A TURBINE TYPE FLOW TRANSDUCER

Maker: ITT Barton
Monterey Park, California

Serial: 7101-2569

submitted by

Engineering Mechanics
Mechanics Division
National Bureau of Standards
Washington, D.C. 20234

A calibration has been performed on the meter described above by counting the total pulses generated during discharge of a weighed quantity of water converted to gallons.

As tested, this assembly consisted of upstream tubing 1 inch inside diameter and 28 inches in length preceded by an elbow, the meter, and exit tubing 20 inches in length. The assembly mounted horizontally with the meter pickoff coil in a vertical position was connected by a straight AN nipple to AN - 16 hose. Test temperature and downstream pressure level were 22.5 ± 3°C and 38 psig, respectively, and the pulse frequency was controlled to within one-half percent of the values listed.

The results given in the attached table are the arithmetic means of ten separate observations taken in groups of five successive runs on each of two different days. The reported values of pulses per gallon have an estimated overall uncertainty of ± 0.19 percent based on a standard error of 0.03 percent and an allowance of ± 0.1 percent for possible systematic error.

For the Director,

L. K. Irwin

L. K. Irwin
Acting Chief
Fluid Meters Section
Mechanics Division, IBS

Results of Water Calibration

ITT Barton Turbine Meter, S/N 7101-2569

Pulses/Sec	Pulses/Gal
236	1348.3
461	1347.8
682	1352.5
922	1352.5
1160	1353.0

213.06/2130440
July 2, 1976

FORM NBS-443
(REV. 12-65)

KRB:plb

U.S. DEPARTMENT OF COMMERCE
NATIONAL BUREAU OF STANDARDS
WASHINGTON, D.C. 20234

213.06/2130440
July 2, 1976

REPORT OF CALIBRATION

OF A TURBINE TYPE FLOW TRANSDUCER

Maker: ITT Barton
Monterey Park, California

Serial: 7101-2570

submitted by

Engineering Mechanics
Mechanics Division
National Bureau of Standards
Washington, D.C. 20234

A calibration has been performed on the meter described above by counting the total pulses generated during discharge of a weighed quantity of water converted to gallons.

As tested, this assembly consisted of upstream tubing 1 inch inside diameter and 28 inches in length preceded by an elbow, the meter, and exit tubing 20 inches in length. The assembly mounted horizontally with the meter pickoff coil in a vertical position was connected by a straight AN nipple to AN - 16 hose. Test temperature and downstream pressure level were 24.3 ± 0.8°C and 38 psig, respectively, and the pulse frequency was controlled to within one-half percent of the values listed.

The results given in the attached table are the arithmetic means of ten separate observations taken in groups of five successive runs on each of two different days. The reported values of pulses per gallon have an estimated overall uncertainty of ± 0.19 percent based on a standard error of 0.03 percent and an allowance of ± 0.1 percent for possible systematic error.

For the Director,

L. K. Irwin

L. K. Irwin
Acting Chief
Fluid Meters Section
Mechanics Division, IBS

Results of Water Calibration

ITT Barton Turbine Meter, S/N 7101-2570

Pulses/Sec	Pulses/Gal
235	1368.4
463	1367.8
685	1369.8
921	1372.3
1151	1372.7

213.06/2130440
July 2, 1976

FORM NBS-443
(REV. 12-65)

HHA:plb

U.S. DEPARTMENT OF COMMERCE
NATIONAL BUREAU OF STANDARDS
WASHINGTON, D.C. 20234

213.06/2130440
July 2, 1976

REPORT OF CALIBRATION

OF TWO TURBINE TYPE FLOW TRANSDUCERS

Maker: ITT Barton
Monterey Park, California

Serial: 7101-2571
7101-2566

submitted by

Engineering Mechanics
Mechanics Division
National Bureau of Standards
Washington, D.C. 20234

A calibration has been performed on each of the meters described above by counting the total pulses generated during discharge of a weighed quantity of water converted to gallons.

For each meter tested, the assembly consisted of upstream tubing 1 inch inside diameter and 28 inches in length preceded by an elbow, the meter, and exit tubing 20 inches in length. Each assembly, mounted horizontally with the meter pickoff coil in a vertical position, was connected to AN - 16 hose 10 inches long. Test temperature and downstream pressure level were 24.2 ± 0.6°C and 35 psig, respectively, and the pulse frequency was controlled to within one percent of the values listed.

The results given in the attached table are the arithmetic means of four separate observations taken in groups of two successive runs on each of two different days. The reported values of pulses per gallon have an estimated overall uncertainty of ± 0.25 percent based on a standard error of 0.05 percent and an allowance of ± 0.1 percent for possible systematic error.

For the Director,

L. K. Irwin

L. K. Irwin
Acting Chief
Fluid Meters Section
Mechanics Division, IBS

Results of Calibration

ITT Barton, Serial 7101-2571

Pulses/Sec	Pulses/Gal
233	1324.3
458	1319.4
682	1318.8
913	1318.7
1208	1319.6

ITT Barton, Serial 7101-2566

Pulses/Sec	Pulses/Gal
231	1371.5
464	1370.2
676	1369.6
911	1369.6
1205	1371.5

213.06/2130440
July 2, 1976

Appendix B. The Test Matrix

A subdivision of the test plan consists of the following test matrix:

Time Period ______

Surface ________

TIRES / SPEED	A	B	C	D	E	F	G
$S - \Delta S$	1	2	3	4	5	6	7
			(LANES)				
S	2	3	4	5	6	7	1
$S + \Delta S$	4	5	6	7	1	2	3

Letters A thru G designate 7 tires while numbers 1 thru 7 identify the 7 lanes comprising the surface. The nominal test speed is S, while ΔS is an incremental change in the speed.

The mean of the 21 skid number measurements represents the skid number of the surface measured during the time period using the average tire at the nominal test speed. The novelty of the test matrix is that it yields the skid gradient of the surface, as well as a measure of the surface and tire nonuniformities.

Suppose we want to compare the effect of making a measurement with tire A with all the other tires. To do this effectively, we want to eliminate any measurement deviations due to skidding in different lanes and at different speeds.

Let a measurement result be represented by the notation

$$(SN + \varepsilon)_{LT(S-\Delta S)}$$

where:

- SN = a nominal skid number measured value,
- $+\varepsilon$ = an increase in the SN value due to testing at lower than the nominal test speed by the increment ΔS,
- L = lane identification of the test measurement, and
- T = the tire identification of the test measurement.

From the test matrix, tire A was used in lanes 1, 2, and 4 at three different speeds. Lane 1 was used with tires A, G, and E at three different speeds, while lane 2 was used with tires B, A, and F at the three different speeds, while lane 4 was used with tires D, C, and A at three different speeds.

Let us write an equation for the measurement results made in each lane

$$2(SN + \varepsilon)_{1A(S - \Delta S)} - (SN)_{1G(S)} - (SN - \varepsilon)_{1E(S + \Delta S)} = \Delta_{AGE} + 3\varepsilon \quad (1)$$

$$2(SN)_{2A(S)} - (SN + \varepsilon)_{2B(S - \Delta S)} - (SN - \varepsilon)_{2F(S + \Delta S)} = \Delta_{ABF} \quad (2)$$

$$2(SN - \varepsilon)_{4A(S + \Delta S)} - (SN)_{4C(S)} - (SN + \varepsilon)_{4D(S - \Delta S)} = \Delta_{ACD} - 3\varepsilon \quad (3)$$

where Δ_{AGE} = twice the difference between using tire A and the average of using tires G and E in lane 1,

Δ_{ABF} = twice the difference between using tire A and the average of using tires B and F in lane 2,

Δ_{ACD} = twice the difference between using tire A and the average of using tires C and D in lane 4.

Note that equations 1, 2, and 3 are each independent of lane effects. Note also that the sum of the three equations is independent of any speed effects (assuming ΔS is small). Consequently, the sum is free of both lane and speed effects. To simplify the notation, eliminate the lane and speed variations from the sum, and we get

$$6(SN)_A - (SN)_B - (SN)_C - (SN)_D - (SN)_E - (SN)_F - (SN)_G = \sum\Delta \quad (4)$$

We may add to this equation [7], the equation

$$(SN)_A - (SN)_A = 0 \quad (5)$$

which simply says that the skid number without lane and speed dispersion is equal to the skid number measurement using tire A without lane and speed dispersion with no measurement error. Then

$$7(SN)_A - \left\{SN_A + SN_B + SN_C + SN_D + SN_E + SN_F + SN_G\right\} = \sum\Delta \quad (6)$$

Now, the measurement performance with tire A can be compared with the performance of all the other tires by writing

$$SN_A = \sum_{i=A}^{G} \frac{SN_i}{7} + \frac{\sum \Delta}{7}$$

$$= \text{mean of all measurements} + \frac{\sum \Delta}{7} \qquad (7)$$

In a similar manner, the test matrix can be rearranged to yield, for example, the measurement performance on lane 1 compared with the performance on all the other lanes. The results are then a measure of surface uniformity.

NBS-114A (REV. 7-73)

U.S. DEPT. OF COMM. BIBLIOGRAPHIC DATA SHEET	1. PUBLICATION OR REPORT NO. NBSIR 77-1213	2. Gov't Accession No.	3. Recipient's Accession No.

4. TITLE AND SUBTITLE Skid Resistance Measurement Tests of New FHWA Reference Systems at the Eastern Field Test Center	5. Publication Date February 1977
	6. Performing Organization Code
7. AUTHOR(S) R. W. Kearns and J. F. Ward	8. Performing Organ. Report No.
9. PERFORMING ORGANIZATION NAME AND ADDRESS NATIONAL BUREAU OF STANDARDS DEPARTMENT OF COMMERCE WASHINGTON, D.C. 20234	10. Project/Task/Work Unit No. 2130440
	11. Contract/Grant No.
12. Sponsoring Organization Name and Complete Address *(Street, City, State, ZIP)* Federal Highway Administration Office of Development Washington, D. C. 20590	13. Type of Report & Period Covered Final Feb-April 1976
	14. Sponsoring Agency Code

15. SUPPLEMENTARY NOTES

16. ABSTRACT *(A 200-word or less factual summary of most significant information. If document includes a significant bibliography or literature survey, mention it here.)*

The Federal Highway Administration (FHWA) is developing a program to improve the method of measuring wet weather pavement skid resistance (SN) and to reduce the variation in results. At the national level, an interim reference system (IRS) is maintained and operated by the National Bureau of Standards. At the regional level, an area reference system (ARS) is maintained and operated at each FHWA Field Test Center. Intercomparisons between these reference systems and the highway measuring systems at the state level provide measurement assurance.

In this report, the first correlations between three identical, newly manufactured systems (ARS 1, 2, 3) and the IRS are given. Computed standard deviations of mid-range predicted SN values are typically less than 0.1 SN. SN is given as a function of test speed for each system, on two test surfaces. Speed gradients of SN are found to be characteristic of the surface.

The test program is explained, from preparations and calibrations of subsystems through dynamic measurement on the surfaces. Controlled and uncontrolled variables are identified, discussed, and in some cases, investigated experimentally. A ranking of the sources of dispersion is given.

A ground station for improved SN calculation precision and on-site statistical analysis, operated in parallel with traditional SN data acquisition methods, is found to perform reliably.

17. KEY WORDS *(six to twelve entries; alphabetical order; capitalize only the first letter of the first key word unless a proper name; separated by semicolons)*

Accident reduction, skidding; correlation, skid resistance; highway safety; measurement, skid resistance; pavement, skid resistance; pavement wetting system; skid resistance, measurement; tire-pavement interface forces; wet pavement skid resistance.

18. AVAILABILITY	19. SECURITY CLASS (THIS REPORT)	21. NO. OF PAGES
[X] Unlimited [ ] For Official Distribution. Do Not Release to NTIS	UNCLASSIFIED	131
[ ] Order From Sup. of Doc., U.S. Government Printing Office Washington, D.C. 20402, SD Cat. No. C13 [X] Order From National Technical Information Service (NTIS) Springfield, Virginia 22151	20. SECURITY CLASS (THIS PAGE) UNCLASSIFIED	22. Price $6.00

USCOMM-DC 29042-P74